https://doi.org/10.5194/essd-2025-789
Preprint. Discussion started: 31 March 2026

Open Access Earth System Science Data Discussions

MORE, a new convection-permitting reanalysis dataset over Italy and Alpine region: Validation and application in weather, climate and hydrology

Paolo Stocchi[1], Francesco Cavalleri[2,3], Mohsin Tariq[4] , Michele Brunetti[1], Stefania Camici[4], Daniele Mastrangelo[1], Fabio Di Sante[6] and Silvio Davolio[1,5]

[1]Institute of Atmospheric Sciences and Climate, National Research Council (CNR-ISAC), Bologna 40129, Italy
[2]Environmental Science and Policy Department (ESP), University of Milan, Milan 20133, Italy
[3] Sustainable Development and Energy Resources Department, Research on Electric Systems (RSE), Milan, Italy
[4]Research Institute for Geohydrological Protection, National Research Council, (CNR-IRPI) Perugia, Italy
[5] Department of Earth Sciences, University of Milan, Milan, Italy
[6] CINECA, Casalecchio di Reno, Bologna, Italy

Correspondence to: Paolo Stocchi (p.stocchi@isac.cnr.it)

Abstract. This study presents a new convection-permitting reanalysis dataset over Italy and Alpine region, produced through dynamical downscaling of ERA5 reanalysis with the non-hydrostatic mesoscale model MOLOCH. MORE (MOloch-downscaled ERA5 REanalysis) is a very high spatial resolution (~1.7 km) gridded dataset, covering the 1990–present period. The dataset includes hourly outputs of a wide range of variables at the surface and on pressure-levels.

MORE validation follows a multiscale framework applied to precipitation and near-surface air temperature using dense and quality-controlled observational datasets. MORE is benchmarked against other convection-permitting products and coarser-resolution reanalyses. Results show that MORE realistically reproduces spatial and temporal variability and improves the simulation of wet-hour frequency, precipitation intensity, sub-daily extremes, particularly during convective regimes, and key climate indicators such as the number of tropical nights, although a systematic cold bias is present in temperature.

As an application example, the May 2023 Emilia-Romagna (northern Italy) catastrophic flood is analyzed. MORE successfully reproduces the meteorological evolution of the two heavy rainfall events, providing added value in the representation of the mesoscale features resulting in localized precipitation extremes. In cascade, hydrological simulations driven by MORE data improve the representation of catchment-scale discharge, and soil moisture dynamics.

Overall, MORE represents the highest-resolution convection-permitting reanalysis currently available for Italy and the Alpine region. Its comprehensive set of variables at hourly resolution makes it a valuable reference for hydrometeorological studies, climate change adaptation, and climate services in regions with complex terrain and high exposure to extremes. The dataset is openly available at DOI: https://doi.org/10.5281/zenodo.18470948 (Stocchi, P. 2026) and will be periodically updated to ensure long-term accessibility, reliability and completeness.

https://doi.org/10.5194/essd-2025-789
Preprint. Discussion started: 31 March 2026

Open Access Earth System Science Data Discussions

1 Introduction

Weather and climate reanalysis datasets have become fundamental tools in meteorological and climate research. These datasets provide spatially and temporally consistent reconstructions of atmospheric and surface conditions, ensuring long-term homogeneity that is crucial for studying climate variability, extreme events, and long-term trends. By assimilating vast amounts of observational data through advanced numerical modeling, reanalyses offer a comprehensive and physically consistent representation of past and present climate state.

Among the most advanced reanalysis products, the European Centre for Medium-Range Weather Forecasts (ECMWF) Reanalysis v5 (ERA5) is a state-of-the-art dataset that has set up a new standard in atmospheric reanalysis (Hersbach et al., 2020). ERA5 provides global coverage from 1940 to the present with a horizontal resolution of 0.25° (approximately 31 km) and hourly outputs, incorporating decades of improvements in data assimilation and development in numerical weather prediction modelling. Building upon ERA5, ECMWF has also released ERA5-Land (Muñoz-Sabater et al., 2021), a specialized reanalysis product designed to improve land surface representation. With an enhanced spatial resolution of 0.1° (~9 km), ERA5-Land refines the depiction of land-atmosphere interactions, offering a more detailed characterization of surface variables such as soil moisture, evaporation, and runoff. Due to their unprecedented level of detail, accuracy, and consistency, both ERA5 and ERA5-Land are among the most reliable datasets currently available for climate and meteorological research (Buizza et al., 2018; Hersbach et al., 2020; Bell et al., 2021). Furthermore, their spatial and temporal resolution makes them crucial not only for atmospheric studies but also for supporting impact assessments across various sectors, including water resource management, agriculture, renewable energy, disaster risk reduction (Kourtis et al., 2023, Shangguan et al., 2022, Vitolo et al., 2020, Olauson, 2018), being also exploited in emerging fields like machine learning (Tomasi et al., 2024; Long et al., 2025).

However, despite their widespread use, global reanalysis datasets exhibit a key limitation: their spatial resolution. These datasets typically feature relatively coarse grid spacing, which, combined with their reliance on convection parameterization, limits their applicability for certain climate impact studies, particularly those aimed at capturing localized atmospheric processes. Various studies (Prein et al., 2015; Kendon et al., 2021; Singh et al., 2021; Zhang et al., 2021; Bandhauer et al., 2022; Lavers et al., 2022; Velikou et al., 2022; Dalla Torre et al., 2024; Chen et al., 2024; Gebrechorkos et al., 2024) have demonstrated that this spatial resolution is often insufficient for capturing the localized impacts of climate variability, such as precipitation patterns, temperature extremes, and the effects of terrain heterogeneity (e.g., mountains, coastal areas, urban regions), and can limit the applications to localized risk assessment, urban planning, and hydrological modeling (Poncet et al., 2024).

A promising solution to this limitation is the dynamic downscaling, a technique that uses regional climate models (RCMs) or meteorological models to increase the spatial resolution of reanalysis and global climate data. Dynamic downscaling consists

https://doi.org/10.5194/essd-2025-789
Preprint. Discussion started: 31 March 2026

in running high-resolution simulations driven by global reanalysis data, such as ERA5, to capture atmospheric processes at local scales (Giorgi and Mearns, 1991). This approach significantly enhances the spatio-temporal accuracy of the reanalysis data, enabling more precise reconstructions of climate impacts at scales relevant to specific applications (e.g., Giorgi et al., 2009, 2015, 2019, 2024; Mearns et al., 2015; Di Luca et al., 2016; Teichmann et al., 2021; Poncet et al., 2024), at the expense of a higher computational cost.

Recent increase in computational resources and advancements in numerical modelling have further fostered the application of downscaling simulations at "convection permitting" scale (i.e.: grid-spacing 1-4 km).

Therefore, several European initiatives, such as the H2020 EUCP and CORDEX-FPS Convection (Coppola et al., 2020) along with numerous studies, have explored the potential of convection-permitting downscaling simulations (Ban et al., 2014; Kendon et al., 2014; Leutwyler et al., 2017; Liu et al., 2017; Berthou et al., 2018; Fumière et al., 2019; Coppola et al., 2020; Pichelli et al., 2021; Ban et al., 2021; Senior et al., 2021; Ha et al., 2022; Soares et al., 2022; Stocchi et al., 2022; Poncet et al., 2024). These studies have provided compelling evidence that Convection-Permitting Regional Climate Models (CP-RCMs) significantly enhance the representation of hourly precipitation characteristics, including the diurnal cycle, spatial distribution, intensity, and extreme events, bringing modeled precipitation dynamics closer to reality. Moreover, CP-RCMs have demonstrated their ability to resolve fine-scale surface heterogeneities (Cortés-Hernández et al., 2024), such as mountainous terrain, coastal regions, and urban environments (Prein et al., 2015; Rowell & Berthou, 2022), offering a more accurate representation of land–atmosphere interactions (Taylor et al., 2013). These improvements are essential for capturing and better representing extreme climate phenomena, such as droughts and summer heatwave. Furthermore, the enhanced physical realism in CP-RCMs has cascading benefits for other key climate variables, including surface energy fluxes (e.g., latent and sensible heat,(Lenderink et al., 2025) and soil moisture, which, although often under-monitored, are crucial for a wide range of applications.

Given these advances, the combination of global reanalysis datasets, such as ERA5, with high-resolution regional models, offers a robust framework for addressing the spatial and temporal limitations inherent in global reanalysis products. This can be pursued with purely dynamical downscaling or by applying data assimilation procedures to enhance the accuracy of the representation of atmospheric variables. Although we fully acknowledge the fundamental differences between these two approaches, for the sake of simplicity, we will refer to both of them as "reanalysis datasets" or “high-resolution atmospheric datasets” throughout the text.

In recent years, UERRA-HARMONIE (Kaiser-Weiss et al., 2019), CERRA (Ridal et al., 2024), COSMO-REA6 (Bollmeyer et al., 2015) and CHAPTER (Bernini et al., 2025) with horizontal resolutions of 11 km, 5 km, 6 km and 3km respectively, have represented major advancements in the development of high-resolution reanalysis datasets over European domains. Substantial efforts have also been dedicated to the Italian territory. Notably, two convection-permitting reanalyses, employing

https://doi.org/10.5194/essd-2025-789
Preprint. Discussion started: 31 March 2026

data assimilation, have been produced by downscaling ERA5: the MEteorological Reanalysis Italian DAtaset High-RESolution (MERIDA-HRES) (Bonanno et al., 2019; Viterbo et al., 2024), generated using the WRF model at 4 km resolution, and the Special Project High-rEsolution ReAnalysis over Italy (SPHERA) (Cerenzia et al., 2022; Giordani et al., 2023) based on COSMO at 2.5 km grid-spacing. Additionally, two convection-permitting hindcast datasets, without data assimilation, have been developed: LAMMA-HINDCAST (Capecchi et al., 2023), which employs the MOdello LOCale in Hybrid coordinates (MOLOCH, Malguzzi et al., 2006; Buzzi et al., 2014) at 2.5 km grid-spacing, and the Very High-Resolution Dynamical Downscaling of ERA5 Reanalysis over Italy (VHR-REA_IT) (Raffa et al., 2021; Reder et al., 2022; Adinolfi et al., 2023) using COSMO at 2.2 km grid-spacing. Recent intercomparisons among these high-resolution datasets over Italy (Cavalleri et al., 2024a; Cavalleri et al., 2024b) highlighted strengths and limitations in capturing precipitation patterns and temperature variability, also revealing significant discrepancies and emphasizing the importance of bias characterization against observational data to ensure their appropriate use in both research and applications.

MORE is obtained through a dynamical downscaling of ERA5 using an updated version of the convection-permitting non-hydrostatic MOLOCH model (Trini Castelli et al., 2020; Giorgi et al., 2023), previously utilized for the LAMMA-HINDCAST reanalysis, operating at a higher spatial resolution of 1.7 km, which is finer than any other existing similar Italian dataset.

MORE provides a comprehensive range of atmospheric variables, 40 in total, including near surface quantities, soil temperature and soil water content at various levels, radiation parameters, geopotential height, temperature (T), moisture and wind components at five vertical levels (950, 850, 700, 500, and 300 hPa). The complete list of variables is available in the dataset metadata (DOI: **https://doi.org/10.5281/zenodo.18470948)** (Stocchi, P. 2026).

As of this writing, MORE represents the highest spatial resolution available dataset of atmospheric reanalysis in Italy. Being an independently generated product that diversifies from existing reanalysis products, it offers substantial added value for meteorological and climatological studies, particularly in ensemble approaches, which aim to optimize the representation of atmospheric processes and strengthen the robustness of analyses (Giordani et al., 2025). In turn, this improves the reliability of reanalysis-based applications, such as impact modeling and extreme event analysis. The MORE dataset will be made publicly available to the scientific community, providing high-resolution atmospheric data at 1.7 km resolution for the period from 1990 to the present, with continuous updates over Italy.

This study aims to introduce the new dataset, evaluate its performance, and present examples of its multidisciplinary applications. The assessment focuses on precipitation and 2 m temperature (t2m) across multiple spatial and temporal scales, highlighting MORE's potential for applications where accurate representation of physical interactions is critical, such as over

https://doi.org/10.5194/essd-2025-789
Preprint. Discussion started: 31 March 2026

123 complex terrain, coastal areas, and whenever high-resolution data are required, including hydrological analysis of convective
124 storms.

125 To evaluate the performance of the MORE reanalysis, validation is undertaken against three independent gridded observational
126 datasets (one for temperature and two for precipitation), using spatially distributed performance diagnostics and statistical
127 summary metrics. This multi-year assessment examines the reanalysis's capability to represent the climatological
128 characteristics of Italy for key meteorological variables. Additionally, the fidelity of MORE in reproducing the intensity and
129 spatial structure of extreme events, such as heavy precipitation and heatwaves, is investigated.

130 Both precipitation and temperature fields are compared against ERA5-Land and CERRA to assess the added value of
131 convection-permitting; furthermore, to contextualize its performance among existing high-resolution reanalysis datasets for
132 Italy, MORE is also compared against LAMMA-HINDCAST and MERIDA-HRES datasets.

133 To demonstrate a potential multidisciplinary application of the MORE reanalysis, we present a meteo-hydrological case study
134 associated with an extreme weather event occurred in May 2023, characterized by record-breaking accumulated precipitation
135 and extensive floods, affecting the Emilia-Romagna (northern Italy) region.

136 Additionally, a climatological application of the MORE dataset is explored in this work, focusing on temperature trends and
137 on a key climate index (Tropical Nights, i.e. TN > 20 °C) providing insights into climatic patterns and shifts over time under
138 warming conditions.

139 After the Introduction, Section 2 outlines the methodology behind MORE, detailing the data used for evaluation and
140 comparison, along with the validation methods applied to rainfall and temperature. Section 3 presents the results of the
141 evaluation and comparison for precipitation and temperature. Section 4 examines the application of MORE in meteorological
142 and hydrological case studies, as well as in climate analysis, presenting and discussing the corresponding results. Finally,
143 Section 5 provides the conclusions.

144 **2 Data and Methods**

145 **2.1 Model and downscaling approach**

146 The dynamical downscaling of ERA5 is performed using the convection-permitting model MOLOCH. Originally developed
147 for research purposes at the Institute of Atmospheric Sciences and Climate (ISAC) of the Italian National Research Council
148 (CNR), MOLOCH is now employed for both operational forecasting and research activities at several national centers (Mariani
149 et al., 2015; Sacchetti et al., 2024). MOLOCH integrates fully compressible dynamical equations and includes
150 parameterizations for boundary layer turbulence, radiation, soil physics, and cloud microphysics. It is designed as a flexible,
151 state-of-the-art numerical weather prediction system that is portable and computationally efficient on parallel computing

https://doi.org/10.5194/essd-2025-789
Preprint. Discussion started: 31 March 2026


Open Access Earth System Science Data Discussions

platforms. MOLOCH operates typically with grid spacing on the order of 1–4 km, allowing for the explicit representation of deep convection without the need for parameterization (Malguzzi et al., 2006; Davolio et al., 2009). A comprehensive overview of MOLOCH, including its physical parameterizations and a range of applications, is provided by Davolio et al. (2020) and Giorgi et al. (2023).

For the dynamical downscaling ERA5 data are used as initial and lateral boundary conditions (at hourly frequency) for MOLOCH simulations at 1.7 km resolution over the Italian territory (domain shown in Figure 1). The reanalysis period (1990–present) is covered by daily model runs. Each 30-h MOLOCH simulation is initialized at 18:00 UTC using ERA5 atmospheric fields, while soil temperature, soil moisture, and snow depth are carried over from the previous day's simulation to ensure physical consistency. To construct the MORE dataset, the first six hours of each daily simulation are treated as spin-up time

https://doi.org/10.5194/essd-2025-789
Preprint. Discussion started: 31 March 2026

and thus discarded, while the remaining 24 hours are retained. A schematic representation of the experimental setup is provided in Figure 2. Model outputs are generated at hourly frequency.

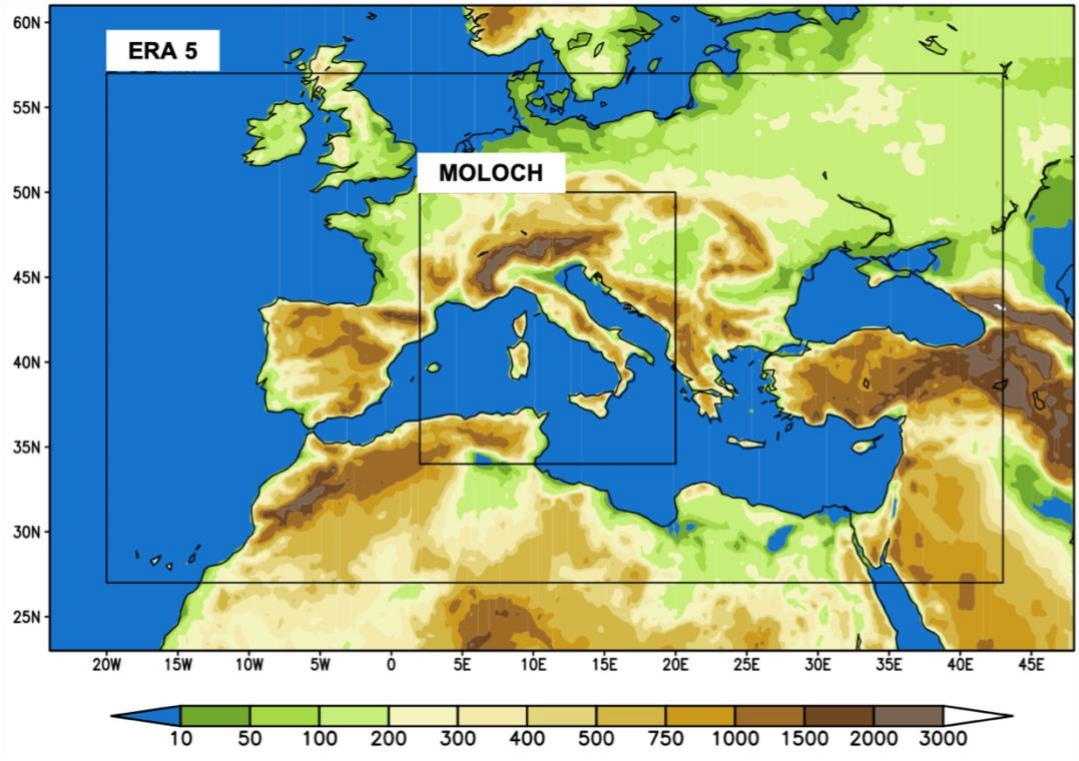

Figure 1: Domains of integration for ERA5 and MOLOCH, overlaid with topography (m). The outer black box represents the ERA5 domain used, approximately corresponding to the Med-CORDEX region, while the inner black box delineates the MOLOCH domain, covering Italy and its surrounding areas

https://doi.org/10.5194/essd-2025-789
Preprint. Discussion started: 31 March 2026

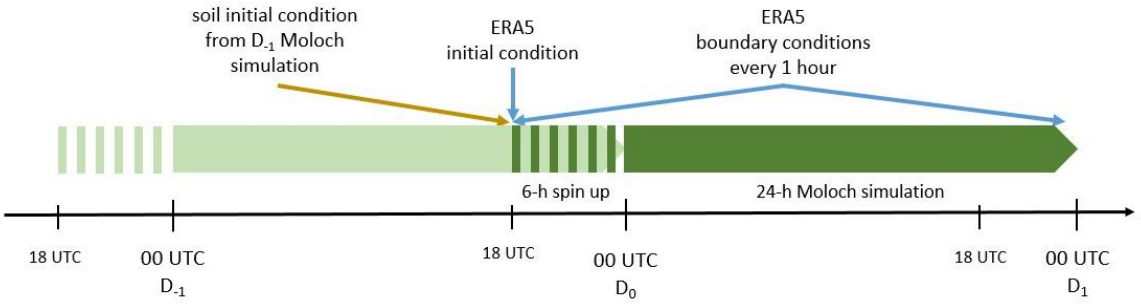

Figure 2: Schematic representation of the modeling setup for generating a single day of MOLOCH downscaling.

2.2 Data sources for evaluation and comparison

Validation of MORE reanalysis for multiple variables, including precipitation and temperature, is performed using three independent gridded observational datasets: GRIPHO and ARCIS for precipitation and UniMi/ISAC-CNR for temperature.

GRIPHO (GRidded Italian Precipitation Hourly Observations, Fantini, 2019) is a gridded precipitation dataset covering Italy at a spatial resolution of approximately 3 km. It is derived from quality-controlled rain-gauge measurements and spans the period 2001–2016. GRIPHO has been widely used in previous studies (Ban et al., 2021; Caillaud et al., 2021; Coppola et al., 2021; Stocchi et al., 2022; Reder et al., 2022; Capecchi et al., 2023) to validate numerical precipitation estimates and constitutes the only available high-resolution gridded hourly precipitation dataset for this region, thus providing a unique reference for evaluation.

ARCIS (Climatological Archive for Central-Northern Italy; Pavan et al., 2019) is a high-resolution (5×5 km) daily gridded precipitation dataset that integrates approximately 1000 quality-controlled and homogenized rain gauge records from various Italian institutions, including Hydrological Services, Agro-Meteorological Services, and Regional/Local Meteorological Agencies. It spans the period 1961–2024, but covers only central and northern Italy.

To complement the precipitation analysis, the E-OBS dataset (Cornes et al., 2018) is also employed to assess the spatial distribution of daily precipitation over the whole Italian domain for the 1990–2020 period. Due to its coarse effective resolution and known limitations in capturing fine-scale variability (Bandhauer et al., 2022), E-OBS is used only for qualitative comparisons, while quantitative analyses rely exclusively on ARCIS.

UniMi/ISAC-CNR is based on daily station data of maximum and minimum temperature, offering high-quality and homogenized observational records, which can be interpolated onto every spatial grid, given its coordinates and the elevation of each grid point. The interpolation method follows the anomaly-based approach proposed by Mitchell and Jones (2005): it reconstructs monthly fields by combining climatological normals (long-term averages for a specified reference period) with anomalies (deviations from these averages). The specific implementation adheres to the methodology described by Brunetti et

https://doi.org/10.5194/essd-2025-789
Preprint. Discussion started: 31 March 2026

al. (2012), as applied in Cavalleri et al. (2024a). Climatological fields are constructed using data from approximately 1500 stations. These values are interpolated via locally weighted linear regression, incorporating elevation and spatial relationships, such as horizontal and vertical distances, slope gradient, aspect, and proximity to the sea, between grid cells and surrounding stations (Brunetti et al., 2014). Anomaly fields are then interpolated on the same nodes using a weighting scheme that combines radial and vertical weighting functions with an angular component taking into account the heterogeneity in spatial distribution of stations around each grid point (González-Hidalgo et al., 2011). For this part of the analysis, we used the stations from Brunetti et al. (2006), along with the station networks from the different Italian regional agencies, with records ranging from about 400 in the first half of the examined period to more than 2500 at the end of this period.

Superimposing climate normal and anomalies components allowed us to provide monthly temperature values for each given grid point. Then, we used the methodology of Di Luzio et al. (2008) to obtain the daily values. Specifically, stations' daily data were converted into relative contributions to the total monthly amounts and spatially interpolated on the same nodes as the monthly data, using these latter as constraints to convert the interpolated relative contributions back into absolute daily amounts.

In this study, MORE has been evaluated against both high-resolution observational datasets and benchmark reanalysis products, focusing on periods with available and reliable observational records. The validation framework is also designed to align with standard climatological reference periods commonly adopted in the literature, allowing for a robust and consistent comparison with previous studies.

Validation is carried out at both daily and hourly temporal scales; accordingly, datasets lacking sub-daily resolution are excluded from hourly-scale analyses. For instance, CERRA, which provides 3-hourly data, is not included in the hourly-scale comparison.

For precipitation, the validation period extends from 01 January 2001, to 31 December 2016, using GRIPHO data, and from 01 January 1991, to 31 December 2020, using ARCIS data.

For temperature, the validation covers the period from 01 January 1991 to 31 December 2020 in order to both evaluate the performance of the MORE dataset and facilitate a direct comparison with previous analysis (Cavalleri et al. 2024a) in which temperature fields from other reanalysis products were validated against the same observational fields (UniMi/ISAC-CNR) and over the same time span. For this reason, the performance maps of other reanalysis products are not reported directly in this work, but only in some cases for the purpose of comparing with MORE. All the datasets used in this analysis are summarized in Table 1 along with their respective time periods, data sources, and spatial resolutions.

https://doi.org/10.5194/essd-2025-789
Preprint. Discussion started: 31 March 2026

Open Access Earth System Science Data Discussions

Dataset	Type	Variables used for validation	Spatial resolution	Temporal resolution	Temporal coverage	Source	Reference
E-OBS	Gridded observations precipitation (Europe)	Precipitation,	~0.1° (~10 km)	Daily	1950–present	ECA & D	*Cornes et al., 2018*
ARCIS	Gridded observations (Italy, North)	Precipitation	5 km	Daily	1961–present	ISPRA	*Pavan et al., 2021*
GRIPHO	Gridded observations (Italy)	Precipitation	3 km	Hourly	2001–2016	ICTP-ESP	*Fantini, 2019*
UniMi-ISAC	Stations	Temperature	Interpolated onto every spatial grid	daily	1920-present	UniMi-ISAC	*Brunetti et al. 2014, Cavalleri et al., 2024a*
ERA5-Land	Reanalysis (global)	Precipitation, Temperature,	~9 km	Hourly	1950–present	ECMWF / Copernicus	*Muñoz-Sabater et al., 2021*
CERRA	Regional reanalysis (Europe)	Precipitation, Temperature,	5.5 km	sub-daily	1984–2021	ECMWF / Copernicus	*Ridal et al., 2024*
LAMMA-HINDCAST	Regional reanalysis (Italy)	Precipitation,	~2.5 km	Hourly	1979–present	LAMMA	*Capecchi et al., 2023*
MERIDA-HRES	Regional reanalysis (Italy)	Precipitation, Temperature	~4 km	Hourly	1986–2022	RSE	*Bonanno et al., 2019; Viterbo et al., 2024*

Table 1: Precipitation datasets used in this study, including their time periods, data sources, and spatial resolutions

https://doi.org/10.5194/essd-2025-789
Preprint. Discussion started: 31 March 2026

238 **2.3 Validation Methods**

239

240 **2.3.1 Precipitation**

241

242 For the precipitation, our analysis focuses on a set of statistical metrics detailed in Table 2, including seasonal mean daily
243 precipitation, seasonal wet-day/hour intensity and frequency, and extreme precipitation indexes, defined as the 99th and 99.9th
244 percentiles of all daily and hourly precipitation occurrences, respectively. Additionally, model performance is assessed through
245 the probability distribution of precipitation intensities, relative bias, spatial variability, and correlation.
246 Metrics are computed for each season: summer (June–July–August, JJA), winter (December–January–February, DJF), spring
247 (March–April–May, MAM), and autumn (September–October–November, SON). To preserve the highest level of detail, both
248 model and observational datasets are maintained on their original grids: given that different remapping procedures can
249 introduce uncertainties and degrade data quality (Diaconescu et al., 2015), we minimize data manipulation whenever possible.
250 On the contrary, for metrics requiring direct grid-point comparison, such as relative bias, spatial correlation, and spatial
251 variability, model data are remapped onto the observational grids used for comparison to ensure consistency in the analysis.
252 An important aspect when comparing model outputs with gridded observational datasets derived from rain gauges is the need
253 to account for their known limitations. In mountainous areas, sparse gauge coverage leads to systematic underestimation.
254 Additional biases arise from wind-induced undercatch, wetting, and evaporation losses (Sevruk, 1985; Frei et al., 2003).
255 Interpolation techniques used in gridded products may further smooth extremes and misrepresent precipitation patterns,
256 especially at high elevations where gauges are typically located in valleys (Isotta et al., 2014). Recent studies show that high-
257 resolution models may outperform observational datasets in complex terrain (Lundquist et al., 2020). Considering that rain
258 gauge undercatch can vary between 4% and 50%, we adopt a precipitation bias range of −5% to +25% in our discussion as a
259 reasonable reference for observational uncertainty. This interval reflects an estimated mean undercatch of up to 20% (Frei et
260 al., 2003; Kotlarski et al., 2014).
261 To quantitatively assess the spatial consistency and systematic biases of the MORE reanalysis dataset, we employ a set of
262 statistical metrics commonly used in meteorological and climatological validation studies (e.g., Ban et al., 2021; Pichelli et al.,
263 2021). Specifically, we compute the Relative Bias, Spatial Correlation, and Spatial Variability (Table 2) between model outputs
264 and reference observations. Spatial Correlation is defined as the Pearson correlation coefficient (Wilks, 2011) of seasonal mean
265 values between model and observed fields across all grid points, providing a measure of the linear association between modeled
266 and observed spatial patterns. Spatial Variability is defined as the ratio of the spatial standard deviation of the temporally
267 averaged model field to that of the corresponding observed field, quantifying their relative amplitude.
268 Both metrics are summarized using a Taylor diagram (Taylor, 2001), which provides an integrated assessment of model–
269 observation agreement in terms of spatial structure and variability (Ban et al., 2021; Stocchi et al., 2022).
270 In addition, to provide a comprehensive, multi-dimensional assessment of reanalysis performance for selected precipitation
271 thresholds, we employ performance diagrams (Roebber, 2009). This graphical tool combines four key categorical verification

https://doi.org/10.5194/essd-2025-789
Preprint. Discussion started: 31 March 2026

metrics derived from a contingency table: the probability of detection (POD), the success ratio (SR), the frequency bias, and the critical success index (CSI) (Table 2) (Wilks, 2011). For our analysis, contingency tables are computed at each grid point and over the full study period. POD measures the fraction of observed events correctly detected (model sensitivity), while SR quantifies the fraction of predicted events that actually occurred (1 – FAR), providing insight into false alarm (FAR) behavior, bias quantifies systematic over, or under-prediction, and CSI provides a balanced measure of overall skill

Performance diagrams allow these metrics to be jointly visualized in a compact form, facilitating the comparison of model skill across precipitation thresholds and enabling a clear evaluation of strengths and weaknesses. Consequently, they are increasingly adopted in regional climate validation studies (e.g., Weisman et al., 2008; Schwartz et al., 2010)

Metrics	Definition	Unit
Mean	Mean daily precipitation	mm/day
Frequency	Wet day (hour)[a] frequency fraction of wet days (hours) per season	[0-1]
Intensity	Wet day (hour) intensity	mm/day (mm/hour)
Heavy Precipitation[b] (p99, p99.9)	99th (99.9th) daily (hourly) precipitation percentile	mm/day (mm/hour)
Probability Density Function (PDF)	Normalized frequency of precipitation events within a certain bin	[0-1]
Relative Bias	$\frac{(\bar{M}-\bar{O})}{\bar{O}} * 100$ where: $\bar{M}$ = temporal average of model values (M_i) over the evaluation period $\bar{O}$= temporal average of observed values (O_i) over the evaluation period	%
Spatial Variability[c] (Taylor Diagram)	$\frac{\sigma_m}{\sigma_o}$ σ_m= spatial standard deviation of temporal average of model values $\bar{M}$ σ_O= spatial standard deviation of temporal average of observed values $\bar{O}$ spatial variability defined as the ratio of spatial standard deviations of the model and observed seasonal mean fields	-
Spatial Correlation[c] (Taylor Diagram)	Spatial (Pearson) correlation of seasonal spatial anomaly fields between model and observations	[-1,1]

https://doi.org/10.5194/essd-2025-789
Preprint. Discussion started: 31 March 2026

Climatological Bias (CBIAS)	$\overline{(M_{ij} - O_{ij})}$ Where: $\bar{M}$ = climatological average of model values $\bar{O}$ = climatological average of observational values $\overline{M_{ij}}$= climatological average of model values at grid point (i,j) $\overline{O_{ij}}$= climatological average of observational values at grid point (ij) The difference between model and observational climatologies	°C
Mean Absolute Error (MAE)	$\frac{1}{N_{ij}} \sum_{i=1}^{n_x} \sum_{j=1}^{n_y} \lvert \overline{M_{ij}} - \overline{O_{ij}} \rvert$ Where: N_{ij} =n_xxn_y is the total number of grid points M_{ij}= climatological average of model values at grid point (i,j) O_{ij}= climatological average of observational values at grid point (i,j) Field average of absolute difference between model and observation	°C
Correlation[c] in time (CORR)	Correlation coefficient in time between model and observational anomalies	-
Mean Absolute Error in time (MAEt)	$\frac{1}{N_{days}} \sum_{t=1}^{N_{days}} \lvert am_t - ao_t \rvert$ Where: N_{days} = number of days in the reference period am_t = model daily anomalies at time t ao_t = observed daily anomalies at time t Average in time of absolute daily differences between model and observation	°C
Probability of Detection (POD)	$POD = \frac{H}{H + M}$ Fraction of observed events correctly predicted (sensitivity) where: H = Hits (events correctly predicted) M = Misses (observed but not predicted) F = False alarms (predicted but not observed)	
Success Ratio (SR)	$SR = \frac{H}{H + F}$ Fraction of predicted events that actually occurred (1 – FAR)	
False Alarm Ratio (FAR)	$FAR = \frac{F}{H + F}$ Fraction of predicted events that did not occur	

https://doi.org/10.5194/essd-2025-789
Preprint. Discussion started: 31 March 2026

Frequency Bias (Bias)	$FBI = \frac{H + M}{H + F}$ Ratio of forecast to observed events (>1: overprediction, <1: underprediction)	
Critical Success Index (CSI)	$CSI = \frac{H}{H + M + F}$ Overall measure of forecast skill combining hits, misses, and false alarms	

Table 2. ***Statistical metrics used for the validation of the precipitation and temperature variable in the MORE dataset.***
[a]A wet day (hour) is a day (hour) with precipitation ≥ 1 mm (≥ 0.1 mm)
[b]Percentiles are calculated using all events (wet and dry) following Schär et al. (Ban et al., 2021)
(Ban et al., 2021)
[c] Correlations have been computed with Climate Data Operators (CDO; Schulzweida, 2023)

2.3.2 Temperature

To evaluate the consistency of the MORE t2m fields, a different approach is required compared to precipitation. While numerous high-resolution datasets exist for precipitation, particularly over the Alpine region, few analogous products are available for temperature in Italy. In particular, the observational t2m dataset UniMi/ISAC-CNR was selected (Cavalleri et al, 2024a) because it is specifically designed to enable accurate comparisons even in areas with complex orography (see section 2.2 for details). Indeed, t2m decreases with elevation at a lapse rate of roughly -6.5°C per kilometer (Rolland, 2003). This implies a high spatial variability of t2m fields in complex terrain. While t2m observations are taken at specific elevations, reanalysis represents a smoothed version of the real orography, due to discretization and numerical stability issues (Wang et al., 2022). Although this effect is reduced for high-resolution reanalyses, the difference between the elevation for observations and reanalysis grid-points may result in a temperature bias. Previous studies (e.g., Luo et al., 2019; Cavalleri et al., 2024a) stress that different elevation can be the primary cause of discrepancies. Aware of this issue, we opt for reconstructing t2m observational fields onto the same longitude, latitude and elevation coordinates of the MORE grid nodes, starting from the UniMi/ISAC-CNR stations' observations. This approach, already proposed by Cavalleri et al. (2024a), allows us to overcome biases due to the static elevation difference with observations, and to evaluate the dynamical ability of MORE to reproduce t2m fields at its native high-resolution, which is the one required to capture complex small-scale phenomena such as thermal inversions and urban heat island effects.

This approach allows the validation of different reanalysis products using the same observations, with performances assessed at each dataset's native resolution. The goal is not to rank them, but to evaluate how errors vary with model resolution and to test whether MORE, by resolving finer-scale features, can maintain the accuracy of near-surface temperature fields while adding local detail.

https://doi.org/10.5194/essd-2025-789
Preprint. Discussion started: 31 March 2026

Three different quantities are considered: the daily average t2m, the minimum, and the maximum daily values. For MORE, which provides hourly values, the minimum and maximum hourly values are considered as daily minimum and maximum, while the 24-hour average is calculated to get the daily average. In contrast, the observational average is computed from the minima and maxima provided by UniMi/ISAC-CNR. The impact of these choices is marginal and is discussed by Cavalleri et al. (2024a).

Given the UniMi/ISAC-CNR observational fields at MORE resolution and elevations, we first compute climatologies for the 1991–2020 period for both datasets, aggregated at seasonal and annual scales. Differences between reanalyses and observations are then assessed by subtracting the observational climatologies from the corresponding reanalysis climatologies at each grid point (Climatological Bias, CBIAS, Table 2). Alongside with the bias maps, we calculate the average bias across Italy to assess general seasonal tendencies, and the spatial mean of the absolute value of the differences (MAE, Table 2) to evaluate the overall agreement.

In addition to climatological means, we also assess day-to-day variability by analyzing daily temperature anomalies, computed by subtracting to each dataset (observations and MORE) its own daily climatological values over the 1991–2020 reference period. To quantify agreement of anomalies over time, we calculate, for each grid point: i) the temporal mean absolute error (MAEt, Table 2), defined as the mean of the absolute values of the daily differences between reanalysis and observational anomalies over the reference period; ii) the correlation coefficient (CORR, Table 2) between the time series of reanalysis and observational anomalies. Spatial averages of both metrics are subsequently computed, following the same approach used for evaluating the mean CBIAS. Finally, the t2m trends are assessed by comparing the annual average t2m anomalies of MORE with the corresponding observational values.

The same validation methodologies were applied in Cavalleri et al. (2024a) to other reanalysis products for the same 1991–2020 period, thus enabling a comparison with MORE performances over the Italian domain. Results of temperature validation are reported in Section 3.2.

3 Evaluation and Comparison Results

3.1 Precipitation

The evaluation of MORE precipitation primarily focuses on the autumn and summer seasons. These seasons are particularly relevant as they reflect distinct synoptic conditions: widespread precipitation associated with mid-latitude cyclones in autumn, and localized, convective rainfall in summer (e.g. Grazzini et al, 2020). Nevertheless, the patterns emerging from these two seasons also provide meaningful insights into the precipitation behavior observed during spring and winter (not shown).

3.1.1 Analysis of Spatial Patterns and Systematic Biases in Daily and Hourly Precipitation

https://doi.org/10.5194/essd-2025-789
Preprint. Discussion started: 31 March 2026

Figures 3 and 4 provide an overview of the spatial distribution of daily and hourly precipitation (as defined in Table 2) derived from observational datasets and the MORE reanalysis, highlighting its ability to realistically reproduce precipitation climatology. Specifically, seasonal means, precipitation intensity, wet-event frequency, and extreme precipitation, defined by the 99th percentile for daily and the 99.9th percentile for hourly precipitation, are analyzed for summer and autumn. Additional results including comparisons with other reanalyses are shown in Figures A1–A4 in Appendix A.

https://doi.org/10.5194/essd-2025-789
Preprint. Discussion started: 31 March 2026

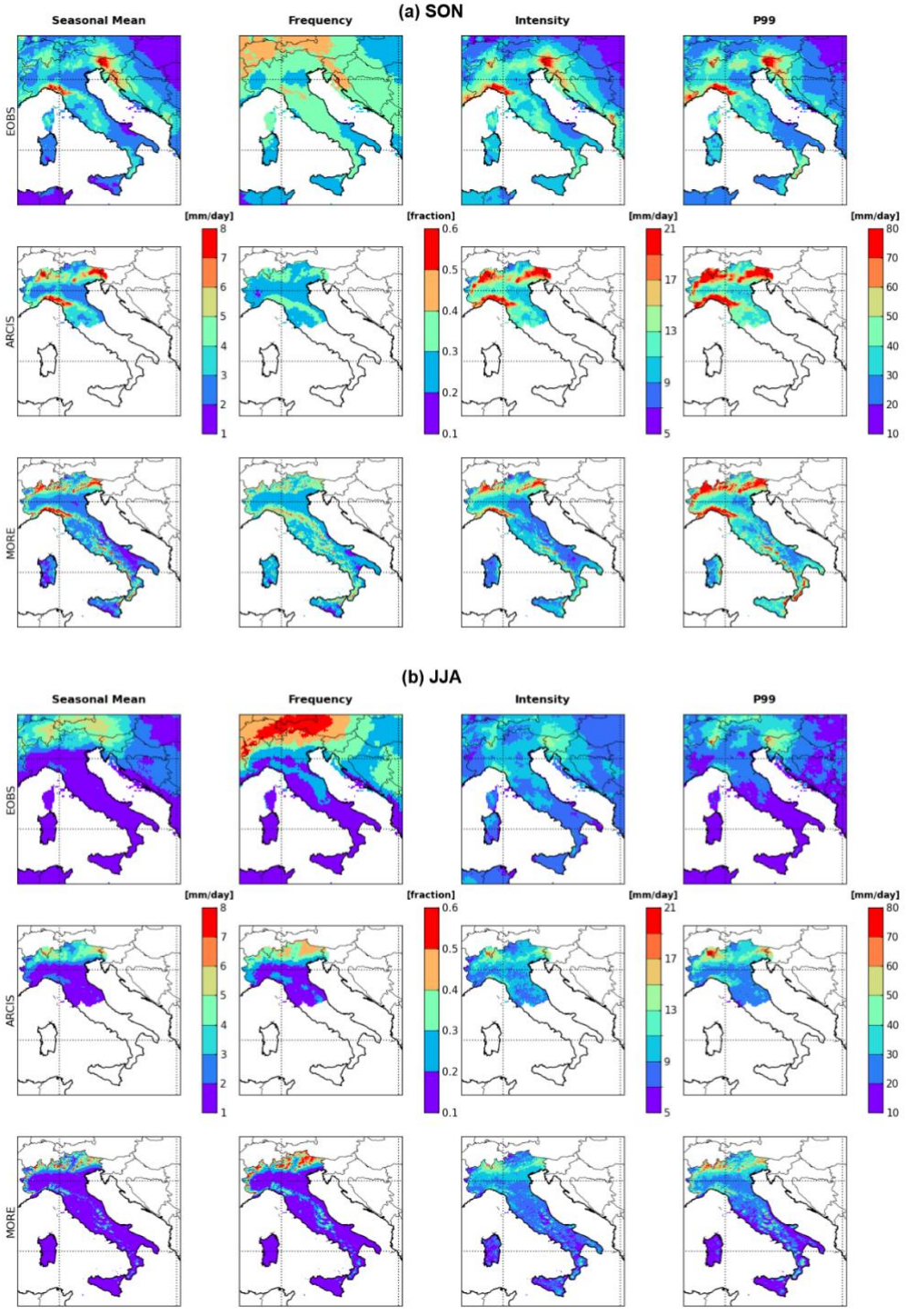

Figure 3: Seasonal means of daily precipitation indices for autumn (SON, panel a) and summer (JJA, panel b) over the period 1991–2020, including mean precipitation, precipitation frequency, precipitation intensity, and heavy precipitation (defined as the 99th percentile; Table 2). Results are shown for observational datasets (EOBS & ARCIS) and the MORE reanalysis.

https://doi.org/10.5194/essd-2025-789
Preprint. Discussion started: 31 March 2026

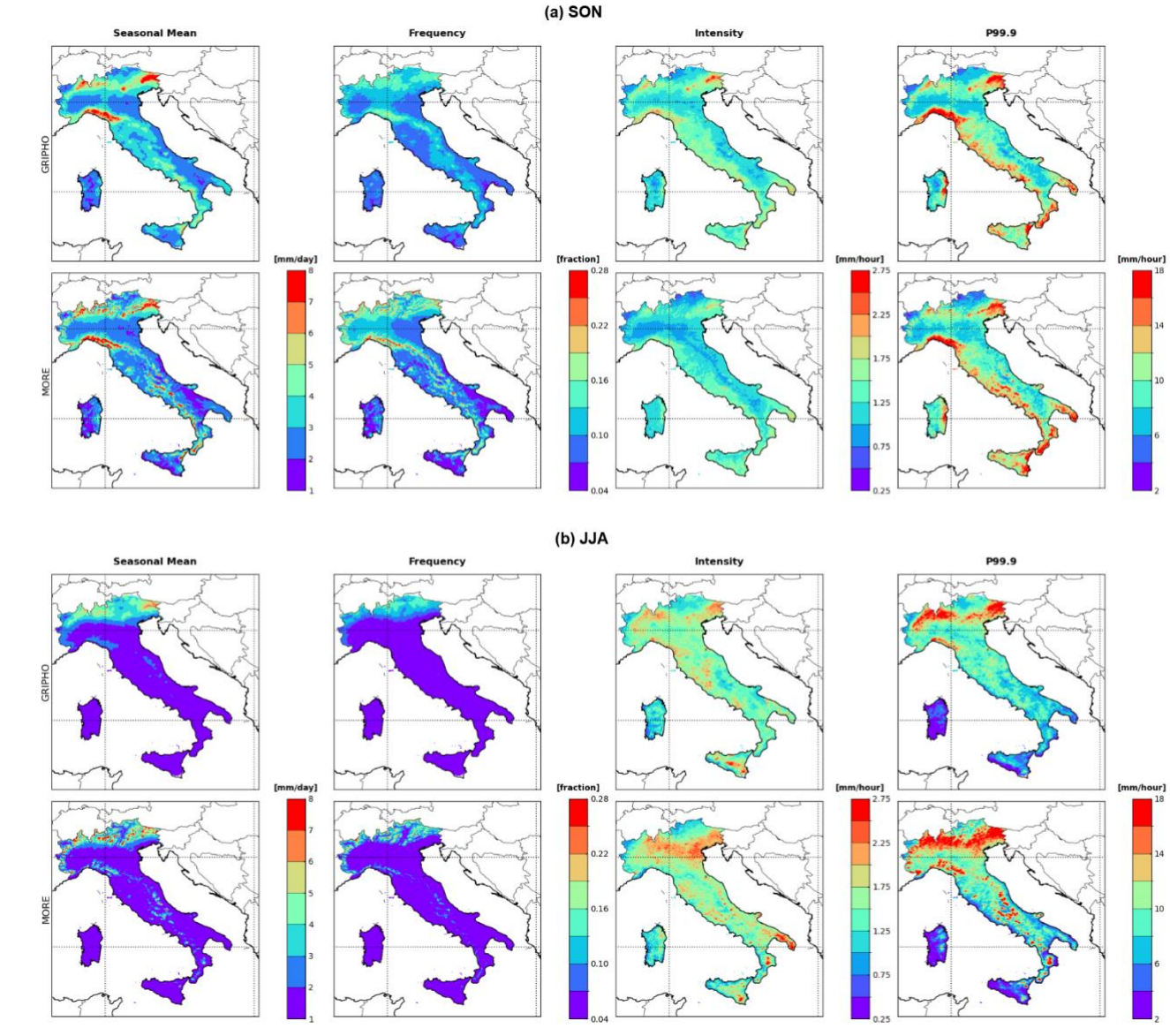

Figure 4: As in Fig. 3, but for hourly precipitation, showing precipitation frequency, intensity, and heavy precipitation indices. Seasonal means are derived from daily precipitation, consistent with Fig. 3. Observations are from the gridded hourly precipitation dataset over Italy (GRIPHO; Fantini et al., 2019) for the period 2001–2016. Heavy hourly precipitation is defined as the 99.9th percentile of all events.

In Figures 3 and 4, the high resolution of MORE allows a highly detailed depiction of orographic influences, with enhanced precipitation over elevated topography in both summer and autumn. During SON, the contrast between mountains and adjacent lowlands is reduced, reflecting the stronger influence of Mediterranean cyclonic activity and Alpine lee-side dynamics (Trigo

https://doi.org/10.5194/essd-2025-789
Preprint. Discussion started: 31 March 2026


Open Access Earth System Science Data Discussions

et al., 1999). Figure 3 shows that MORE captures the spatial patterns of mean daily precipitation, intensity, frequency, and extremes when compared to observations (E-OBS and ARCIS). Compared to other reanalyses (Figures A1–A2 in Appendix A), MORE provides a more realistic representation of localized convective events, particularly during the warm season, likely due to its explicit treatment of convection and finer spatial resolution (Ban et al., 2021; Stocchi et al., 2022). Comparable skill is observed with high-resolution regional models such as LAMMA-HINDCAST and MERIDA-HRES, while ERA5-Land and CERRA tend to overestimate wet-day frequency and underestimate precipitation intensity and extremes in summer.

Figures 4 present the same precipitation statistics as in Figures 3, but at the hourly scale (except for the seasonal mean, which is derived from daily precipitation), validated against the GRIPHO dataset, the only high-resolution gridded hourly dataset available for Italy. MORE closely reproduces the observed hourly precipitation patterns, capturing both intensity and extremes with high fidelity. Comparisons with other reanalyses are provided in Figures A3–A4 in Appendix A, where ERA5-Land overestimates wet hours and underestimates intensity, and MORE exhibits superior skill, even slightly reducing extreme precipitation overestimation compared to LAMMA-HINDCAST and MERIDA-HRES, particularly in summer (Figure A4 in Appendix A).

A more detailed discussion of precipitation biases across reanalyses is presented in Figures 5–8, which provide a comprehensive overview of the relative biases for all daily and hourly precipitation indices (as defined in Table 2) during autumn and summer. Figures 5 and 6 depict the relative biases of daily precipitation indices with respect to ARCIS, evaluated over the ARCIS domain, while Figures 7 and 8 illustrate analogous results for hourly precipitation indices, assessed over the Italian territory using GRIPHO

https://doi.org/10.5194/essd-2025-789
Preprint. Discussion started: 31 March 2026

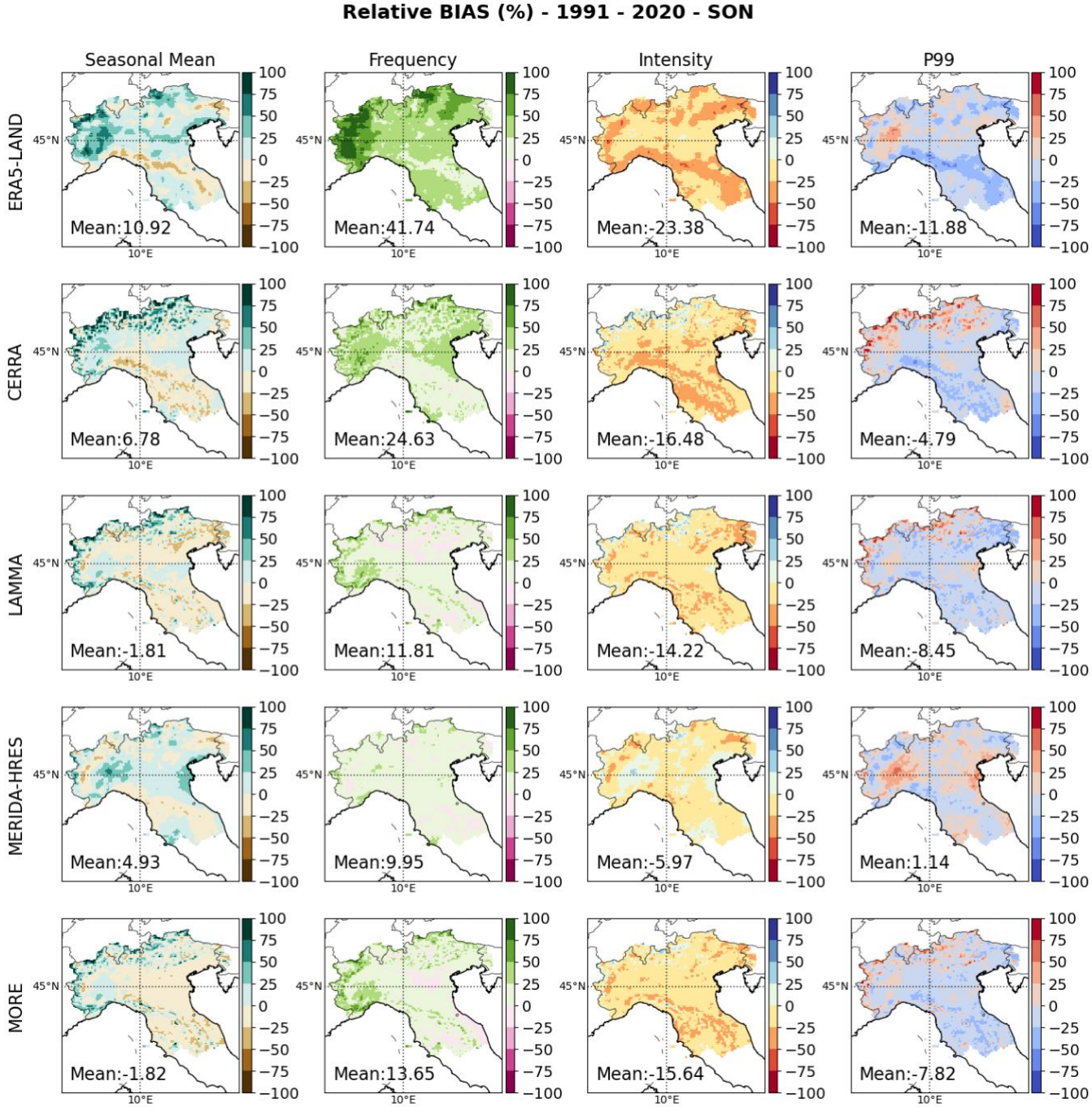

Figure 5: Relative bias (%) of daily precipitation indices in the autumn season (SON) over the period 1991–2020. Bias is calculated for each index (Table 2) with respect to ARCIS observations, over the ARCIS observation area, considering all reanalysis datasets listed in Table 1.

https://doi.org/10.5194/essd-2025-789
Preprint. Discussion started: 31 March 2026

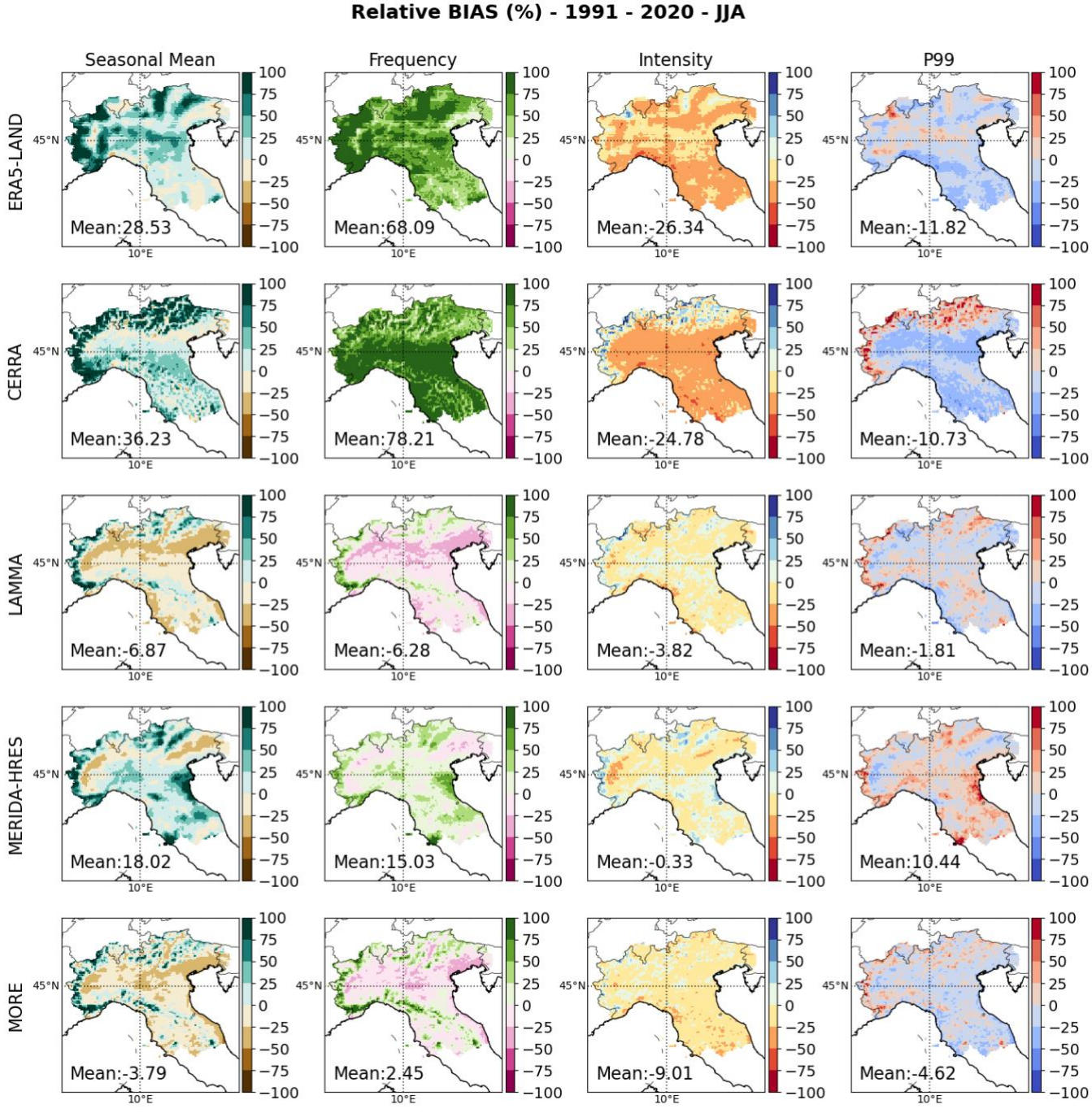

Figure 6: As Figure 5, but for the summer season (JJA)

https://doi.org/10.5194/essd-2025-789
Preprint. Discussion started: 31 March 2026

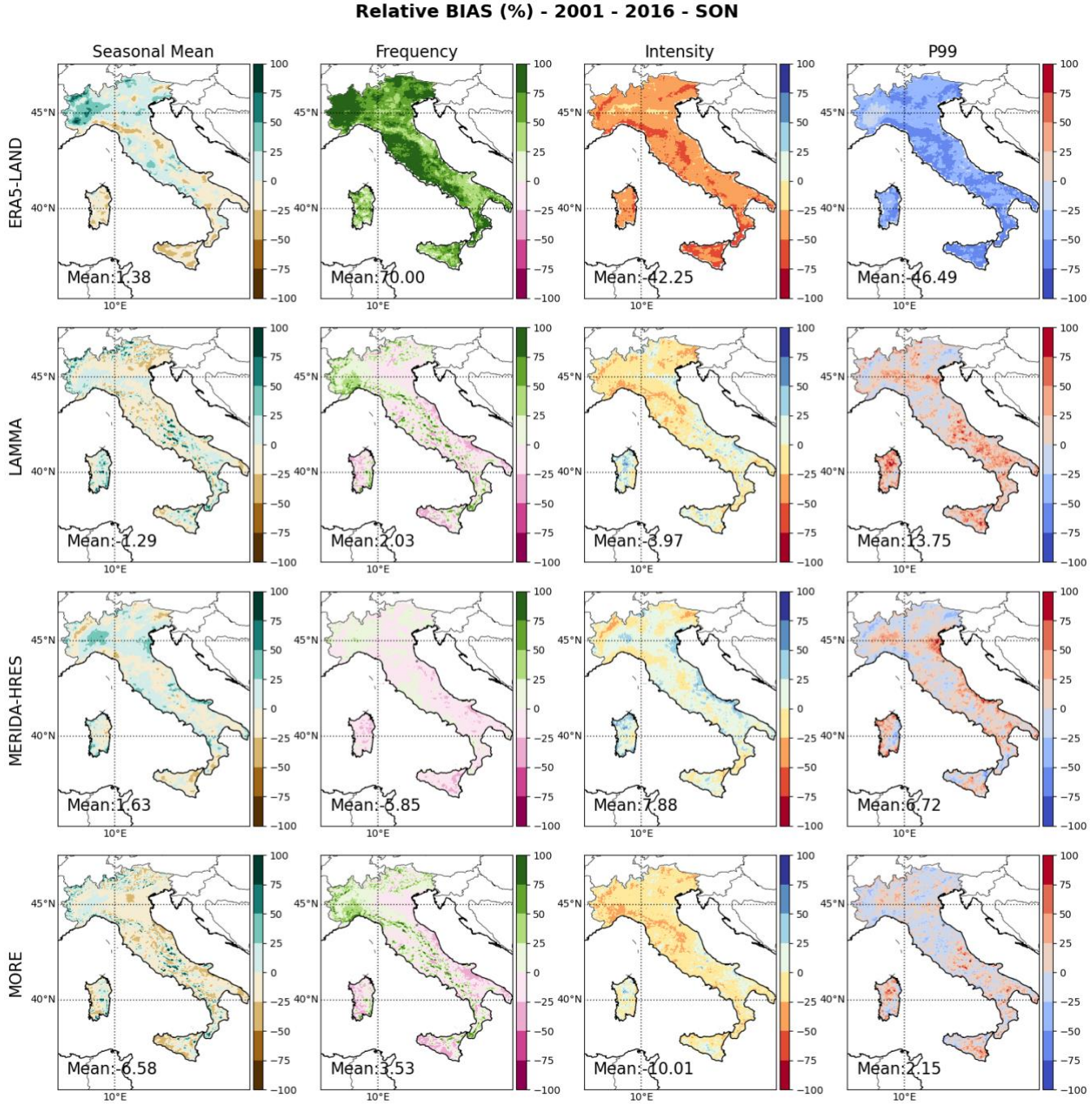

Figure 7: Relative bias (%) of hourly precipitation indices in autumn (SON). The relative bias of the seasonal mean (first column) is derived from daily precipitation, to ensure consistency with the seasonal mean relative bias shown in Fig. 5 and Fig. 6 (calculated using ARCIS). Biases are computed over Italy with respect to GRIPHO observations for the period 2001–2016, considering all hourly reanalysis datasets listed in Table 1.

https://doi.org/10.5194/essd-2025-789
Preprint. Discussion started: 31 March 2026

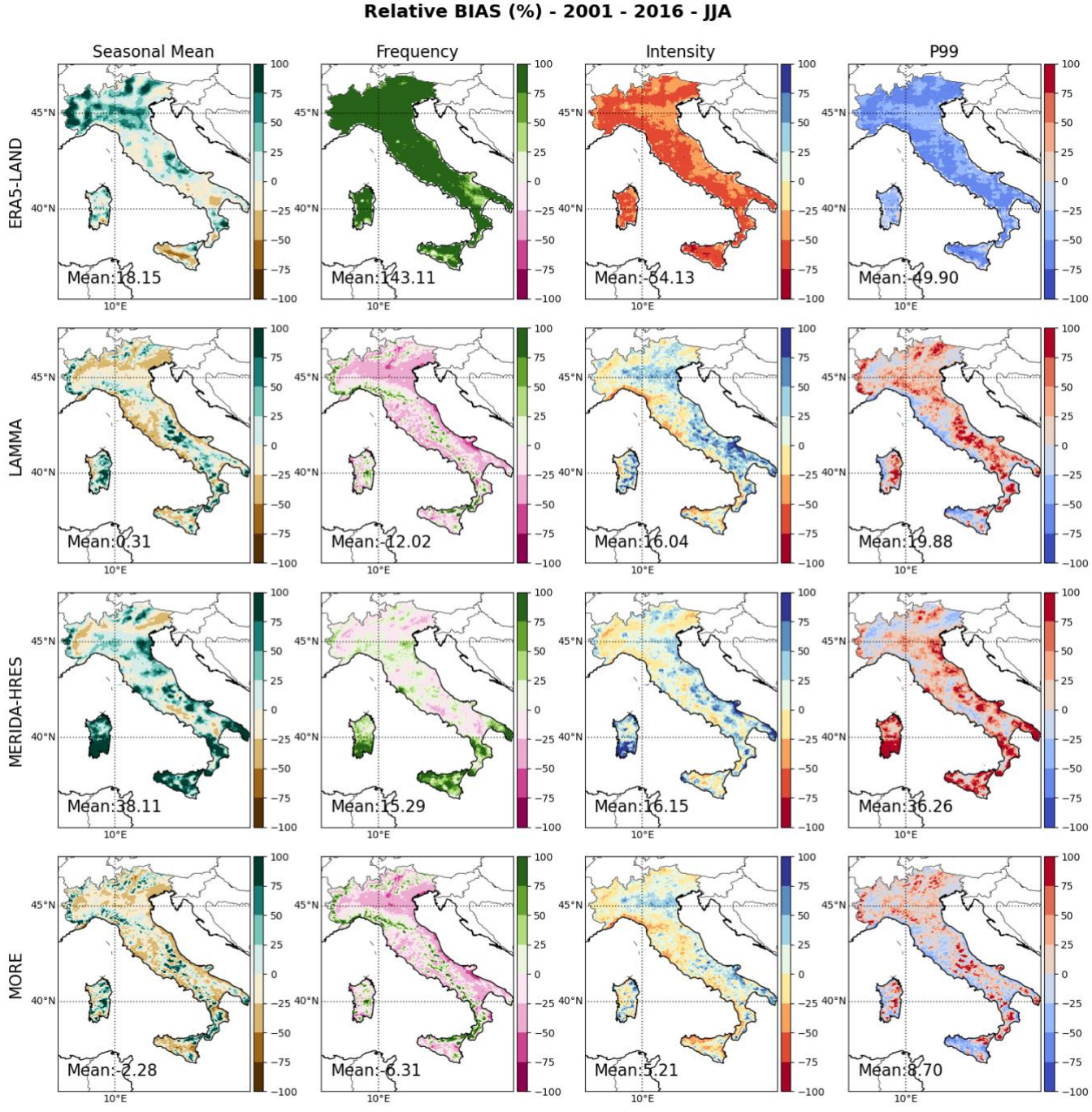

Figure 8: As Figure 7, but for the summer season (JJA)

https://doi.org/10.5194/essd-2025-789
Preprint. Discussion started: 31 March 2026


Open Access Earth System Science Data Discussions

As discussed in Section 2.3.1, for both daily and hourly metrics, a bias range of −5% to +25% is considered acceptable. The biases shown in Figures 5 and 6 highlight that relative biases in MORE are generally modest and substantially lower compared to those in ERA5-Land and CERRA, particularly during the summer season. Unlike ERA5-Land and CERRA, which tend to overestimate wet-day frequency in summer and autumn and underestimate precipitation intensity and extremes in summer, MORE provides a more accurate representation. The performance of MORE is comparable to that of other high-resolution regional reanalyses, with most biases falling within the acceptable range.

On average, ERA5-Land, CERRA, and MERIDA-HRES overestimate mean daily precipitation and wet-day frequency, especially during JJA. This overestimation is more pronounced in ERA5-Land and CERRA, while MORE and LAMMA-HINDCAST, both based on the MOLOCH model, show better agreement with observations. Conversely, all reanalyses generally underestimate precipitation intensity and extremes, particularly in JJA. An exception is MERIDA-HRES, which systematically overestimates heavy precipitation events in both seasons, with a stronger signal during JJA.

Overall, MORE demonstrates notably improved performance in terms of relative bias, mitigating the overestimation of wet-hour frequency characteristic of coarser-resolution products and more accurately reproducing daily precipitation intensity, especially in summer.

At the hourly scale (Figures 7 and 8), the behavior observed for daily metrics is further amplified: MORE shows systematically smaller biases and a robust improvement in relative bias metrics, particularly during JJA. This enhanced performance is likely linked to its higher spatial resolution, which allows for a better representation of convective processes that are more frequent and intense in summer. ERA5-Land, by contrast, consistently overestimates the frequency of wet hours while underestimating precipitation intensity across almost all seasons. As a result, the daily mean precipitation (Figures 3 and 4) may appear realistic but is in fact the product of compensating errors between frequency and intensity.

In contrast, MORE and the other high-resolution datasets better reduce wet-hour frequency and simulate more intense precipitation events (Figures 7 and 8). MORE slightly underestimates wet-hour frequency but captures both precipitation intensity and extremes (e.g., heavy precipitation) quite well, showing a clear improvement compared to LAMMA-HINDCAST. MERIDA-HRES, although generally characterized by small biases during SON (Figure 7), diverges in JJA, where it shows larger biases. Specifically, it tends to overestimate wet-hour frequency, particularly in southern Italy, and overestimates extreme precipitation, as highlighted by the 99.9th percentile (Figure 8).

Figure 9 summarizes the uncertainties of the different reanalysis datasets over the Italian domain for both daily and hourly precipitation using box plots, which display the median (black line), interquartile range (25th–75th percentiles), and 5th–95th percentiles, providing insight into both central tendency and spatial variability of the biases.

https://doi.org/10.5194/essd-2025-789
Preprint. Discussion started: 31 March 2026

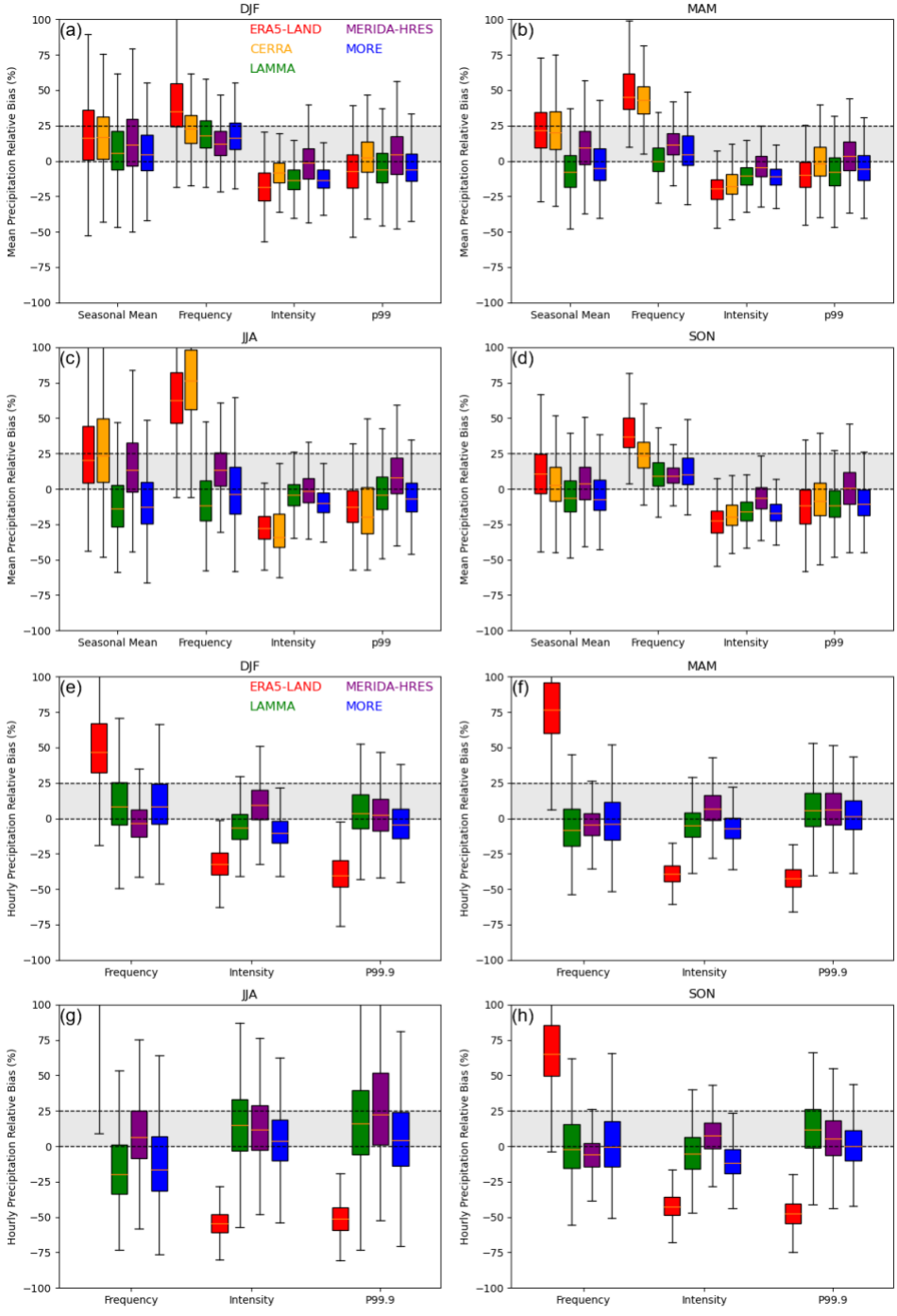

Figure 9: Box plots of reanalysis dataset biases (%) for the indices listed in Table 2, shown for daily (a–d) and hourly (e–h) precipitation across all seasons over Italy. The grey shading indicates the acceptable uncertainty range (0–25%) in the observational data, mainly due to systematic rain gauge undercatch, typically around 20%. Panels a–d show daily precipitation biases relative to ARCIS observations over the ARCIS domain (northern Italy) for the period 1991–2020, while panels e–h show hourly precipitation biases relative to GRIPHO observations across the GRIPHO domain (Italy) for the period 2001–2016

https://doi.org/10.5194/essd-2025-789
Preprint. Discussion started: 31 March 2026

Open Access Earth System Science Data Discussions

435

436 Seasonal spatial distributions of relative biases for the various precipitation indices are shown, with ARCIS (Figure 9a–d) and
437 GRIPHO (Figure 9e–h) serving as reference observational datasets for daily and hourly precipitation within their respective
438 coverage domains. Overall, MORE exhibits good agreement with observations for both daily and hourly precipitation across
439 all indices, with most mean relative bias values falling within the acceptable uncertainty range. A key finding is that high-
440 resolution datasets, especially MERIDA-HRES, consistently exhibit lower mean relative biases and narrower uncertainty
441 ranges, particularly for wet-hour frequency. This added value is evident at the daily scale (Figure 9a-d), particularly in summer,
442 and becomes even more pronounced at the hourly scale (Figure 9e-h). For instance, ERA5-Land, in summer, shows wet-hour
443 frequency biases with uncertainty intervals that may exceed 180%, while high-resolution datasets confine these uncertainties
444 to a much narrower range (approximately 80%). Among all indices, uncertainty ranges are largest for wet-hour frequency.
445

446 **3.1.2 Evaluation of Spatial Correlation and Variability of Daily and Hourly Precipitation**

447

448 To assess the ability of MORE to reproduce the spatial patterns and variability of precipitation, we utilize Taylor diagrams,
449 which integrate the spatial correlation coefficient and the ratio of spatial standard deviation (Table 2). This diagnostic is applied
450 to both daily (Figure10a-h) and hourly (Figure 11a-f) precipitation.
451

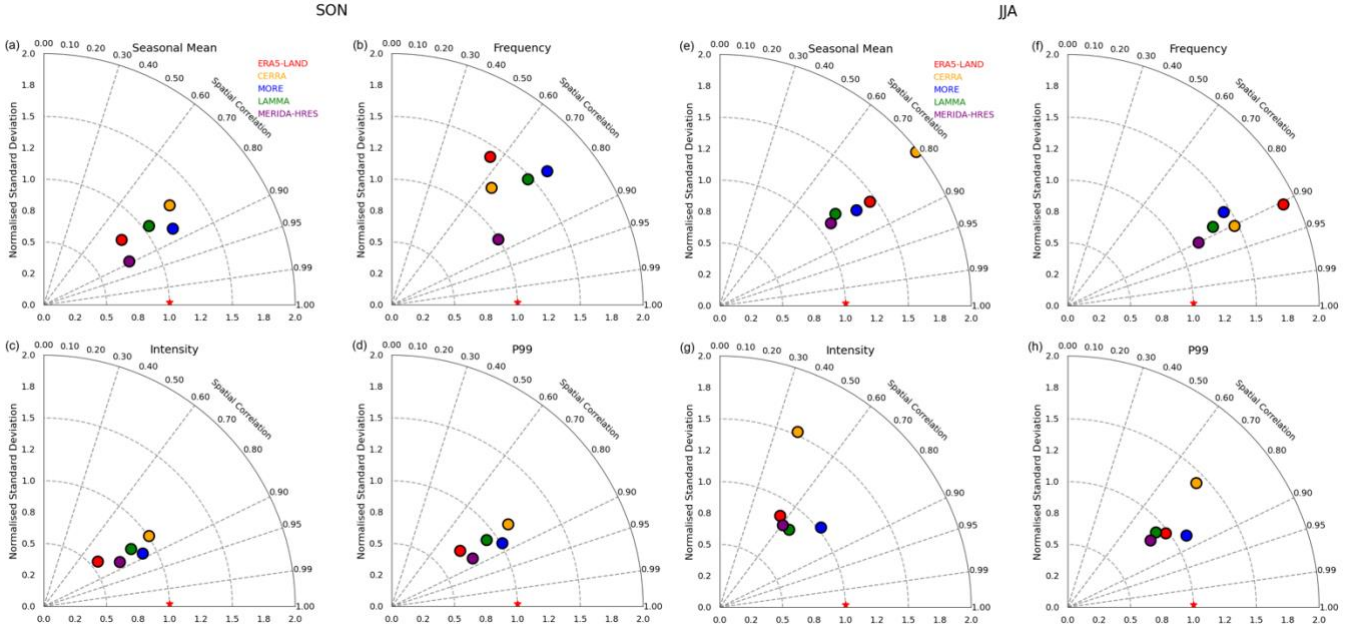

452

453 **Figure 10:Spatial Taylor diagrams showing the performance of different datasets in reproducing the spatial variability of seasonal**
454 **daily precipitation over Northern Italy for SON (a-d) and JJA (e-h). The analysis considers mean seasonal precipitation (a,e), daily**
455 **precipitation frequency (b,f), daily precipitation intensity (c,g), and extreme daily precipitation, defined as the 99th percentile (d,h).**
456 **The diagrams display spatial correlation (azimuthal angle) and the ratio of spatial standard deviations (radial distance), with each**

https://doi.org/10.5194/essd-2025-789
Preprint. Discussion started: 31 March 2026

dataset represented by a different colored symbol. ARCIS observations serve as the reference, with all statistics computed relative to ARCIS within its observational domain for the period 1991–2020.

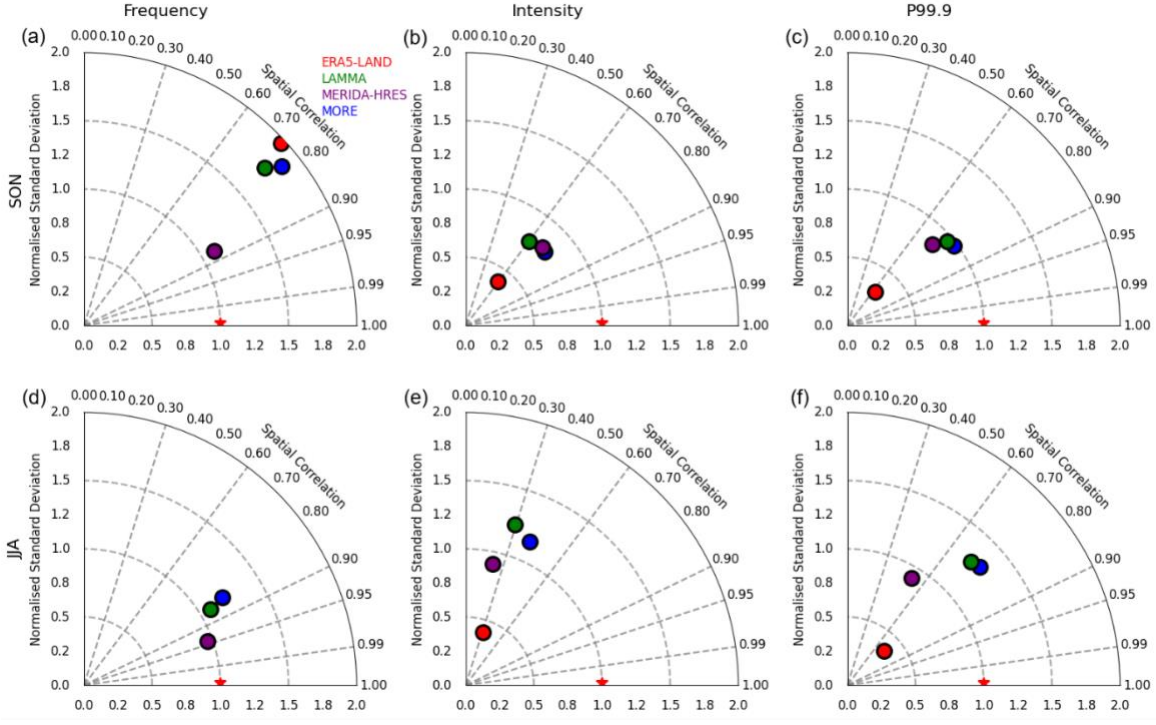

Figure 11: Spatial Taylor diagrams evaluating the performance of different datasets in reproducing the spatial variability of seasonal hourly precipitation over Italy for the SON (a-c) and JJA seasons(d-f). The analysis is presented for hourly precipitation frequency (a,d), hourly precipitation intensity (b,e), and extreme hourly precipitation, defined as the 99.9th percentile (c,f). The diagrams display the spatial correlation (azimuthal angle) and the ratio of spatial standard deviations (radial distance), with different colored symbols representing individual datasets. Observational reference is provided by the GRIPHO dataset, with all statistics computed relative to GRIPHO observations within the GRIPHO observational domain for the period 2001-2016. Note: ERA5_LAND R.std for JJA frequency is 2.78 (d), outside the diagram scale and not visible

For almost all the seasons and precipitation indices at both daily and hourly time scale, spatial correlation coefficients exceed 0.7, and spatial standard deviations are generally close to 1, highlighting the good skill of MORE in reproducing both the spatial correlation and amplitude of spatial variability. This is especially evident at the daily timescale during JJA (Figure 10a-h). This reflects a robust representation of spatial precipitation patterns in terms of mean, frequency, intensity and extremes. Similar performance is also observed for the other high-resolution datasets which outperform the coarser-resolution products in terms of both spatial correlation and variability metrics.

At the hourly scale (Figure 11a-f), on the whole Italian domain covered by GRIPHO, discrepancies in spatial variability become more pronounced, particularly between high-resolution datasets and ERA5-Land, for all indices. MORE maintains good skill in reproducing spatial correlation coefficients (0.7) and normalized spatial standard deviations for the majority of seasons and indices. However, some limitations emerge during the summer months in representing hourly precipitation

https://doi.org/10.5194/essd-2025-789
Preprint. Discussion started: 31 March 2026

intensity (Figure 11e), when MORE tends to overestimate spatial variability, a behavior also evident in the other convection-permitting datasets.

It is important to emphasize that the variability overestimation by some reanalysis datasets does not necessarily reflect poor model performance. Part of the discrepancy may stem from observational uncertainties, particularly in complex orographic areas, where the limited density of rain gauges and the interpolation methods used to produce gridded observational datasets can result in an underestimation of local precipitation maxima and spatial variability (Isotta et al., 2014). Moreover, when comparing against the GRIPHO dataset, it is crucial to consider that it is derived from a non-uniform station network, with a significantly higher density of rain gauges in the northern part of Italy than in the central and southern regions (Fantini, 2019). This spatial inhomogeneity in observational coverage can influence the accuracy of the reference data, particularly in regions with sparser stations.

Overall, MORE demonstrates a performance comparable to that of the other convection-permitting datasets, yielding a more realistic representation of precipitation patterns and variability than coarser-resolution reanalysis products.

3.1.3 Assessing the Skill in Representing Precipitation Using Performance Diagrams

To evaluate the ability of reanalyses to reproduce observed precipitation characteristics, we employ Performance Diagrams (Roebber, 2009), a compact tool that simultaneously displays multiple verification metrics for binary (yes/no) precipitation events, as detailed in Section 2.3.1 and summarized in Table 2. A precipitation event is defined as the exceedance of a specified threshold over a given time interval. Thresholds are applied at both daily and annual timescales, enabling the evaluation of dataset performance across a range of precipitation intensities and temporal aggregations (Capecchi et al., 2023). Annual thresholds are set at approximately 700, 900, 1100, 1400, 1600, and 1800 mm/year, corresponding to the 25th, 50th, 75th, 90th, 95th, and 98th percentiles of the observed mean annual precipitation distribution derived from the GRIPHO dataset. Daily thresholds, on the other hand, are defined at 1, 2, 5, 10, 20, and 50 mm/day.

The Performance Diagrams in Figure 12 present the evaluation against the GRIPHO dataset for daily precipitation, providing a detailed assessment across multiple thresholds.

https://doi.org/10.5194/essd-2025-789
Preprint. Discussion started: 31 March 2026

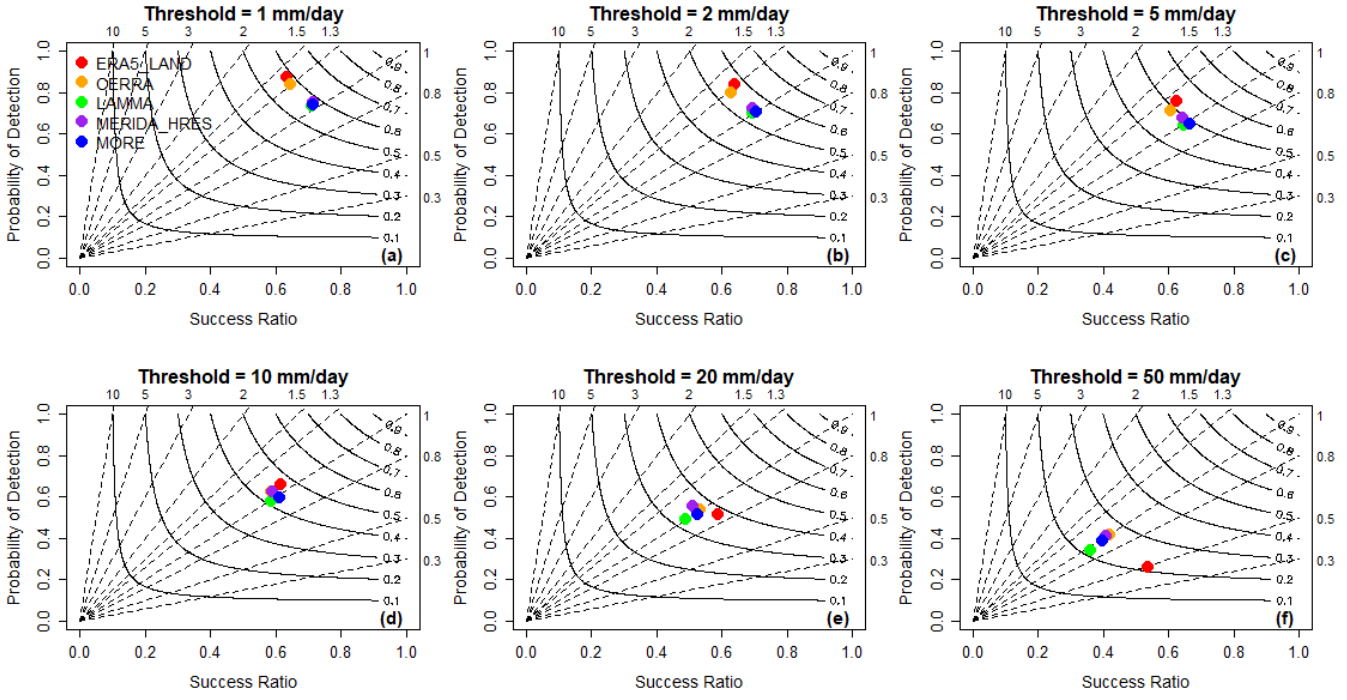

Figure 12:Performance diagram for daily precipitation over the period 2001–2016, comparing reanalysis datasets against GRIPHO observations within the GRIPHO domain. The x-axis shows the Success Ratio (SR), and the y-axis the Probability of Detection (POD). Curved isopleths represent the Critical Success Index (CSI), while dashed diagonal lines indicate bias values

MORE generally exhibits good skill, with POD and SR values exceeding 0.5 for most thresholds, except at the highest threshold of 50 mm/day. Consistent with the results shown in Figures 5-8 and Figs. A1–A4, and as highlighted in earlier studies (Kendon et al., 2012; Ban et al., 2021), the parameterized convection used in regional climate model simulations and in reanalyses such as ERA5-Land and CERRA tend to overproduce widespread light rainfall and underestimate daily maxima. This behavior is evident for the lower thresholds (1, 2, and 5 mm/day) (Figure 12), where ERA5-Land and CERRA points lie above the 1:1 bias line (bias ≈ 1.3), despite relatively high POD values (>0.75) and acceptable SR. In contrast, the convection-permitting reanalyses (MORE, MERIDA-HRES, and LAMMA) show comparable performance, outperforming ERA5-Land and CERRA, although both POD and SR decrease progressively at higher thresholds.

The decline in SR at the highest thresholds highlights the increasing challenge of capturing rare and spatially localized precipitation extremes, often confined to orographically complex regions. It is important to note that the construction of performance diagrams requires a strict one-to-one spatial correspondence between simulated and observed events. At convection-permitting resolutions, this approach can lead to an excessive penalization of the models (double penalty; Rossa et al., 2008), as simulated events that are slightly displaced relative to observations are classified as both misses and false alarms, despite representing physically consistent precipitation.

https://doi.org/10.5194/essd-2025-789
Preprint. Discussion started: 31 March 2026

Another aspect that emerges from our performance analysis is that skill scores calculated against GRIPHO are systematically higher than those obtained with ARCIS (see Appendix A, Fig. A5). This discrepancy likely reflects the coarser spatial resolution of ARCIS (5 km) and the smoothing introduced by its interpolation methods, which attenuate localized intense rainfall events (as discussed in Section 2.3), while GRIPHO (3 km) better preserves such extremes, providing potentially a more robust verification dataset. In addition, the ARCIS dataset is partly based on historical time series from manual networks, where daily precipitation was measured in the early morning and assigned to the observation day, although it referred to the preceding 24-hour period. Despite subsequent corrections through automatic weather stations and homogenization procedures, residual uncertainties in event timing of about ±1 day may persist (Pavan et al., 2018). For this reason, ARCIS-based results are reported in Appendix A (Fig. A5). These findings emphasize the importance of carefully considering the characteristics of the observational dataset employed for model evaluation, particularly in relation to the analyzed variable and temporal scale.
Finally, the annual-scale performance diagrams, complementing the daily analysis, are also provided in Appendix A (Figs. A6–A7). These confirm the general conclusions: MORE outperforms ERA5-LAND and CERRA across most thresholds and shows comparable skill to other high-resolution convection-permitting datasets, although with slightly better performance than LAMMA.

3.1.4 PDF analysis for Assessing the Representation of Precipitation Distributions and Extremes

To evaluate how well MORE reanalysis reproduces not only the mean but also the full distribution and variability of observed precipitation, including rare and extreme events (Wilks, 2011), we computed the Probability Density Functions (PDFs) of precipitation at both daily and hourly scales. This approach provides a comprehensive view of model performance beyond simple averages, allowing the assessment of how well the frequency and intensity of precipitation events are captured across different time resolutions. Such analysis is particularly relevant for hydrological applications and impact-oriented studies, where both light and extreme precipitation events play a crucial role (Maraun et al., 2010; Kendon et al., 2012).
Figures 13 and 14 show the Probability Density Functions (PDFs) of daily and hourly precipitation, respectively, evaluated for the different reanalysis datasets against observations.
The highest observed daily precipitation values, located in the tails of the PDFs, reach approximately 600 mm/day in NI (Figures 13a,b). For hourly precipitation, the maximum observed amounts reach approximately 200 mm in northern and southern Italy, and about 150 mm in central Italy (Figures 14a,b,c).

https://doi.org/10.5194/essd-2025-789
Preprint. Discussion started: 31 March 2026

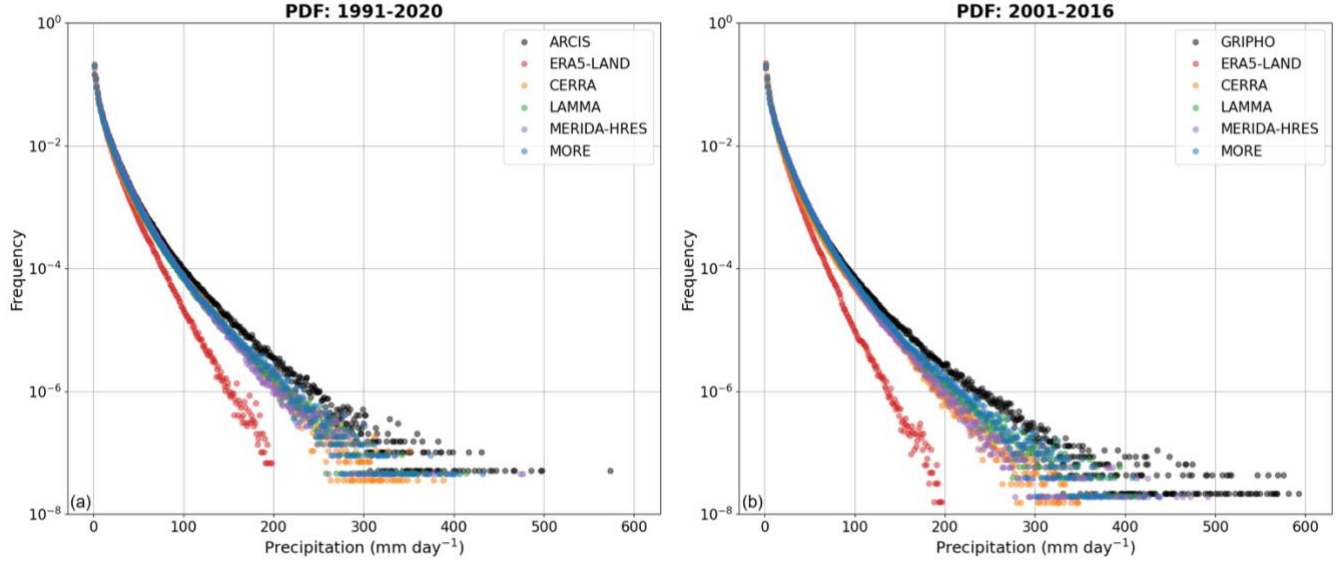

Figure 13:Probability Density Function (PDF) of daily precipitation, evaluated for different reanalysis datasets against: a) ARCIS observations within the ARCIS observational domain (Northern Italy) for the period over the 1991–2020; b) GRIPHO observations within the same domain but for the period 2001-2016. All datasets have been interpolated onto the corresponding observational grid resolution (ARCIS: 5 km; GRIPHO: 3 km). The horizontal axis shows precipitation intensity (mm/day), while the vertical axis indicates the relative frequency of events within each intensity bin. This figure illustrates the ability of each dataset to capture the observed distribution of daily precipitation, from light to extreme events.

https://doi.org/10.5194/essd-2025-789
Preprint. Discussion started: 31 March 2026

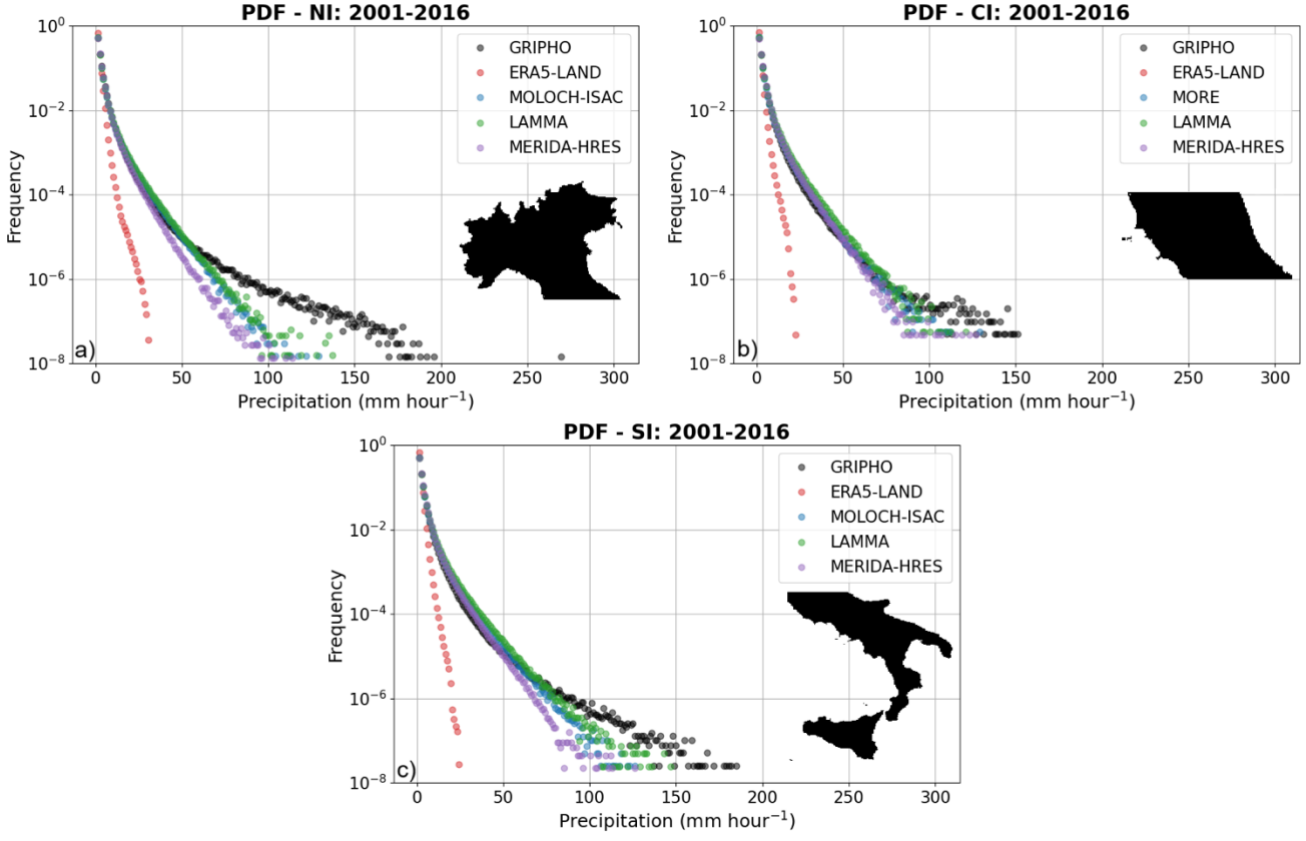

Figure 14:Probability Density Function (PDF) of hourly precipitation for the period 2001–2016, evaluated for different reanalysis datasets against GRIPHO observations over three subdomains a) Northern Italy (NI), b) Central Italy (CI), and c) Southern Italy (SI). The three subdomains are shown in each panel. All datasets have been interpolated onto the GRIPHO grid at a spatial resolution of 3 km. The horizontal axis represents precipitation intensity (mm/hour), while the vertical axis indicates the relative frequency of events within each intensity bin. This figure assesses the ability of each dataset to reproduce the observed distribution of hourly precipitation, including both light and intense events.

MORE reproduces the distribution of daily precipitation events with notable accuracy, in line with the other convection-permitting reanalysis and closely matching the observed frequencies across most intensity bins (Figures 13a and 13b). However, a systematic underestimation becomes apparent for higher intensity thresholds, particularly above 200 mm/day, consistent with the limitations already highlighted in the analysis of the performance diagrams. This limitation is more pronounced when comparing with the GRIPHO observational dataset (Figure 13b), likely due to its finer spatial resolution (3 km), which allows for a more detailed representation of local-scale extremes. As a result, GRIPHO captures a greater number of high-intensity events that may be smoothed out in coarser observational references.

https://doi.org/10.5194/essd-2025-789
Preprint. Discussion started: 31 March 2026

At the hourly scale (Figures 14a-c) the analysis is further stratified into three macro-regions: Northern Italy (NI), Central Italy (CI), and Southern Italy (SI), to highlight the differing precipitation regimes across the peninsula. This regional breakdown also allows assessment of the models' ability to capture the spatial variability of precipitation, which is essential for accurate climate simulations and hydro-meteorological impact studies.

MORE demonstrates good agreement with the observed probability distributions over NI, CI, and SI. Nonetheless, the dataset exhibits reduced capability in representing the most intense precipitation events in the tails of the PDFs, those exceeding 100 mm/h, especially over NI (Figure 14a), a region more frequently affected by such extremes. This behavior is also observed in other high-resolution datasets such as MERIDA-HRES and LAMMA-HINDCAST. However, MERIDA-HRES appears to exhibit greater difficulty in representing the most extreme precipitation values compared to MORE and LAMMA-HINDCAST. Overall, this reflects a common limitation among convection-permitting models (CPMs) operating at horizontal resolutions of approximately 2–4 km. These models may still be inadequate to simulate highly localized and intense convective events, which likely require even finer spatial resolutions, potentially below 1 km, to resolve the mesoscale and storm-scale dynamics responsible for such extremes (Bryan et al., 2003; Wyngaard, 2004; Ban et al., 2014; Leutwyler et al., 2016; Vergara-Temprado et al., 2020).

In contrast, ERA5-Land displays a clear tendency to underestimate precipitation occurrences at both daily and hourly scales, particularly failing to represent high-end extremes. This underestimation is consistent with findings from previous studies and is commonly attributed to the use of parameterized convection schemes, which are known to inadequately capture the intensity and frequency of sub-daily extremes (Ban et al., 2021; Pichelli et al., 2021; Stocchi et al., 2022). The inability of such models to resolve explicitly convective processes limits their effectiveness in simulating short-duration, high-intensity precipitation events, which are often critical for hydrological impact assessments and risk management in complex orographic regions such as Italy.

3.2. MORE temperature fields assessment

Regarding temperature, the evaluation encompasses all four seasons over the period 1991–2020, to facilitate a comparison with prior validations of reanalysis products employing the same methodological framework (Cavalleri et al, 2024a). The analysis distinctly separates systematic errors, reflected in biases of seasonal climatologies, from errors arising from daily variability, assessed comparing daily temperature anomalies. This approach enables a detailed assessment of dataset performance in reproducing different t2m features. Finally, MORE ability in reproducing t2m trends is assessed.

3.2.1 Climatological biases

As a first step, the seasonal climatological averages (1991-2020) of t2m fields are computed for MORE, UniMi/ISAC-CNR and for the other reference reanalyses (see Appendix A, Figure A8). The higher level of detail provided by MORE is evident

https://doi.org/10.5194/essd-2025-789
Preprint. Discussion started: 31 March 2026

in both seasons, better describing the features over complex terrains such as Alps and Apennines. Then, CBIAS fields are calculated for each season at the native MORE resolution (Figure 15, row a). Overall, a cold bias of approximately -1°C is observed, which is more pronounced during winter, especially over Central Italy and Sicily. In summer, the cold bias becomes more evident over Southern Italy and Sicily, while some localized warm biases (<1°C) are also present in certain Alpine valleys and areas of the Po Valley.

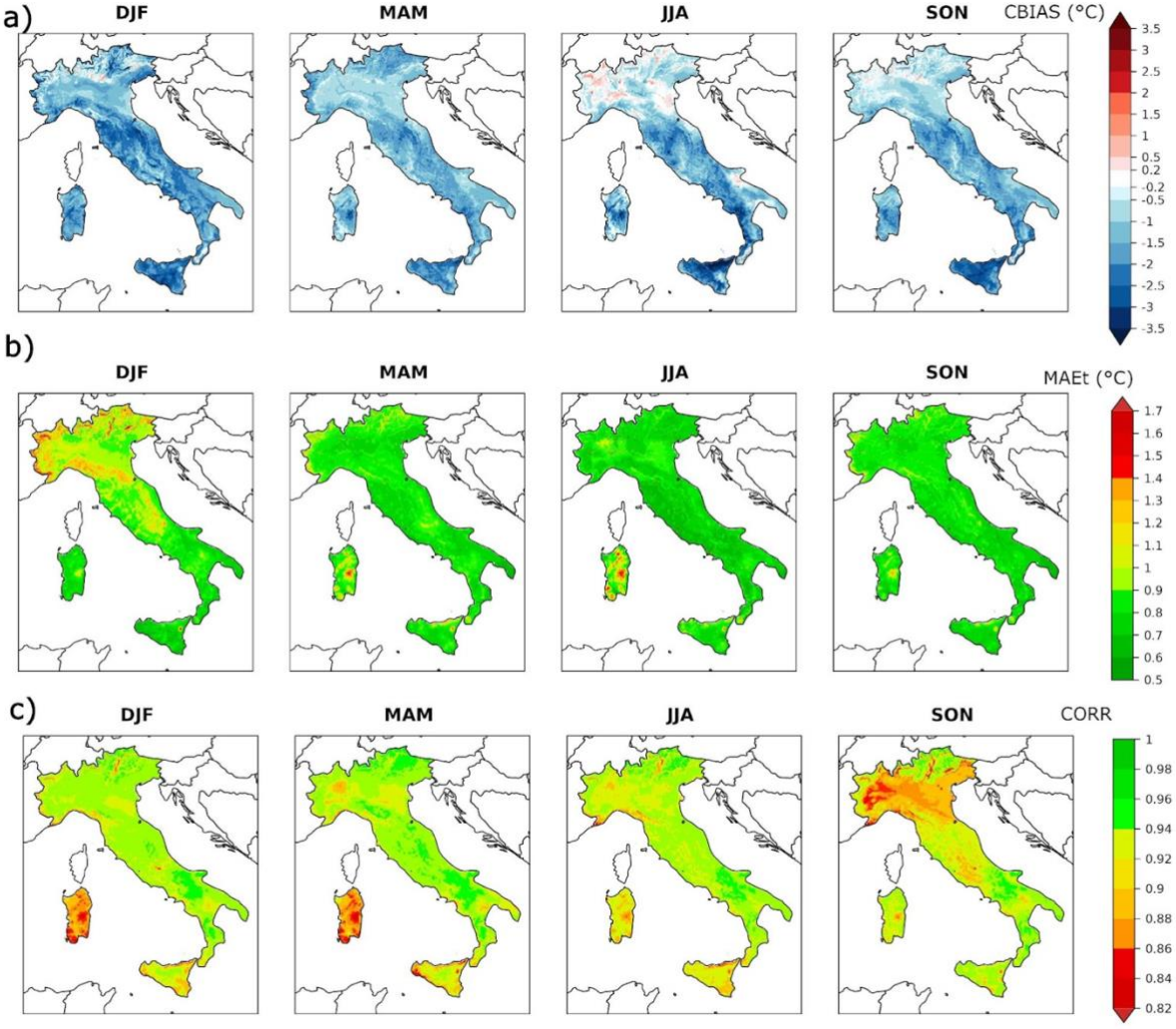

Figure 15: seasonal performance of MORE t2m fields. Row a) CBIAS at the MORE resolution over the climatological period 1991-2020. Row b) MAE in time between MORE daily t2m anomalies and corresponding UniMi/ISAC-CNR ones. Row c) CORR between MORE daily t2m anomalies and corresponding UniMi/ISAC-CNR ones. Row c) CORR between MORE daily t2m anomalies and corresponding UniMi/ISAC-CNR ones.

https://doi.org/10.5194/essd-2025-789
Preprint. Discussion started: 31 March 2026

The performance of MORE t2m fields is compared with that of other regional reanalyses that have been previously validated using the same observational dataset and methodology and over the same time period considered in this study. In particular, validation results for ERA5, ERA5-Land and CERRA are available in Cavalleri et al. (2024a), while MERIDA-HRES is evaluated in Viterbo et al. (2024). Each reanalysis is assessed at its native spatial resolution; therefore, these comparisons are not intended to rank the reanalyses from best to worst, but rather to provide context regarding the magnitude of their native-resolution errors. Table 3 reports the Average CBIAS and the MAE over the entire Italian territory for MORE and other reanalyses. While the Average CBIAS provides the main direction of the deviation (colder or warmer), the MAE provides the average deviation from the observations regardless of the sign. Negative biases means that the reanalysis is colder than the observations. Although all products generally exhibit a cold climatological bias to varying extent, MORE and MERIDA-HRES are the reanalyses with the strongest bias among those analyzed (up to -1.5°C). MORE shows slightly worse CBIAS than MERIDA-HRES, by approximately 0.1°C to 0.3°C across all seasons, except in winter, when the bias in MORE is marginally better (by about 0.1°C). MORE presents a climatological MAE of 0.1 to 0.2 °C larger than CERRA and ERA5-Land ones, but smaller than MERIDA-HRES in most seasons (except winter).

	Average Bias (CBIAS)					***Mean Absolute Error (MAE)***				
	DJF	***MAM***	***JJA***	***SON***	***Annual***	***DJF***	***MAM***	***JJA***	***SON***	***Annual***
ERA5-Land	*-1.31*	*-1.25*	*-0.92*	*-0.97*	*-1.11*	*1.39*	*1.26*	*0.98*	*1.03*	*1.14*
CERRA	*-1.19*	*-0.92*	*-0.85*	*-1.15*	*-1.03*	*1.25*	*1.02*	*1.04*	*1.18*	*1.08*
MERIDA HRES	*-1.49*	*-1.41*	*-1.45*	*-1.39*	*-1.40*	*1.56*	*1.44*	*1.52*	*1.44*	*1.45*
MORE	*-1.57*	*-1.27*	*-1.06*	*-1.22*	*-1.32*	*1.59*	*1.28*	*1.14*	*1.24*	*1.32*

Table 3. ***Average bias (left) and MAE (right) of climatological seasonal and annual t2m fields against UniMi/ISAC-CNR observations, for MORE and the other reanalyses considered.***

Additionally, CBIAS on the seasonal daily minima and maxima t2m are computed for MORE (not shown) and other reanalyses. The average biases are reported in Table 4. In the case of climatological minimum t2m, different patterns emerge among the products. MORE displays biases between -0.7 and 0.1 °C, particularly low in summer and autumn, indicating a mix of over and underestimations in these seasons. In contrast, the bias tends to be predominantly negative in winter and spring. Among the other datasets, MERIDA-HRES systematically underestimates minimum temperatures by about -1 to -1.5°C.

https://doi.org/10.5194/essd-2025-789
Preprint. Discussion started: 31 March 2026

ERA5-Land also shows a consistent cold bias, though it is less pronounced in spring and summer. On the other hand, CERRA exhibits a behavior similar to MORE, with more spatially variable deviations and average biases near zero, especially in autumn and at the annual scale. Regarding maximum temperatures, MORE shows a slightly stronger cold bias than the other products, ranging from -1.5 to -2°C. However, most datasets display biases between -1 and 1.5°C across seasons and annually, except for summer when biases in other products remain negative but closer to 0°C. This pattern has been observed in previous studies. In particular, while several factors may contribute, spatial resolution and the representation of topographic and surface processes are among the possible influences on the simulation of daytime maximum temperatures.

	Average Bias on Mimimum Temperatures (CBIAS)					***Average Bias on Maximum Temperatures (CBIAS)***				
	DJF	***MAM***	***JJA***	***SON***	***Annual***	***DJF***	***MAM***	***JJA***	***SON***	***Annual***
ERA5-Land	*-0.92*	*-0.89*	*-0.50*	*-1.70*	*-0.79*	*-0.97*	*-0.99*	*-0.42*	*-1.25*	*-1.41*
CERRA	*-0.14*	*-1.25*	*-0.85*	*0.15*	*-0.19*	*-1.47*	*-1.15*	*-0.27*	*-1.30*	*-1.29*
MERIDA HRES	*-1.44*	*-1.37*	*-1.29*	*-1.47*	*-1.04*	*-1.35*	*-1.32*	*-0.78*	*-1.40*	*-1.42*
MORE	*-0.72*	*-0.46*	*-0.06*	*-0.19*	*-0.39*	*-1.94*	*-1.42*	*-1.65*	*-1.51*	*-1.67*

Table 4. ***Average bias of climatological seasonal and annual daily minima (left) and maxima (right) t2m fields against UniMi/ISAC-CNR observations, for MORE and the other reanalyses considered.***

3.2.2 Daily anomalies

Shifting the focus to day-to-day variability, MORE t2m anomalies (with respect to MORE t2m 1991-2020 climatologies) are compared with the observed anomalies. MORE generally shows MAEt values ranging between 0.5°C and 1°C across most of the territory, with the exception of Sardinia (Figure 15, row b). In Sardinia, higher errors are located over mountainous areas, particularly in spring and summer. The highest MAEt values were observed in winter, when errors exceed 1°C on average over the Apennines and the Alpine region, reaching up to 1.5°C in some Alpine valleys. Values of CORR above 0.9 are recorded over most of the territory and during most seasons, with the exception of Sardinia in winter and spring (Figure 15, row c). The lowest CORR are found during autumn in the Po Valley, particularly in its western sector and in some Alpine

https://doi.org/10.5194/essd-2025-789
Preprint. Discussion started: 31 March 2026

valleys, where CORR drops below 0.85. These spatial and seasonal differences between the two indicators help to highlight areas of reduced model performance from different perspectives. While CORR reflects the ability of the reanalysis to correctly capture the day-to-day variability, MAEt quantifies the magnitude of these discrepancies. For example, in the Alpine region during winter, CORR is high, indicating that the reanalysis correctly tracks the direction of anomalies, but the MAEt is relatively large, suggesting that the amplitude of the anomalies is overestimated. Conversely, in the Po Valley during autumn, CORR values are low, indicating difficulty in capturing the day-to-day sign changes of anomalies, yet the MAEt remains low and comparable to other regions, suggesting that the errors are relatively small.

Compared to other reanalysis products in terms of spatial averages of anomaly error indicators (Table 5), MORE exhibits slightly higher MAEt values compared to MERIDA-HRES and ERA5-Land, but substantially lower than CERRA. In terms of CORR, MORE shows values that are comparable to those of MERIDA-HRES and ERA5-Land, and systematically higher than those of CERRA. In summary, the t2m fields provided by MORE demonstrate a performance that is fully consistent with the current state-of-the-art high-resolution regional reanalysis products over Italy. Importantly, these results are achieved while operating at an even higher spatial resolution (~1.7 km) compared to the previously available datasets.

3.2.3 Trends

Finally, the ability of MORE to reproduce the warming trend over the Italian territory and its spatial patterns is validated using the annual mean of the daily 2-meter temperature (t2m) anomaly in order to reduce noise.

The warming trends are estimated using the Sen's Slope method over the period 1991–2020. The mean trend obtained with MORE is +0.39 °C per decade, with a 95% confidence interval of [0.36, 0.46], corresponding to approximately +1.28 °C over 30 years. The corresponding trend from the UniMi/ISAC-CNR observational dataset is +0.44 °C per decade, with a confidence interval of [0.35, 0.50], amounting to +1.32 °C over the same period. The maps of these trends (Figure 16, left and central panels) show similar spatial patterns. To investigate the small differences in these similar patterns, a spatial map of the deviation in trend between MORE and the observations (Figure 16, right panel) was obtained. The distribution of these deviations indicates that 95% of the differences lie within the range of –0.2 to +0.1 °C per decade. Trend underestimations of about –0.1 to –0.2 °C per decade are found over the Eastern Po Valley, parts of the central Apennines, and some areas in the northern sectors of Sardinia and Sicily. Milder underestimations also occur in South-Western areas and in the western Alps, while overestimations of up to +0.2 °C per decade are mainly observed in South-Eastern areas and in some valleys in Eastern Alps and Prealps. These patterns are similar to those found in other reanalyses based on ERA5 downscaling (see Figure 9 in Cavalleri et al., 2024a), suggesting that such inhomogeneities may be inherited from the ERA5 dataset itself. Nevertheless, more than 98% of the grid points lie within the range [–0.2, +0.2] °C per decade, which corresponds to a deviation from the

https://doi.org/10.5194/essd-2025-789
Preprint. Discussion started: 31 March 2026

observed trend of no more than ±0.6 °C over 30 years, below the half of the magnitude of the warming signal. Those deviations are in line with the ones of other regional downscalings (Cavalleri et al. 2024a).

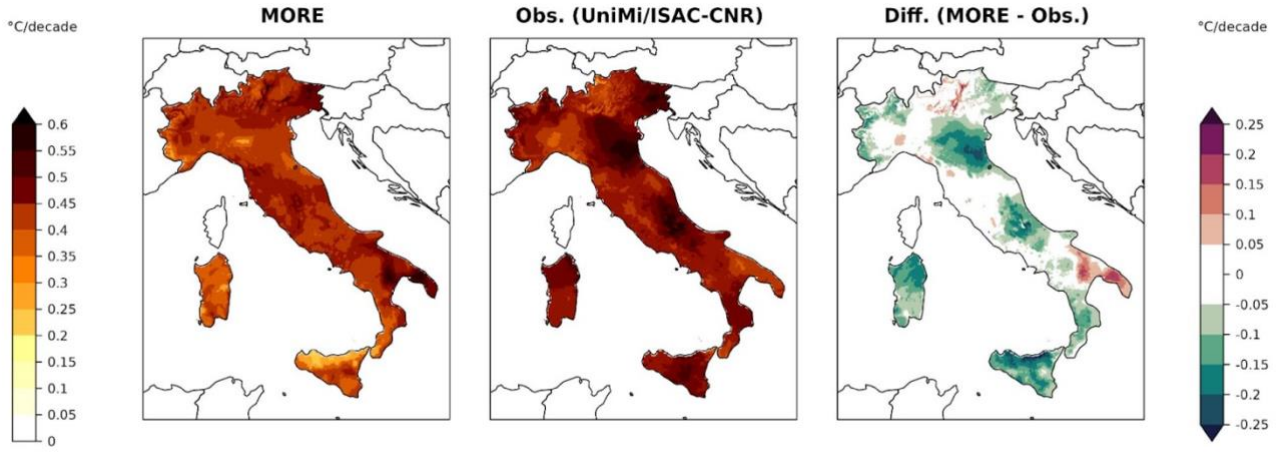

Figure 16: decadal trends in the annual t2m anomaly for MORE (left panel), and UniMi/ISAC-CNR observations (central panel); decadal trends of the differences between MORE and observational annual t2m anomalies (right panel).

4. Application of MORE

To illustrate the potential of the MORE reanalysis, we present its application across meteorological, hydrological, and climatological perspectives. This approach emphasizes the dataset's high-resolution capabilities and its relevance for diverse atmospheric and environmental analyses.

4.1 Meteorological case studies: May 2023 extreme precipitation events

In view of possible applications to natural risk prevention and adaptation, besides a general validation of the reanalysis, it is also extremely relevant to assess its capability of reproducing extreme precipitation events characterized by high-impact at the ground. To attain this aim, a case study affecting Emilia Romagna region, northern Italy, in spring 2023 has been selected as a test bed.

The extensive flooding episode was characterized by two almost "twin" rainfall events, occurring one after the other at about two weeks distance, 01-03 May and 15-17 May. Within this period, thus between the two main events, scattered precipitation contributed to maintain high values of moisture content in the soil, a critical factor determining the flood severity (Cremonini

https://doi.org/10.5194/essd-2025-789
Preprint. Discussion started: 31 March 2026

et al., 2024). River overflow and breaching, landslides and flooding of lowland areas resulted in a dramatic toll of 16 casualties and many billions of damages (Brath, 2023; ARPAE, 2023a,2023b).

The precipitation distribution was very similar in the two events, induced by the presence of a Mediterranean cyclone and by orographic forcing (Dorrington et al., 2024). In the first event, cyclogenesis occurred in the central Mediterranean, whilst in the second one, the cyclone formed in the lee of the Atlas Mountains and then moved northward over central Italy. Although the detailed characteristics of the two cyclones and of the environment were slightly different, in both events the low surface pressure played a key role in driving moist easterlies from the Adriatic, impinging on the northern Apennines (as properly shown by the reanalysis, see Appendix A Figure A9). Thermal contrast and convergence at the foothill of the Apennines enhanced the orographic uplift and triggered convective activity especially along the Adriatic coast.

The slow mesoscale evolution and the persistence of the low-level flow configuration were responsible for extreme amounts of rainfall, exceeding 200 mm in less than 48 hours in each event, over a wide area of the northern Apennines. Considering the precipitation accumulated during the whole period from 01 to 17 May, a 200-year return time was estimated (Barnes et al., 2023). The total accumulated precipitation simulated by MORE and ERA5Land is compared with the observations (Figure 17) obtained by interpolation of the national rain gauge network managed by the Italian Department of Civil Protection (Italian Civil Protection and CIMA Research Foundation, 2014).

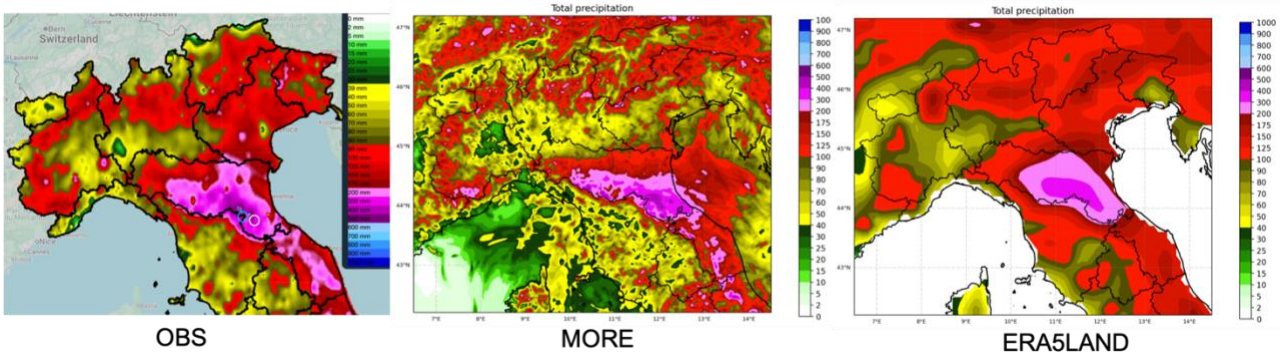

Fig.17: Accumulated precipitation between 01 and 17 May 2023. Observations (interpolation of national raingauge network (Dewetra-DPC), MORE and ERA5LAND. The two circles in the OBS panel, indicate the locations of the Trebbio and Rullato rain gauge stations, shown in blue and white, respectively

MORE demonstrates to reproduce the intensity of the extreme event, with the highest amount localized over the mountain sector in the central-eastern part of the region. Although with a slight underestimation of the rainfall peaks, MORE clearly improves with respect to ERA5Land, according to the general statistical validation discussed before and presents also a much more detailed spatial distribution of the rainfall, likely correlated with the orographic features that the high resolution captures. The temporal evolution of the hourly precipitation in two rain gauges located in the rainiest area (Figure 18), highlights on the one hand the accurate timing of MORE in reproducing all the precipitation spells in the period, but on the other hand a slight

https://doi.org/10.5194/essd-2025-789
Preprint. Discussion started: 31 March 2026

744 eastward shift of the rainfall peaks. In fact, while at Trebbio (blue circle in Figure 17) MORE underestimates the total rainfall
745 amount, only a few tens of kilometres to the east at Rullato (white circle in Figure 17) it overestimates precipitation

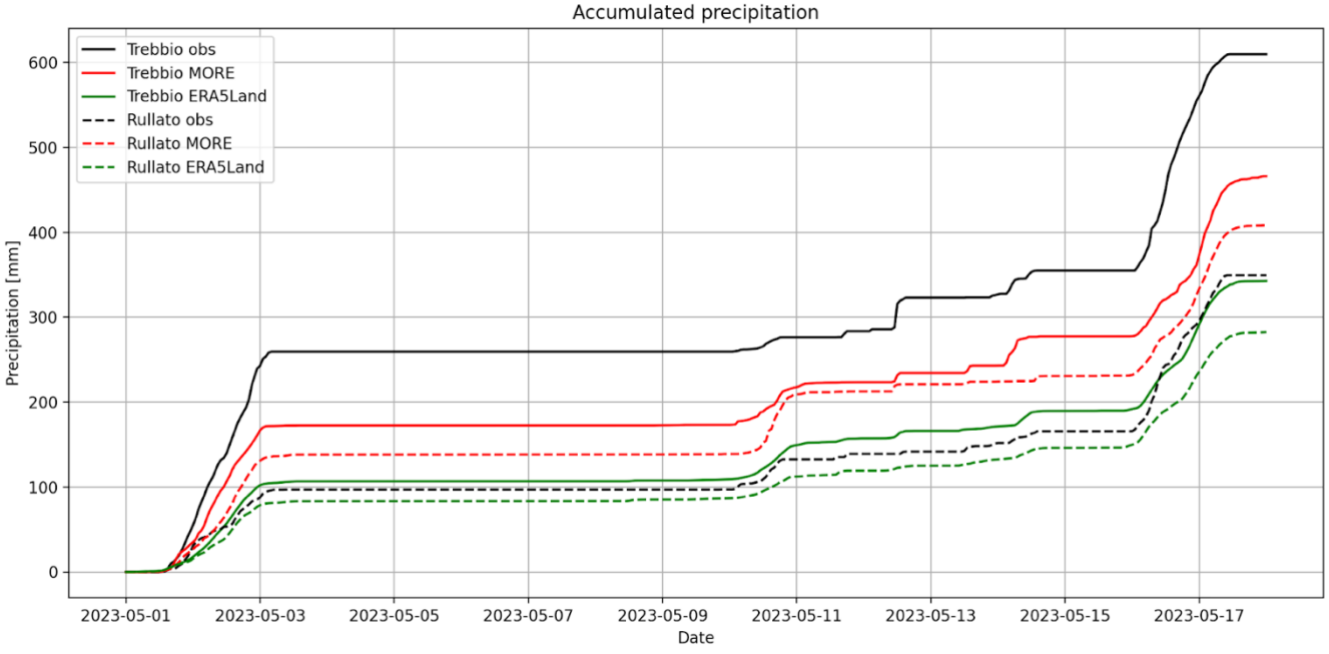

746
747 ***Fig.18: Hourly rainfall evolution for the whole period 01-17 May 2023 at two rain gauge stations located in the Apennines area***
748 ***affected by the most intense precipitation. Trebbio (solid line): 570 m.a.s.l., Lat: 44.137, Lon: 11.837; Rullato (dashed line): 600***
749 ***m.a.s.l, Lat: 43.946, Lon: 12.077. Black, red and green lines refer to observations, MORE and ERA5LAND, respectively.***

750 It is worth noting that the two above rain gauges pertain to different watersheds, so it may be interesting to investigate to what
751 extent this uncertainty in the location affects the river discharge that can be reconstructed by forcing an hydrological model
752 with MORE rainfall fields. This is done in the following Section where hydrological applications of MORE are presented.
753
754 **4.2 Hydrological case study: May 2023 floods events**
755
756 This hydrological analysis aims at evaluating the capability of the MORE dataset to reproduce the flood events that affected
757 the Reno (992 km2), Lamone (202 km2) and Savio (576 km2), river basins (Emilia-Romagna region) in May 2023. To this
758 end, the MISDc model (Brocca et al., 2011; Camici et al., 2025) is employed. MISDc is a semidistributed conceptual
759 hydrological model designed to simulate the main hydrological processes occurring within the soil and along the river network,
760 including infiltration, surface runoff, excess runoff, percolation and river routing. Soil-related processes are computed at the
761 grid scale over two layers (superficial and root zone), whereas river routing is performed at the sub-basin scale. It is important
762 to note that the model does not simulate levee overflows or the consequent reduction in water volume caused by flooding.
763 Nonetheless, MISDc has been widely used for the hydrological validation of precipitation products (e.g., Camici et al., 2020,
764 2018; Brocca et al., 2020; Almagro et al., 2021; El Khalki et al., 2023) and has shown strong performance in reproducing flood

https://doi.org/10.5194/essd-2025-789
Preprint. Discussion started: 31 March 2026

765 peaks across various river basins worldwide (e.g., Brocca et al., 2013; Masseroni et al., 2017; Cislaghi et al., 2020; Nguyen et
766 al., 2020; Ding et al., 2022). For more detailed information on the MISDc model's equations, parameters, and calibration
767 procedures, the reader is referred to Camici et al. (2025).
768 The model utilizes high-resolution air temperature and precipitation data from the MORE dataset as input, and is calibrated
769 against the river discharge measurements observed in the 2023-2024 period at the outlet sections of the investigated basins.
770 Calibration is performed by minimizing an objective function based on the Kling-Gupta Efficiency (KGE) index (Gupta et al.,
771 2009). It has to be specified that a perfect match between observation and simulation is characterized by a KGE value equal
772 to 1. In order to rigorously assess the possible added value of employing high-resolution meteorological data for flood risk
773 monitoring, an analogous calibration and simulation procedure is conducted by using the lower-resolution ERA5-Land
774 meteorological dataset as input to the MISDc model.
775 Figure 19 illustrates the MISDc results in terms of river discharge evolution for the period 1–31 May 2023 at the outlet sections
776 of the Reno, Lamone, and Savio river basins. As shown, the MORE meteorological dataset enables a more accurate
777 reproduction of the observed river discharge, with KGE values exceeding 0.84 for the Reno and Savio basins, and a value of
778 0.62 for the Lamone basin. Overall, the MORE dataset outperforms ERA5-Land data, as evident from both the discharge time
779 series and the corresponding KGE values of 0.46, 0.65, and 0.70 for the Reno, Lamone, and Savio basins, respectively (Figure
780 19).

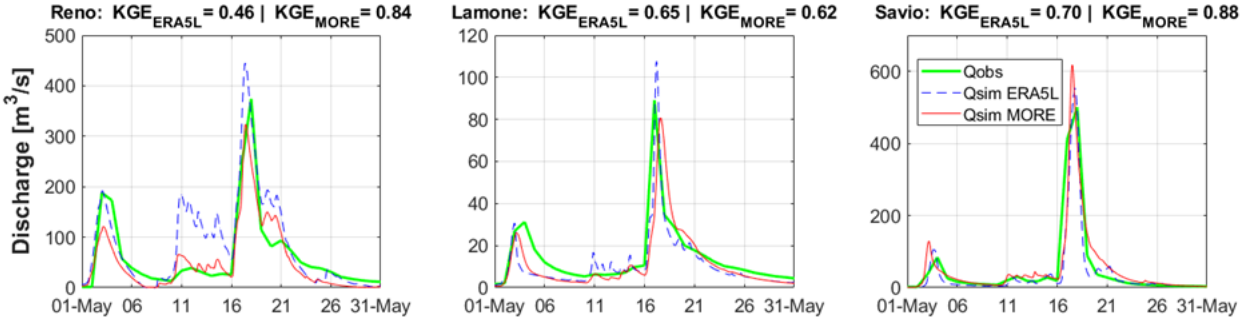

781
782 ***Figure 19: River discharge evolution for the period 01-31 May 2023 at the closure sections of Reno, Lamone and Savio river basins.***
783 ***Blue dashed and red lines represent the modeled river discharge by using ERA5_Land and MORE data as input to the hydrological***
784 ***model, green lines refer to in situ observations.***

785 However, beyond river discharge, it would be interesting to investigate whether the meteorological data input into the
786 hydrological model can 'get the right answers for the right reasons' (Kirchner, 2006). The rationale behind this concept is that
787 the hydrological model, through calibration, adjusts model parameters to reproduce the target variable. However, this does not
788 necessarily ensure that internal hydrological processes and states, such as soil moisture, evapotranspiration, or snowmelt, are
789 accurately represented. Given that this analysis focuses on a flood event, particular attention should be paid to the
790 spatiotemporal evolution of surface soil moisture, which plays a crucial role in determining runoff response (Cremonini et al.,
791 2024).

https://doi.org/10.5194/essd-2025-789
Preprint. Discussion started: 31 March 2026

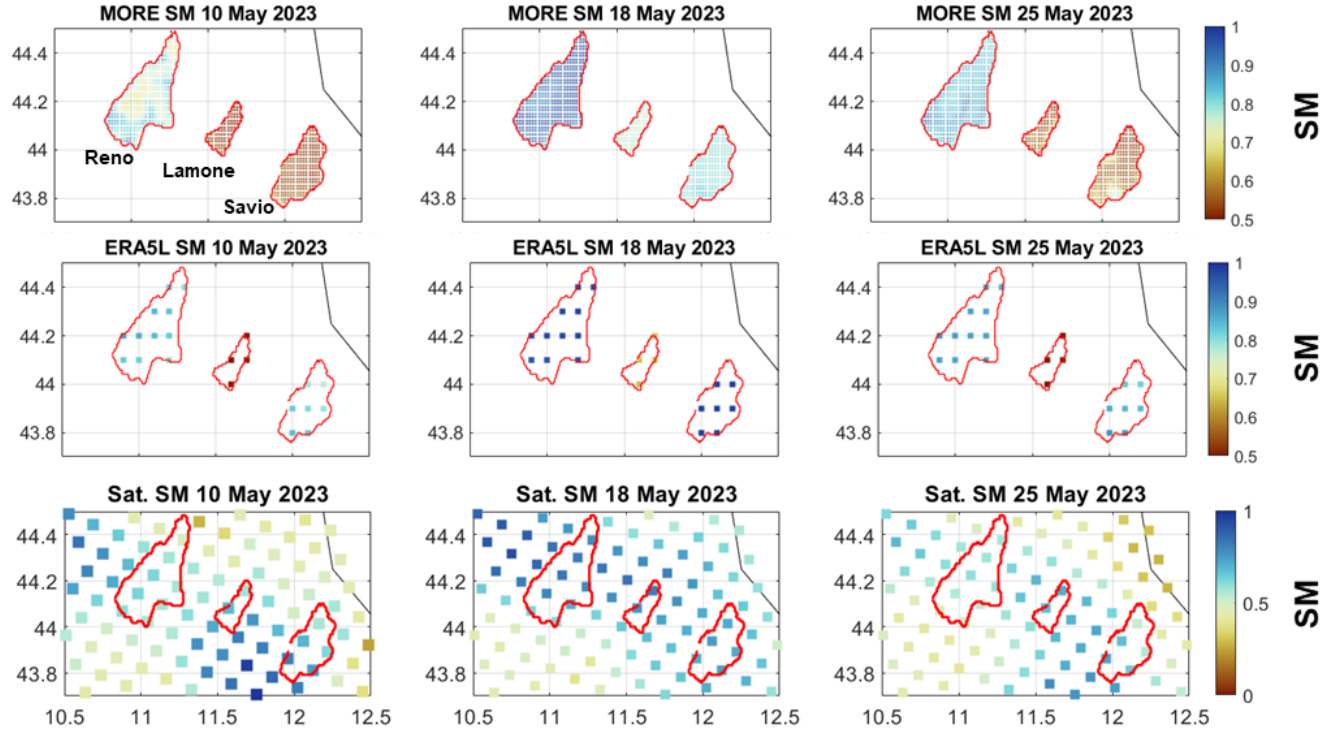

Figure 20: Relative soil moisture pattern for 10, 18 and 25 May 2023 over three study basins, Reno, Lamone and Savio. The first and second rows illustrate the modelled soil moisture by using MORE and ERA5L datasets as input into the MISDc model. The third row shows the satellite-based ASCAT soil moisture pattern.

The first row shows modelled soil moisture using MORE as meteorological input, while in the second row the ERA5-Land data are considered. For comparison, the third row displays daily satellite-based surface soil moisture from Metop Advanced SCATterometer Surface Soil Moisture Near Real Time 12.5 km sampling (ASCAT, https://hsaf.meteoam.it/Products/Detail?prod=H29).

The results reveal substantial differences in the MISDc spatial representation of soil moisture between the two meteorological datasets. The higher spatial resolution of MORE allows the MISDc model to capture finer-scale variability in soil moisture, which is particularly important for accurately simulating hydrological processes in small catchments. In contrast, coarser-resolution inputs such as ERA5-Land tend to smooth out local heterogeneities, potentially compromising model performance in such contexts (Brocca et al., 2024). In addition, the temporal evolution of soil moisture is also noteworthy. Following the earlier precipitation event, soil conditions on 10 May were already wet, with values exceeding 0.53 across all soil moisture products. Saturation levels further increased by 18 May, reaching particularly high values over the Reno basin. These saturated conditions, combined with the intense rainfall on 17–18 May, significantly contributed to the severity of the flood impacts in the region (Arrighi and Domeneghetti, 2024). Following the event, soil moisture values decreased but remained above 0.55, indicating a hydrological memory effect associated with the flood. While this temporal behaviour is reasonably well captured

https://doi.org/10.5194/essd-2025-789
Preprint. Discussion started: 31 March 2026

by both the MORE-forced simulations and ASCAT satellite observations, the ERA5-Land-derived soil moisture fails to reproduce this variability. Specifically, ERA5-Land shows limited spatiotemporal dynamics, suggesting it may be unsuitable for applications requiring detailed soil moisture characterization at the catchment scale. This finding is particularly relevant, as the MORE dataset offers spatial and temporal resolutions well-suited for a wide range of hydrological applications, particularly in small catchments. These include not only the modelling of extreme flood events, but also the downscaling of satellite products and the validation of high-resolution satellite-based observations.

4.3 Climate analysis: Long-term trends and variability of key climate indices

Finally, one last application of MORE, from a climatic perspective, concerns its use in the calculation of climate indices based on daily values. In particular, one indicator from a set of extreme temperature and precipitation indicators suggested by ETCCDI (Expert Team on Climate Change Detection and Indices; Karl et al., 1999) is considered, the Tropical Nights (TR). This index counts the number of nights per year during which the minimum temperature does not drop below 20°C.
Rather than focusing solely on the spatial distribution of this index, the analysis aimed to evaluate MORE's ability to reproduce the temporal trend in the number of TR over the study period (1991–2020), based on the MORE ability in reproducing t2m trends, assessed in Section 3.2.3. Figure 21 presents both the average number of TR and the decadal trend in TR for the observational dataset UniMi/ISAC-CNR, MORE, and other reanalyses. The 1991-2020 climatological averages of TR (Figure 21, top panels), provide useful insights about regions most frequently affected by tropical nights.

https://doi.org/10.5194/essd-2025-789
Preprint. Discussion started: 31 March 2026

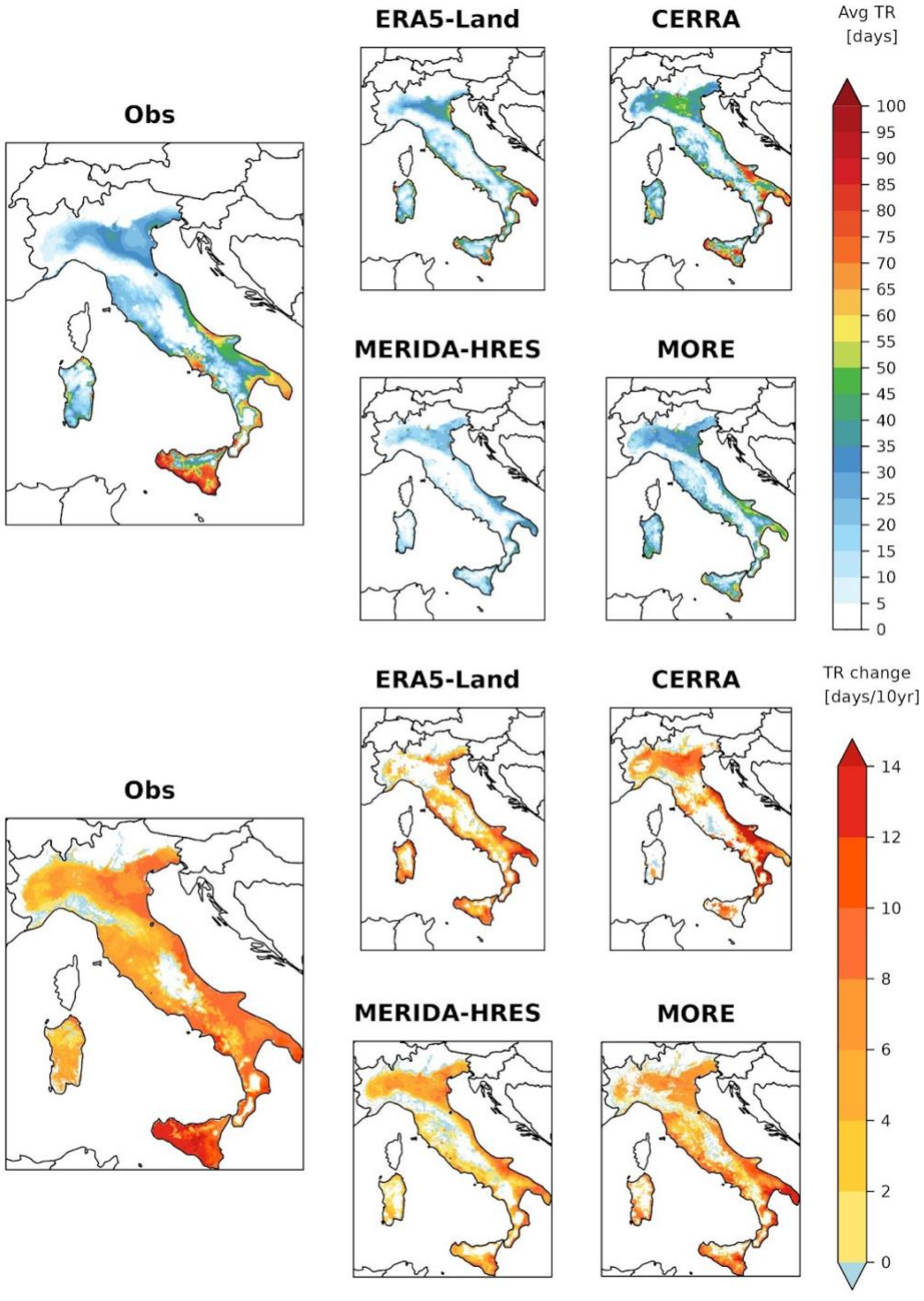

Figure 21: Top panels: Climatology of Tropical Nights (number of days per year with TN > 20 °C), averaged over the period 1991–2020. The leftmost panel shows observations; the four panels on the right show results from the reanalysis datasets: ERA5-Land, CERRA, MORE, and MERIDA-HRES (clockwise from top left). Bottom panels: Corresponding decadal trends in the number of Tropical Nights. The panel layout is the same as above.

https://doi.org/10.5194/essd-2025-789
Preprint. Discussion started: 31 March 2026

Among all reanalyses, MORE shows the strongest agreement with observations, both in the spatial distribution and the frequency of TR. According to observations, regions such as southeastern Italy and several coastal areas of central and southern Italy, including islands, experience over two months of TR per year, with parts of Sicily exceeding three months. MORE reproduces this pattern well, despite a known cold bias in minimum temperatures that results in some underestimation, particularly in Apulia and Sicily. Still, its performance is generally slightly more consistent with the observations than that of MERIDA-HRES, which is the other product capable of capturing TR patterns quite well. ERA5-Land captures the signal over Apulia reasonably well but underestimates TR in Marche and Campania regions. CERRA performs better in these two regions, though with greater spatial irregularity.

In terms of trends (Figure 21, bottom panels), MORE also aligns closely with observations, showing similar average trends (+6.18 and +6.31 TR per decade, respectively) as well as nearly identical InterQuartile Ranges (IQR, 4.00–8.18 for MORE and 4.12–8.67 for observations). This suggests that MORE effectively captures the spatial variability of TR trend.

In contrast, the other reanalyses display greater discrepancies. ERA5-Land reports a comparable average trend (+6.00 TR per decade) but with a broader IQR (2.86–8.89), and it fails to detect significant increases over the Po Valley. CERRA shows a higher average trend (+7.25 TR per decade) and the widest IQR (4.24–10.00), overestimating the warming signal in some areas while missing it across central Italy and Sicily. MERIDA-HRES underestimates the trend (+4.29 TR per decade; IQR 1.76–6.36) and is overall less consistent with the observed patterns than MORE.

5 Data availability

The dataset used and analysed in this study is the MOloch-downscaled ERA5 REanalysis (MORE), Version 1. This release includes hourly near-surface air temperature and precipitation over Italy and the Alpine region for the period 1991–2020, corresponding exactly to the data validated and discussed in this manuscript.

MORE V1 is openly available through the Zenodo repository at: **[https://doi.org/10.5281/zenodo.18470948]** (Stocchi, P. 2026), which ensures long-term preservation and permanent access.

Additional variables and temporal extensions, described but not analysed in this study, are maintained in the CNR-ISAC repository and will be released under a separate DOI once consolidated.

The Zenodo V1 release serves as the official reference for this publication, while the full operational dataset remains accessible internally.

6 Conclusions

This study presents a comprehensive evaluation of MORE, a dataset of high-resolution (~1.7 km) convection-permitting regional reanalysis over Italy, generated through dynamical downscaling of ERA5 with the non-hydrostatic MOLOCH model.

https://doi.org/10.5194/essd-2025-789
Preprint. Discussion started: 31 March 2026

The dataset covers the 1990–present period and is designed to capture fine-scale meteorological processes, particularly in complex terrain.

A multiscale validation framework is employed, assessing daily and hourly precipitation and daily near-surface air temperature. Precipitation is evaluated against high-quality gridded observations (GRIPHO, ARCIS), while temperature fields are assessed using UniMi/ISAC-CNR station data projected onto the native grid and elevation of MORE to avoid orographic mismatches to introduce additional biases. MORE is benchmarked against other convection-permitting products (LAMMA-HINDCAST, MERIDA-HRES) and coarser-resolution reanalyses (ERA5-Land, CERRA).

The results show that MORE realistically reproduces the spatial and temporal variability of precipitation across Italy, with particular skill during summer convective regimes. Relative biases in mean precipitation, wet-day frequency, and intensity generally fall within −5% to +25% and are lower than those of ERA5-Land and CERRA. MORE also outperforms or matches other CPM reanalyses, especially in capturing extremes and localized heavy rainfall at sub-daily scales, reflecting the added value of its high spatial resolution and explicit convection representation. Taylor and performance diagrams further corroborate its high spatial correlation and realistic variability, while PDFs confirm faithful reproduction of both moderate and extreme events, with underestimation in the tails for rare events (>100 mm/h, >200 mm/day).

Temperature validation demonstrates that MORE captures key spatial and temporal features of near-surface air temperature climatology and variability, including daily anomalies and long-term trends. Despite a systematic cold bias (~1 °C, stronger in winter and in specific regions), temporal correlations on daily anomalies exceed 0.9 and mean absolute errors against observational anomalies remain below 1 °C for most regions and seasons. The dataset reliably reproduces spatial patterns and trends of climate indicators, such as the number of Tropical Nights and its increase, aligning closely with observations and outperforming or matching other reanalyses.

Beyond climatological validation, MORE shows strong potential for practical applications. A case study (May 2023 Emilia-Romagna flood) demonstrates its capability to reproduce mesoscale dynamics of extreme precipitation events. Total accumulated rainfall agrees well with interpolated rain gauge data, and hourly time series at representative stations capture the timing and evolution of rainfall spells, with only minor spatial shifts. Hydrologically, MORE-driven simulations improve representation of catchment-scale discharge, rainfall, and soil moisture dynamics, confirming its utility for impact modeling, flood forecasting, and hazard mitigation.

Overall, MORE represents a major advancement in regional reanalysis for Italy, to our knowledge, is currently the highest-resolution dataset available for the Italian territory and the Alps. Its high spatial and temporal resolution, together with convection-permitting dynamics, allows for a substantially improved representation of key meteorological variables. Additionally, MORE provides a comprehensive set of atmospheric variables across multiple pressure levels, making it a valuable reference for climate analyses, characterization of extreme events, climate services, hazard prediction, and environmental impact assessments. Importantly, MORE also has the potential to serve as a high-quality training dataset for AI-based downscaling and reanalysis-driven forecast systems, enabling the development of advanced machine learning applications in climate and weather prediction. Future developments may include extending its spatial and temporal coverage,

https://doi.org/10.5194/essd-2025-789
Preprint. Discussion started: 31 March 2026

validating additional variables, and integrating MORE into multi-sector workflows for risk assessment, adaptation planning, and early warning systems. Its combination of resolution, physical realism, and multi-variable availability positions MORE as a pivotal tool for both research and operational applications

Appendix A: Supplementary Figures

https://doi.org/10.5194/essd-2025-789
Preprint. Discussion started: 31 March 2026

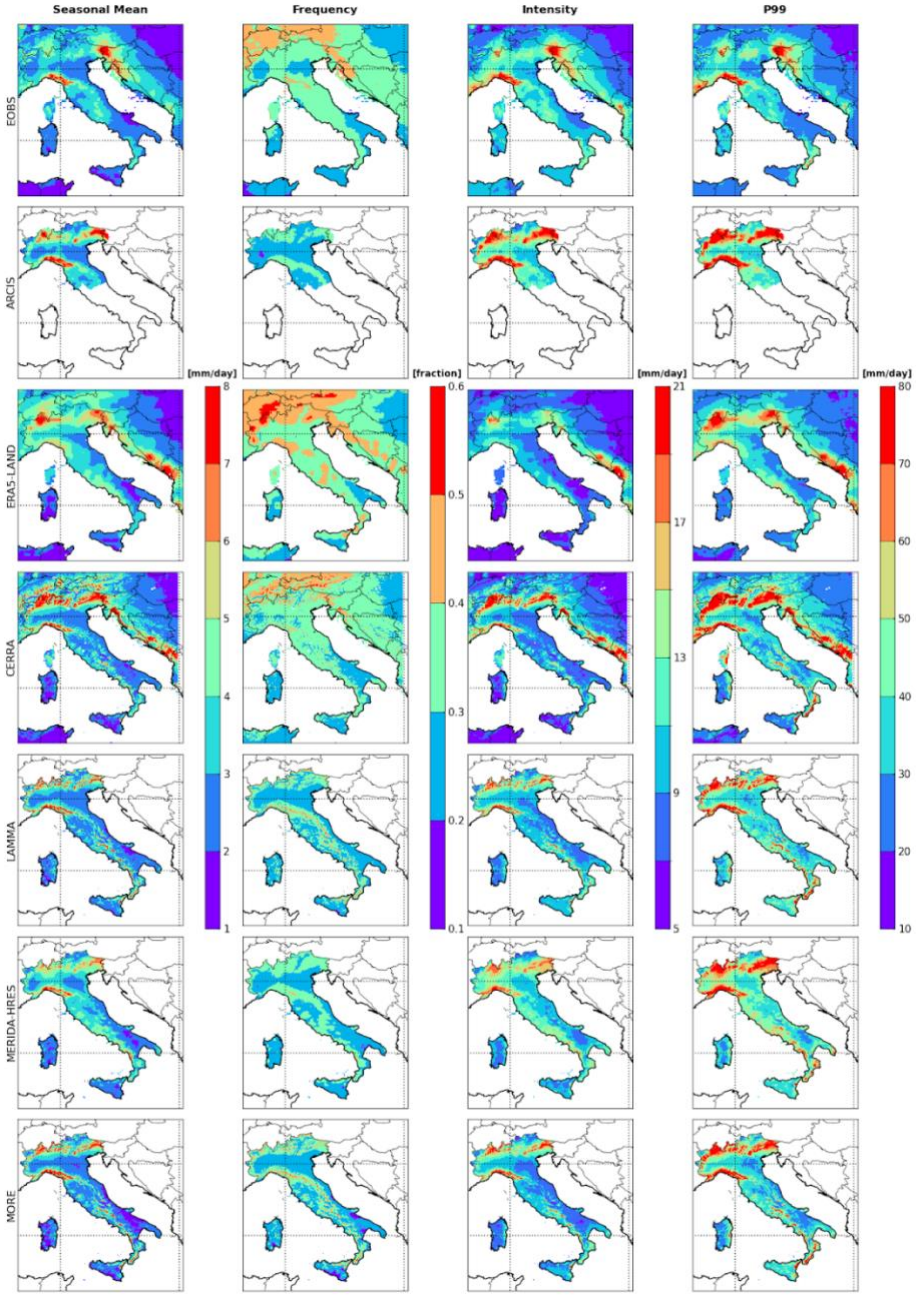

Figure A1: Seasonal means of daily precipitation indices for autumn (SON) over the period 1991–2020, including mean precipitation, precipitation frequency, precipitation intensity, and heavy precipitation (defined as the 99th percentile; Table 2). Results are shown for observational datasets (EOBS & ARCIS), MORE, and the reanalysis datasets listed in Table 1.

https://doi.org/10.5194/essd-2025-789
Preprint. Discussion started: 31 March 2026

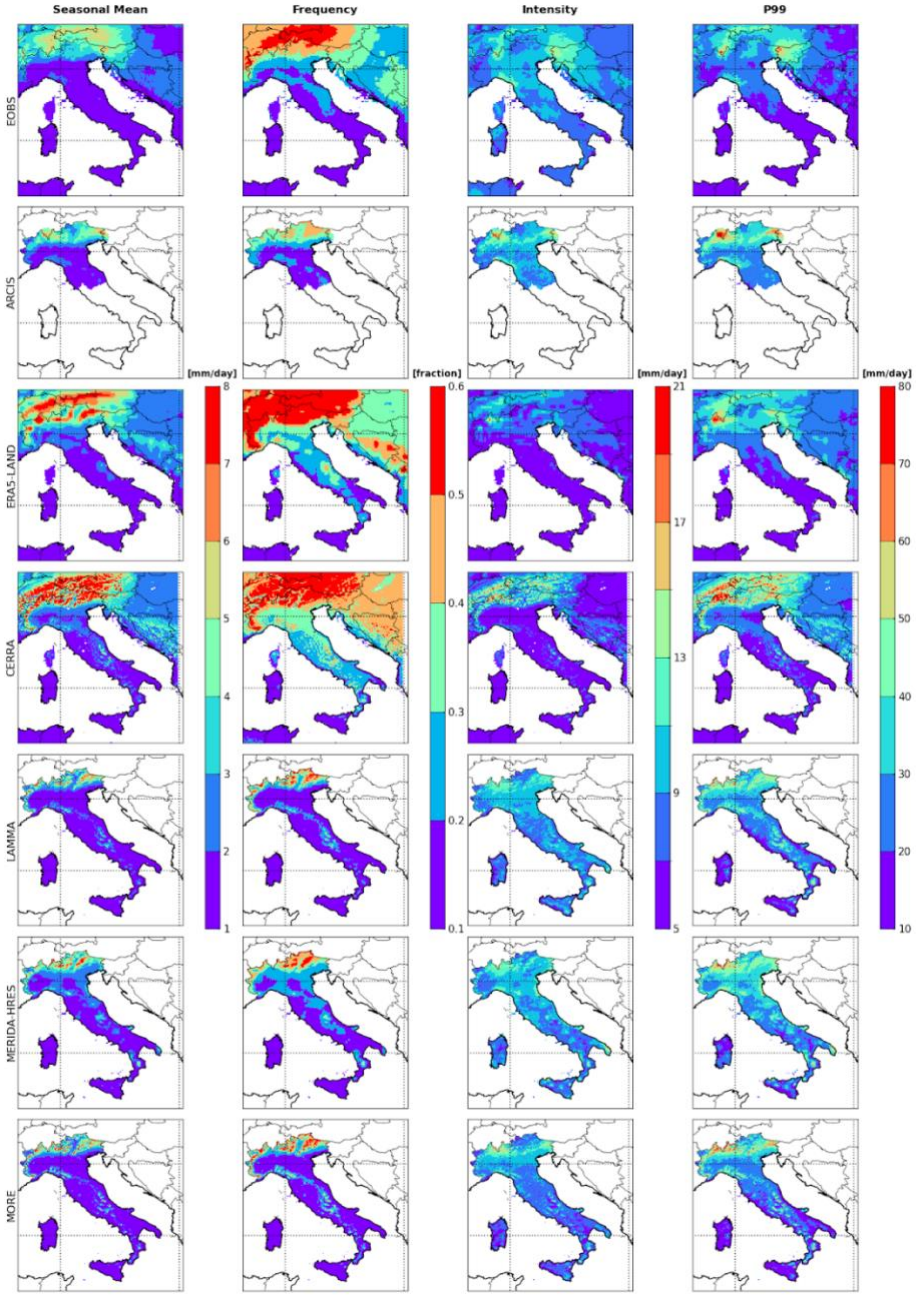

Figure A2: As Fig. A1, but for the summer (JJA) season

https://doi.org/10.5194/essd-2025-789
Preprint. Discussion started: 31 March 2026

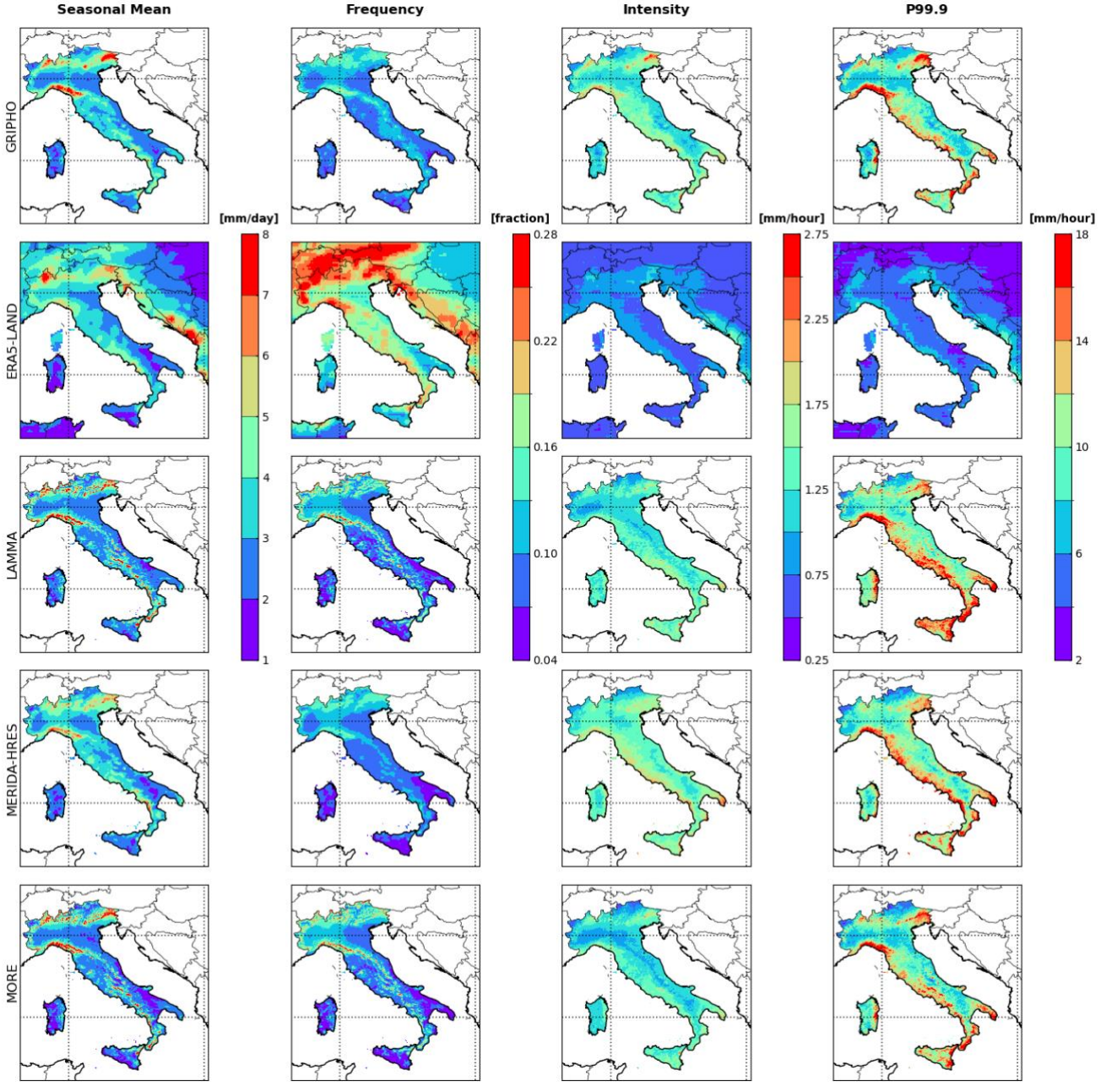

Figure A3: As in Fig. A1, but for hourly precipitation, including frequency, intensity, and heavy precipitation indices. Seasonal means are calculated from daily precipitation, consistent with Fig. A1. Observations are based on the gridded hourly precipitation dataset over Italy (GRIPHO; Fantini et al., 2019) for the period 2001–2016. Heavy hourly precipitation is defined as the 99.9th percentile of all events.

https://doi.org/10.5194/essd-2025-789
Preprint. Discussion started: 31 March 2026

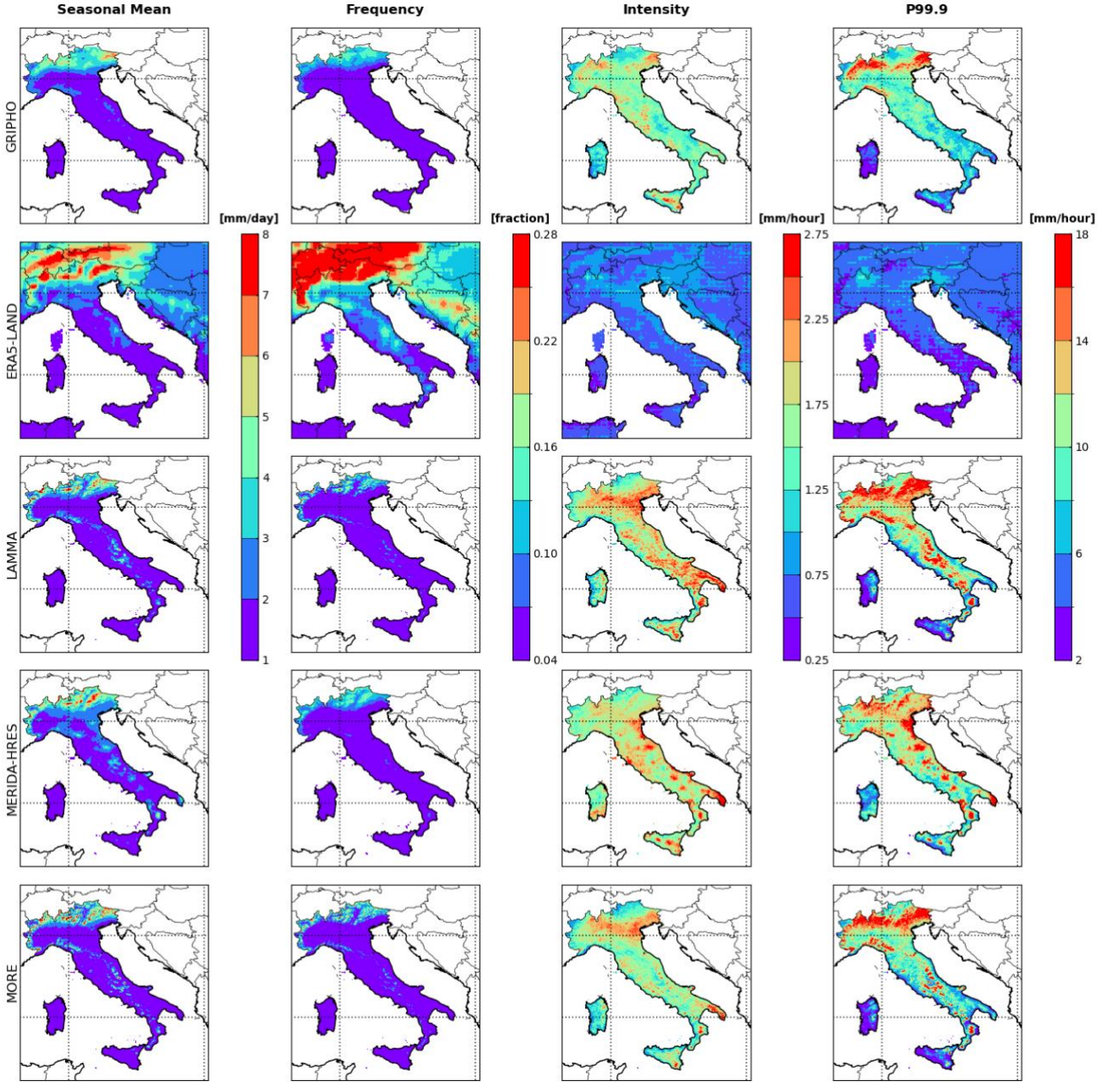

928
929 ***Figure A4: As Fig. A3, but for the summer season.***
930
931
932
933

https://doi.org/10.5194/essd-2025-789
Preprint. Discussion started: 31 March 2026

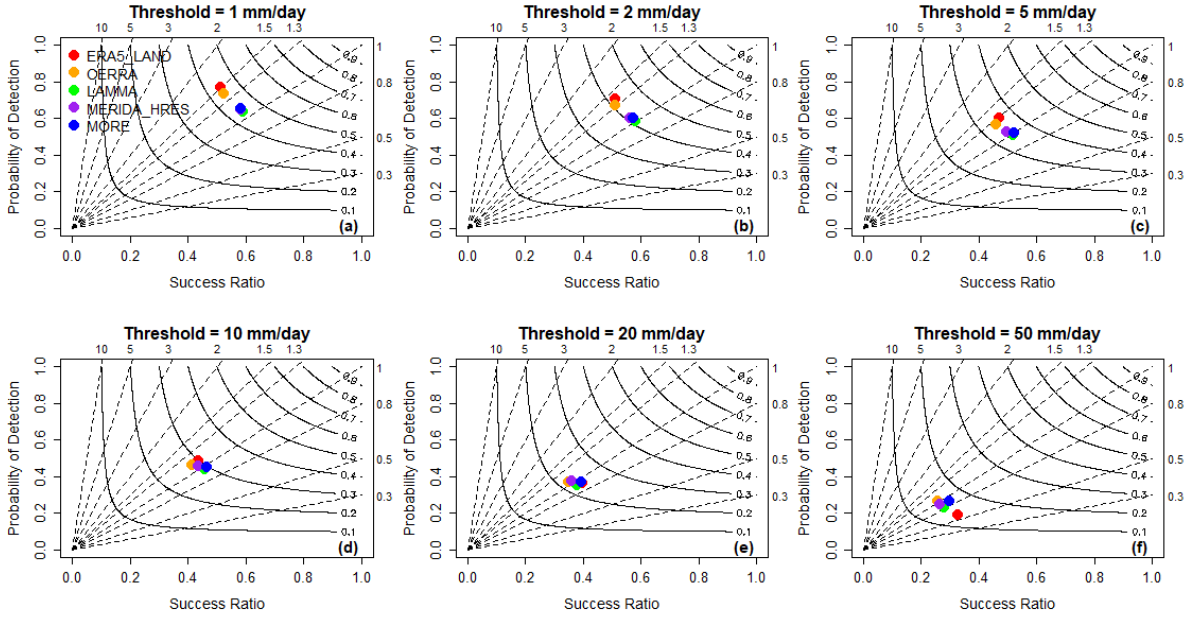

Figure A5: Performance diagram illustrating the average skill scores for daily precipitation over the 1991–2020 period, evaluated for different reanalysis datasets against ARCIS observations within the ARCIS observational domain. The horizontal axis shows the Success Ratio (SR), while the vertical axis displays the Probability of Detection (POD). Curved isopleths represent values of the Critical Success Index (CSI), and dashed diagonal lines indicate the bias

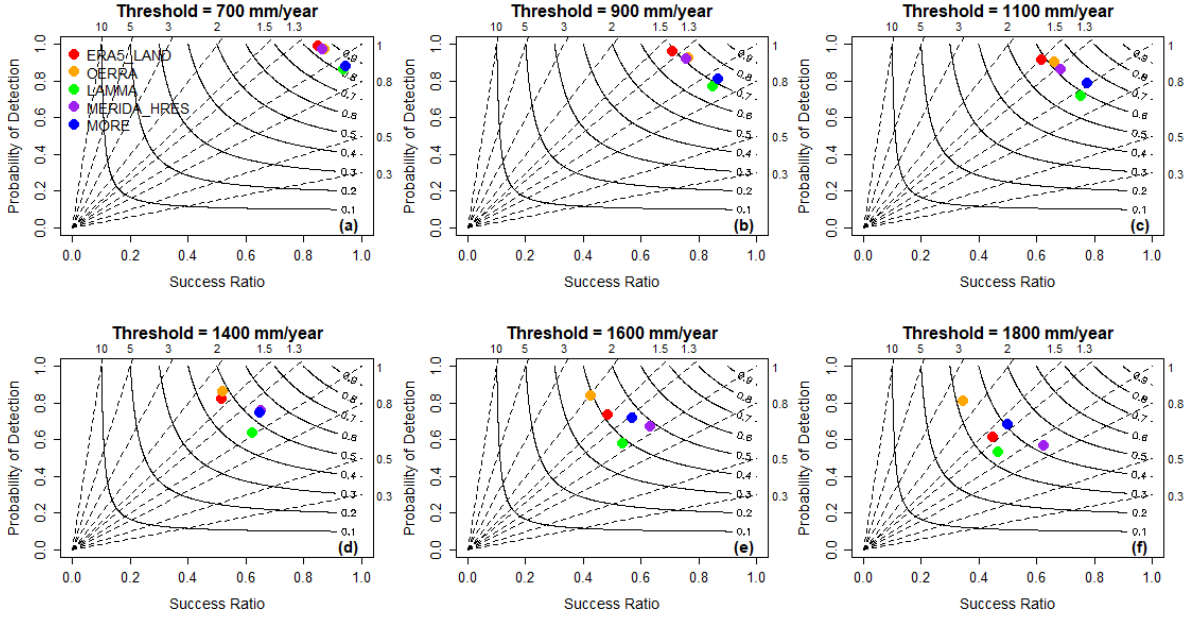

Figure A6: Performance diagram displaying the average skill scores for total annual precipitation over the 1991–2020 period, evaluated for different reanalysis datasets with respect to ARCIS observations within the ARCIS observational domain. The horizontal axis represents the success ratio (SR), while the vertical axis indicates the probability of detection (POD). Curved isopleths correspond to critical success index (CSI) values, and dashed diagonal lines denote the bias

https://doi.org/10.5194/essd-2025-789
Preprint. Discussion started: 31 March 2026

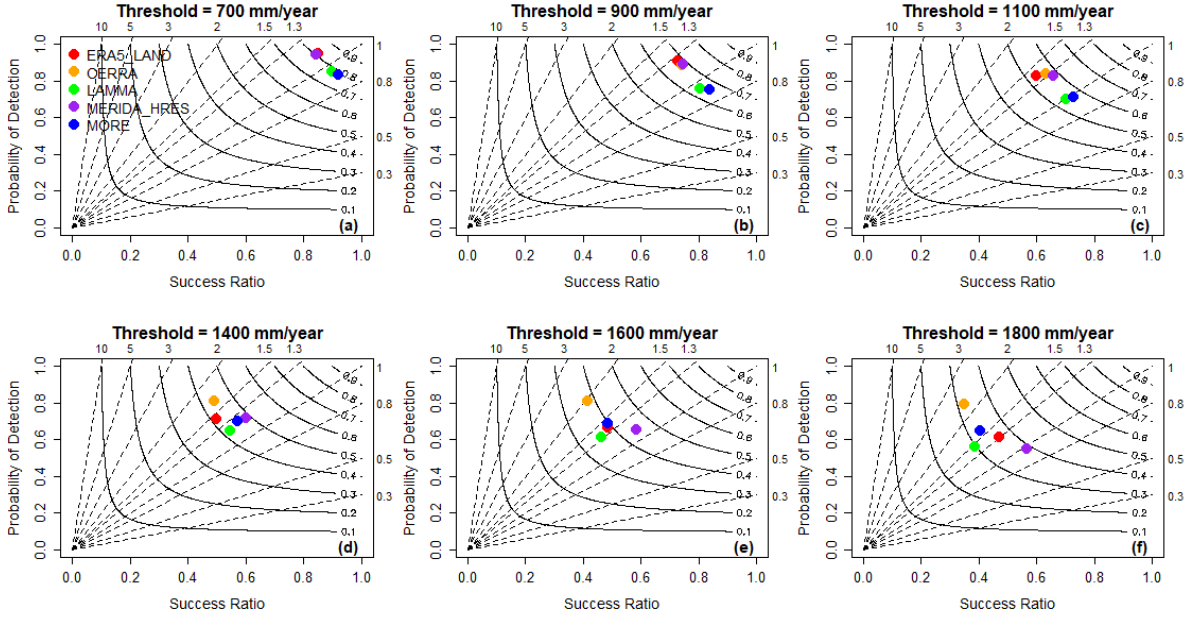

Figure A7: As figure A6 but based on GRIPHO observations dataset within the GRIPHO observational domain over the 2001–2016 period

https://doi.org/10.5194/essd-2025-789
Preprint. Discussion started: 31 March 2026

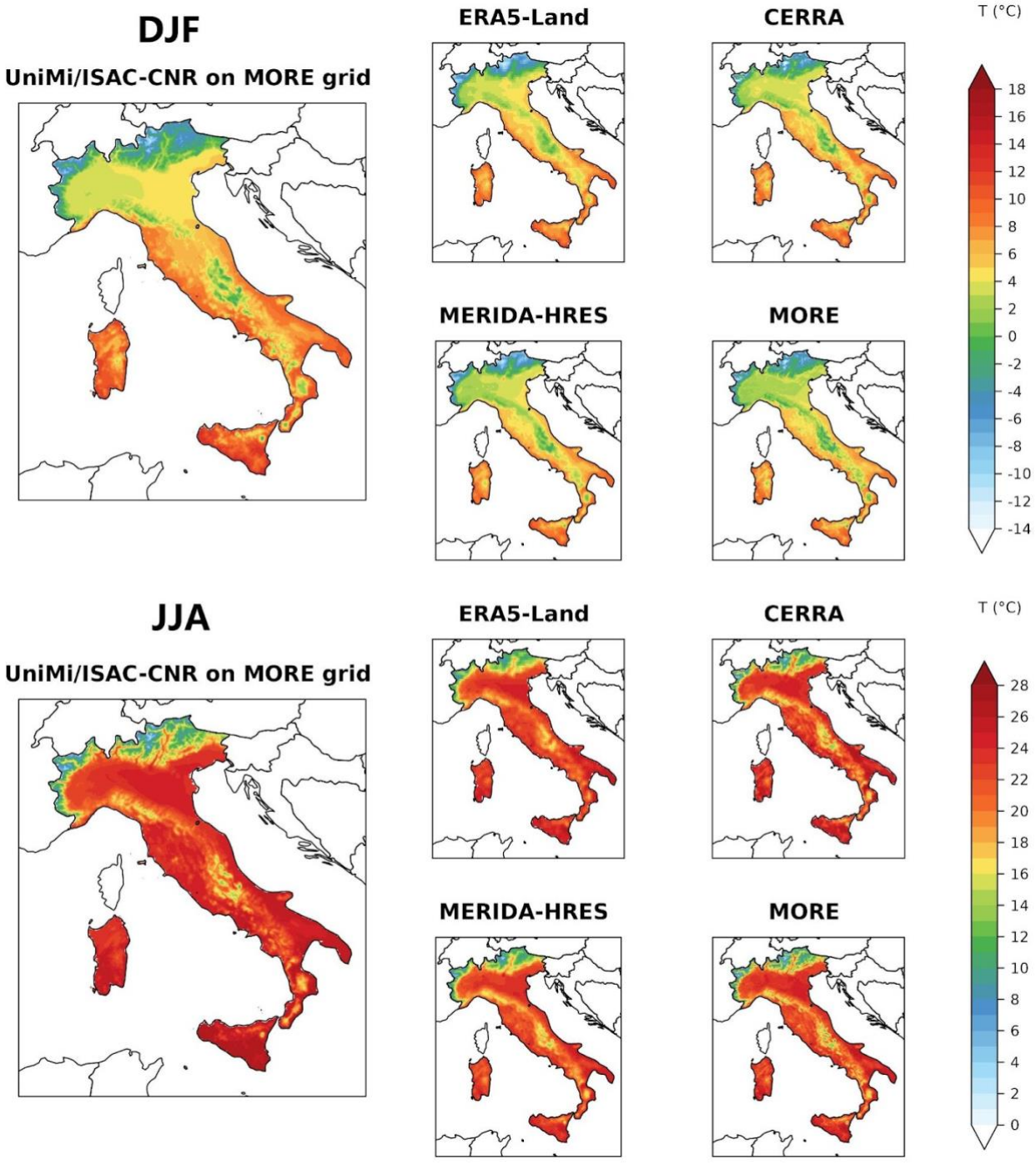

Figure A8: Winter (top) and summer (bottom) climatologies (1991–2020) of 2-meter temperature (t2m) from UniMi/ISAC-CNR observations on the MORE grid (left), compared with reanalyses from ERA5-Land, CERRA, MERIDA HRES, and MORE (four panels on the right). Note: Colorbars differ between winter and summer plots.

https://doi.org/10.5194/essd-2025-789
Preprint. Discussion started: 31 March 2026

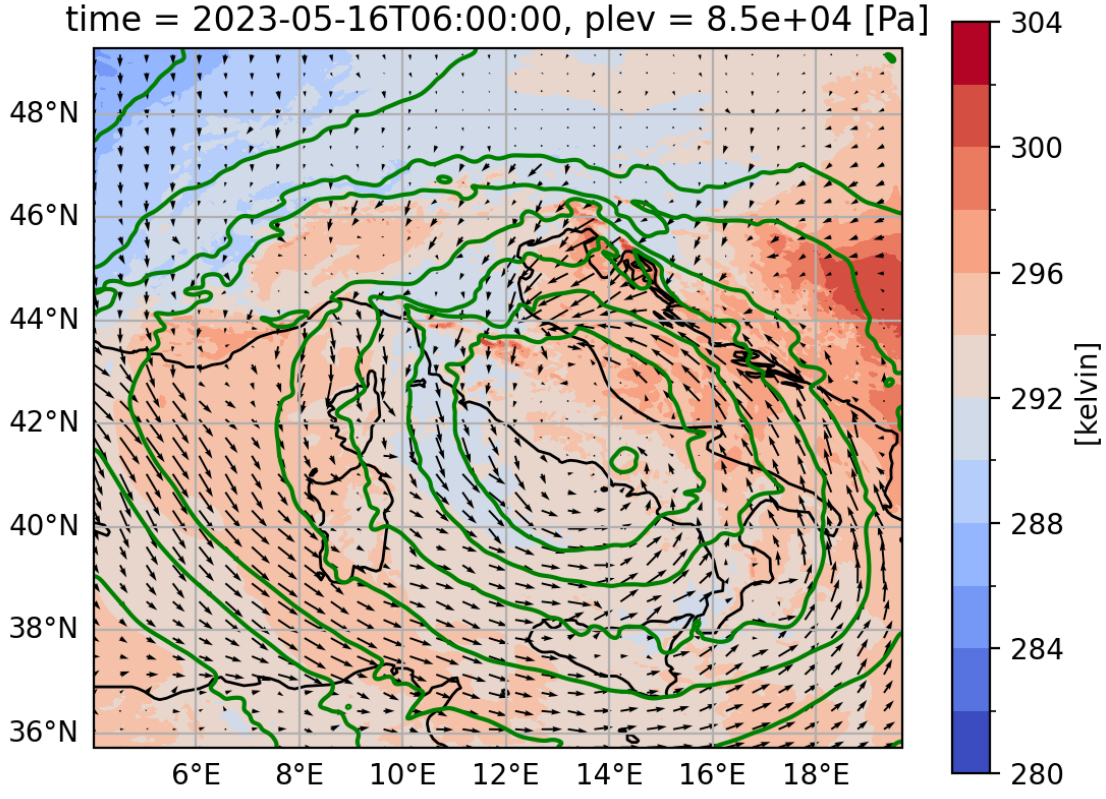

Figure A9: Geopotential height (m) and equivalent potential temperature at 850 hPa, wind vectors at 10 metres, as simulated by MORE at 06 UTC, 16 May 2023, during the most intense phase of precipitation of the second event.

Author contributions

PS contributed to the conceptualization, methodology, formal analysis, investigation, visualization, original draft writing, simulations, funding acquisition, review, and editing. FC contributed to the conceptualization, investigation, temperature validation and analysis, original draft writing, review, and editing. MT contributed to the investigation, precipitation validation and analysis, data homogenization, review and editing. MB contributed to the conceptualization, methodology, and preparation of the observational dataset, review and editing. SC contributed to the conceptualization, hydrological analyses and simulations, original draft writing, review and editing. DM contributed to the analysis, visualization, review and editing. FD contributed to software development, HPC support, and simulation activities. SD contributed to the conceptualization, supervision, funding acquisition, original draft writing, review and editing.

https://doi.org/10.5194/essd-2025-789
Preprint. Discussion started: 31 March 2026

Competing interests

The authors declare no competing interests

Disclaimer

Any opinions, findings, and conclusions or recommendations expressed in this work are those of the authors and do not necessarily reflect the views of the institutions or funding agencies involved

Acknowledgements

We acknowledge the European Centre for Medium-Range Weather Forecasts (ECMWF) for providing access to computing and storage resources through the Special Project [spitstoc-2023], which enabled the production of the simulations used in this work (https://www.ecmwf.int/en/research/special-projects/spitstoc-2023)

Financial support

Financial support is acknowledged from Next Generation EU, Mission 4, Component 1, CUP B53D23006850006, project "unveilINg pasT Events foR dROught risk mitiGATION (INTERROGATION)"

This research has been partially conducted in the framework of the project "Geosciences for society: resources and their evolution" supported by the Italian Ministry of University and Research (MUR) through the funds 'Dipartimenti di Eccellenza 2023/2027', and by the Program PRIN2022—CCHP-ALPS Project (2022CN4RWK), Italian Ministry for University and Research, Funded by the EU Next-Generation Programme. The PhD of F.C. was activated pursuant to DM 352 and is co-sponsored by PNRR funds (from the EU Next Generation programme) and R.S.E. s.p.a. (Research Fund for the Italian Electrical System under the Three-Year Research Plan 2025-2027 (MASE, Decree n.388 of November 6th, 2024), in compliance 450 with the Decree of April 12th, 2024)

References

Adinolfi, M., Raffa, M., Reder, A., et al.: Investigation on potential and limitations of ERA5 reanalysis downscaled on Italy by a convection-permitting model, *Clim. Dyn.*, **61**, 4319–4342, https://doi.org/10.1007/s00382-023-06803-w, 2023.

Almagro, A., Oliveira, P. T. S., and Brocca, L.: Assessment of bottom-up satellite rainfall products on estimating river discharge and hydrologic signatures in Brazilian catchments, *J. Hydrol.*, **603**, 126897, 2021.

ARPAE: Rapporto degli eventi meteorologici di piena e di frana dell'1–4 maggio 2023, Tech. Rep., https://www.arpae.it/it/notizie/rapporto_meteo_20230501-04.pdf (last access: 18 July 2025), 2023a.

ARPAE: Rapporto dell'evento dal 16 al 18 maggio 2023, Tech. Rep., https://www.arpae.it/it/notizie/rapporto_idro_meteo_20230516-18.pdf (last access: 18 July 2025), 2023b.

https://doi.org/10.5194/essd-2025-789
Preprint. Discussion started: 31 March 2026

1006 Arrighi, C. and Domeneghetti, A.: Brief communication: On the environmental impacts of 2023 flood in Emilia-Romagna
1007 (Italy), *Nat. Hazards Earth Syst. Sci. Discuss.*, **2023**, 1–10, 2023.
1008
1009 Ban, N., Schmidli, J., and Schär, C.: Evaluation of the convection-resolving regional climate modeling approach in decade-
1010 long simulations, *J. Geophys. Res.*, **119**, 7889–7907, https://doi.org/10.1002/2014JD021478, 2014.
1011
1012 Ban, N., et al.: The first multi-model ensemble of regional climate simulations at kilometer-scale resolution, part I: Evaluation
1013 of precipitation, *Clim. Dyn.*, **57**, 275–302, 2021.
1014
1015 Bandhauer, M., Isotta, F., Lakatos, M., et al.: Evaluation of daily precipitation analyses in E-OBS (v19.0e) and ERA5 by
1016 comparison to regional high-resolution datasets in European regions, *Int. J. Climatol.*, **42**, 727–747, 2022.
1017
1018 Barnes, C., Faranda, D., Coppola, E., Grazzini, F., Zachariah, M., Lu, C., Kimutai, J., Pinto, I., Pereira, C. M., Sengupta, S.,
1019 Vahlberg, M., Singh, R., Heinrich, D., and Otto, F.: Limited net role for climate change in heavy spring rainfall in Emilia-
1020 Romagna, Imperial College London, Report, https://doi.org/10.25561/104550, 2023.
1021
1022 Bell, B., Hersbach, H., Berrisford, P., Dahlgren, P., Horányi, A., Jánvier, M., et al.: The ERA5 global reanalysis: Preliminary
1023 extension to 1950, *Q. J. R. Meteorol. Soc.*, **147**, 1–15, 2021.
1024 Bernardet, L. R., Grasso, L. D., Nachamkin, J. E., Finley, C. A., and Cotton, W. R.: Simulating convective events using a high-
1025 resolution mesoscale model, *J. Geophys. Res.*, **105**, 14963–14982, 2000.
1026
1027 Bernini, L., Lagasio, M., Milelli, M., Oberto, E., Parodi, A., Hachinger, S., Kranzlmüller, D., and Tartaglione, N.: Convection-
1028 permitting dynamical downscaling of ERA5 for Europe and the Mediterranean basin, *Q. J. R. Meteorol. Soc.*,
1029 https://doi.org/10.1002/qj.5014, 2025.
1030
1031 Berthou, S., Kendon, E. J., Chan, S. C., Ban, N., Leutwyler, D., Schär, C., and Fosser, G.: Pan-European climate at convection-
1032 permitting scale: A model intercomparison study, *Clim. Dyn.*, https://doi.org/10.1007/s00382-018-4114-6, 2018.
1033
1034 Bollmeyer, C., Keller, J., Ohlwein, C., et al.: Towards a high-resolution regional reanalysis for the European CORDEX
1035 domain, *Q. J. R. Meteorol. Soc.*, **141**, 1–15, 2015.
1036
1037 Bonanno, R., et al.: A new high-resolution meteorological reanalysis Italian dataset: MERIDA, *Q. J. R. Meteorol. Soc.*, **145**,
1038 1756–1779, 2019.

https://doi.org/10.5194/essd-2025-789
Preprint. Discussion started: 31 March 2026

Brath, A.: Rapporto della Commissione tecnico-scientifica, Tech. Rep., https://www.regione.emilia-romagna.it/alluvione/rapporto-della-commissione-tecnico-scientifica (last access: 18 July 2025), 2023.

Brunetti, M., Lentini, G., Maugeri, M., Nanni, T., Simolo, C., and Spinoni, J.: Projecting North Eastern Italy temperature and precipitation secular records onto a high-resolution grid, *Phys. Chem. Earth*, **40–41**, 9–22, https://doi.org/10.1016/j.pce.2009.12.005, 2012.

Brunetti, M., Maugeri, M., Nanni, T., Simolo, C., and Spinoni, J.: High-resolution temperature climatology for Italy: Interpolation method intercomparison, *Int. J. Climatol.*, **34**, 1278–1296, 2014.

Bryan, G. H., Wyngaard, J. C., and Fritsch, J. M.: Resolution requirements for simulations of deep moist convection, *Mon. Weather Rev.*, **131**, 2394–2416, 2003.

Buizza, R., Poli, P., Rixen, M., et al.: Advancing global and regional reanalyses, *Bull. Am. Meteorol. Soc.*, **99**, ES139–ES144, 2018.

Buzzi, A., Davolio, S., Malguzzi, P., Drofa, O., and Mastrangelo, D.: Heavy rainfall episodes over Liguria in autumn 2011: Numerical forecasting experiments, *Nat. Hazards Earth Syst. Sci.*, **14**, 1325–1340, https://doi.org/10.5194/nhess-14-1325-2014, 2014.

Buzzi, A., Davolio, S., and Fantini, M.: Cyclogenesis in the lee of the Alps: A review of theories, *Bull. Atmos. Sci. Technol.*, **1**, 433–457, https://doi.org/10.1007/s42865-020-00021-6, 2020.

Caillaud, C., Somot, S., Alias, A., Bernard-Bouissières, I., Fumière, Q., Laurantin, O., Seity, Y., and Ducrocq, V.: Modelling Mediterranean heavy precipitation events at climate scale: An object-oriented evaluation of the CNRM-AROME convection-permitting regional climate model, *Clim. Dyn.*, **56**, 1717–1752, https://doi.org/10.1007/s00382-020-05558-y, 2021.

Camici, S., Ciabatta, L., Massari, C., and Brocca, L.: How reliable are satellite precipitation estimates for driving hydrological models: A verification study over the Mediterranean area, *J. Hydrol.*, **563**, 950–961, 2018.

Camici, S., Massari, C., Ciabatta, L., Marchesini, I., and Brocca, L.: Which rainfall score is more informative about the performance in river discharge simulation?, *Hydrol. Earth Syst. Sci.*, **24**, 4869–4885, 2020.

https://doi.org/10.5194/essd-2025-789
Preprint. Discussion started: 31 March 2026

1072 Camici, S., Dari, J., Filippucci, P., Massari, C., Mantovani, S., Avanzi, F., Delogu, F., Baez-Villanueva, O. M., Vreugdenhil,
1073 M., Volden, E., Fernandez, D. P., and Brocca, L.: High-resolution satellite observations for developing advanced decision
1074 support systems for water resources management in the Po River, *J. Hydrol.*, **662**, 134047,
1075 https://doi.org/10.1016/j.jhydrol.2025.134047, 2025.
1076
1077 Capecchi, V., Pasi, F., Gozzini, B., and Brandini, C.: A convection-permitting and limited-area model hindcast driven by
1078 ERA5 data: Precipitation performances in Italy, *Clim. Dyn.*, **61**, 1411–1437, https://doi.org/10.1007/s00382-022-06633-2,
1079 2023.
1080
1081
1082 Cavalleri, F., Lussana, C., Viterbo, F., Brunetti, M., Bonanno, R., Manara, V., Lacavalla, M., Sperati, S., Raffa, M., Capecchi,
1083 V., Cesari, D., Giordani, A., Cerenzia, I. M. L., and Maugeri, M.: Multi-scale assessment of high-resolution reanalysis
1084 precipitation fields over Italy, *Atmos. Res.*, **312**, 107734, https://doi.org/10.1016/j.atmosres.2024.107734, 2024.
1085
1086 Cavalleri, F., Viterbo, F., Brunetti, M., Bonanno, R., Manara, V., Lussana, C., Lacavalla, M., and Maugeri, M.: Inter-
1087 comparison and validation of high-resolution surface air temperature reanalysis fields over Italy, *Int. J. Climatol.*, **44**, 2681–
1088 2700, 2024a.
1089
1090 Cerenzia, I. M. L., Giordani, A., Paccagnella, T., and Montani, A.: Towards a convection-permitting regional reanalysis over
1091 the Italian domain, *Meteorol. Appl.*, **29**, e2092, https://doi.org/10.1002/met.2092, 2022.
1092
1093 Chen, T.-C., Collet, F., and Di Luca, A.: Evaluation of ERA5 precipitation and 10 m wind speed associated with extratropical
1094 cyclones using station data over North America, *Int. J. Climatol.*, **44**, 729–747, https://doi.org/10.1002/joc.8339, 2024.
1095
1096 Cislaghi, A., Masseroni, D., Massari, C., Camici, S., and Brocca, L.: Combining a rainfall–runoff model and a regionalization
1097 approach for flood and water resource assessment in the western Po Valley, Italy, *Hydrol. Sci. J.*, **65**, 348–370, 2020.
1098
1099 Collier, E. and Mölg, T.: BAYWRF: a high-resolution present-day climatological atmospheric dataset for Bavaria, *Earth Syst.*
1100 *Sci. Data*, **12**, 3097–3112, https://doi.org/10.5194/essd-12-3097-2020, 2020.
1101
1102 Coppola, E., et al.: A first-of-its-kind multi-model convection-permitting ensemble for investigating convective phenomena
1103 over Europe and the Mediterranean, *Clim. Dyn.*, **55**, 3–34, 2020.
1104

https://doi.org/10.5194/essd-2025-789
Preprint. Discussion started: 31 March 2026

Coppola, E., Fantini, A., Giorgi, F., et al.: A new spatially distributed added value index for regional climate models: The EURO-CORDEX and the CORDEX-CORE highest resolution ensembles, *Clim. Dyn.*, **57**, 1403–1424, 2021.

Cornes, R. C., van der Schrier, G., van den Besselaar, E. J. M., and Jones, P. D.: An ensemble version of the E-OBS temperature and precipitation datasets, *J. Geophys. Res.-Atmos.*, **123**, 9391–9409, https://doi.org/10.1029/2017JD028200, 2018.

Cortés-Hernández, V. E., Caillaud, C., Bellon, G., et al.: Evaluation of the convection-permitting regional climate model CNRM-AROME on the orographically complex island of Corsica, *Clim. Dyn.*, **62**, 4673–4696, https://doi.org/10.1007/s00382-024-07232-z, 2024.

Cremonini, L., Randi, P., Fazzini, M., Nardino, M., Rossi, F., and Georgiadis, T.: Causes and impacts of flood events in Emilia-Romagna (Italy) in May 2023, *Land*, **13**, 1800, https://doi.org/10.3390/land13111800, 2024.

Dalla Torre, D., Di Marco, N., Menapace, A., Avesani, D., Righetti, M., and Majone, B.: Suitability of ERA5-Land reanalysis dataset for hydrological modelling in the Alpine region, *J. Hydrol.: Reg. Stud.*, **52**, 101718, https://doi.org/10.1016/j.ejrh.2024.101718, 2024.

Davolio, S., Buzzi, A., Malguzzi, P., Drofa, O., and Mastrangelo, D.: Orographic triggering of long-lived convection in three dimensions, *Meteorol. Atmos. Phys.*, **103**, 35–44, 2009.

Davolio, S., Malguzzi, P., Drofa, O., Mastrangelo, D., and Buzzi, A.: The Piedmont flood of November 1994: A testbed of forecasting capabilities of the CNR-ISAC meteorological model suite, *Bull. Atmos. Sci. Technol.*, **1**, 263–282, 2020.

De Martin, F., Davolio, S., Miglietta, M. M., and Levizzani, V.: A conceptual model for the development of tornadoes in the complex orography of the Po Valley, *Mon. Weather Rev.*, **152**, 1357–1377, 2024.

Diaconescu, E. P., Gachon, P., and Laprise, R.: On the remapping procedure of daily precipitation statistics and indices used in regional climate model evaluation, *J. Hydrometeorol.*, **16**, 2301–2310, https://doi.org/10.1175/JHM-D-15-0025.1, 2015.

Di Luca, A., Argüeso, D., Evans, J. P., De Elía, R., and Laprise, R.: Quantifying the overall added value of dynamical downscaling and the contribution from different spatial scales, *J. Geophys. Res.*, **121**, 1575–1590, https://doi.org/10.1002/2015JD024009, 2016.

https://doi.org/10.5194/essd-2025-789
Preprint. Discussion started: 31 March 2026

1138 Di Luzio, M., Johnson, G. L., Daly, C., Eischeid, J. K., and Arnold, J. G.: Constructing retrospective gridded daily precipitation
1139 and temperature datasets for the conterminous United States, *J. Appl. Meteorol. Climatol.*, **47**, 475–497, 2008.
1140
1141 Ding, Z., Lü, H., Ahmed, N., Zhu, Y., Gou, Q., Wang, X., et al.: Soil moisture data assimilation in MISDc for improved
1142 hydrological simulation in the upper Huai River Basin, China, *Water*, **14**, 3476, 2022.
1143
1144 Done, J., Davis, C. A., and Weisman, M.: The next generation of NWP: Explicit forecasts of convection using the Weather
1145 Research and Forecasting (WRF) model, *Atmos. Sci. Lett.*, **5**, 110–117, 2004.
1146
1147 Dorrington, J., Wenta, M., Grazzini, F., Magnusson, L., Vitart, F., and Grams, C. M.: Precursors and pathways: Dynamically
1148 informed extreme event forecasting demonstrated on the historic Emilia-Romagna 2023 flood, *Nat. Hazards Earth Syst. Sci.*,
1149 **24**, 2995–3012, 2024.
1150
1151 El Khalki, E. M., Tramblay, Y., Saidi, M. E., Marchane, A., and Chehbouni, A.: Hydrological assessment of different satellite
1152 precipitation products in semi-arid basins in Morocco, *Front. Water*, **5**, 1243251, 2023.
1153
1154 Fantini A (2019) Climate change impact on flood hazard over Italy. Ph.D. thesis, Universita degli Studi di Trieste.
1155 http://hdl.handle.net/11368/2940009
1156
1157 Frei C, Christensen JH, Dèquè M, Jacob D, Jones RG, Vidale PL (2003) Daily precipitation statistics in regional climate
1158 models: evaluation and intercomparison for the European Alps. J Geophys Res 108:4124
1159
1160 Fumière Q, Déqué M, Nuissier O, Somot S, Alias A, Caillaud C, Laurantin O, Seity Y (2020) Extreme rainfall in Mediterranean
1161 France during the fall: added value of the CNRM-AROME convection-permitting regional climate model. Clim Dyn.
1162 https://doi.org/10.1007/s00382-019-04898-8
1163
1164 Gebrechorkos, S. H., Leyland, J., Dadson, S. J., Cohen, S., Slater, L., Wortmann, M., ... & Darby, S. E. (2023). Global scale
1165 evaluation of precipitation datasets for hydrological modelling. Hydrology and Earth System Sciences Discussions, 2023, 1-
1166 33.
1167
1168 Giordani, A., Ruggieri, P., & Di Sabatino, S. (2026). Added value of a multi-model ensemble of convection-permitting rainfall
1169 reanalyses over Italy. *Atmospheric Research, 328,* 108402. https://doi.org/10.1016/j.atmosres.2025.108402
1170

https://doi.org/10.5194/essd-2025-789
Preprint. Discussion started: 31 March 2026

Giordani, A., Cerenzia, I.M.L., Paccagnella, T., & Di Sabatino, S. (2023). SPHERA, a new convection-permitting regional reanalysis over Italy: Improving the description of heavy rainfall. Quarterly Journal of the Royal Meteorological Society, 149(752), 781–808. https://doi.org/10.1002/qj.4428

Giorgi, F., Coppola, E., Giuliani, G., Ciarlo`, J. M., Pichelli, E., Nogherotto, R., Raffaele, F., Malguzzi, P., Davolio, S., Stocchi, P., & Drofa, O. (2023). *The Fifth Generation Regional Climate* Modeling System, RegCM5: Description and Illustrative Examples at Parameterized Convection and Convection-Permitting Resolutions. Journal of Geophysical Research: Atmospheres, 128(6), e2022JD038199. https://doi.org/10.1029/2022JD03819

Giorgi, F. Thirty years of regional climate modeling: where are we and where are we going next? *J. Geophys. Res. Atmos.* **124**, 5696–5723 (2019)

Giorgi F, Gutowski WJ Jr (2015) Regional dynamical downscaling and the CORDEX initiative. Annu Rev Environ Resour 40:467–490

Giorgi F, Jones C, Asrar GR et al (2009) Addressing climate information needs at the regional level: the CORDEX framework. World Meteorol Organ Bull 58(3):175

Giorgi, F., & Mearns, L. O. (1991). Approaches to the simulation of regional climate change: A review. *Reviews of Geophysics, 29*(3), 191–216. https://doi.org/10.1029/91RG00973

Gohm, A., Mayr, G. J., Fix, A., and Giez, A.: On the onset of bora and the formation of rotors and jumps near a mountain gap, Q. J. Roy. Meteorol. Soc., 134, 21–46, https://doi.org/10.1002/qj.206, 2008.

González-Hidalgo, J.C., Brunetti, M., and De Luis, M.: A new tool for monthly precipitation analysis in Spain: MOPREDAS database (monthly precipitation trends December 1945–November 2005), International Journal of Climatology 31.5, 715-731, 2011.

Grazzini F, Craig GC, Keil C, Antolini G, Pavan V. Extreme precipitation events over northern Italy. Part I: A systematic classification with machine-learning techniques. Q J R Meteorol Soc. 2020;146:69–85. https://doi.org/10.1002/qj.3635

Gupta, H. V., Kling, H., Yilmaz, K. K., and Martinez, G. F.: Decomposition of the mean squared error and NSE performance criteria: Implications for improving hydrological modelling, *J. Hydrol.*, **377**, 80–91, 2009.

Ha, M. T. et al. Precipitation frequency in Med-CORDEX and EURO-CORDEX ensembles from 0.44° to convection-permitting resolution: impact of model resolution and convection representation. *Clim. Dyn*. https://doi.org/10.1007/s00382-022-06594-6 2022

Hersbach H, Bell B, Berrisford P et al (2020) The ERA5 global reanalysis. Q J R Meteorol Soc 146(730):1999–2049

Kaiser-Weiss, Andrea K., et al. "Added Value of Regional Reanalyses for Climatological Applications." Environmental Research Communications 1, no. 7 (July 2019): 071004. https://doi.org/10.1088/2515-7620/ab2ec3

Karl, T.R., N. Nicholls, and A. Ghazi, 1999: CLIVAR/GCOS/WMO workshop on indices and indicators for climate extremes: Workshop summary. Climatic Change, 42, 3-7.

Kendon, E. J., Roberts, N. M., Senior, C. A., & Stott, P. A. (2021). Challenges and outlook for convection-permitting climate models. Nature Climate Change, 11(7), 490–499. https://doi.org/10.1038/s41558-021-01059-2

Kendon, E.J.; Roberts, N.M.; Fowler, H.; Roberts, M.J.; Chan, S.C.; Senior, C.A. Heavier summer downpours with climate change revealed by weather forecast resolution model. Nat. Clim. Chang. 2014, 4, 570–576. https://doi.org/10.1038/nclimate2258.

Kendon, E. J., Roberts, N. M., Fowler, H. J., & Roberts, M. J. (2012). *Realism of rainfall in a very high-resolution regional climate model*. Journal of Climate, 25(17), 5791–5806.

Kirchner, J. W. (2006). Getting the right answers for the right reasons: Linking measurements, analyses, and models to advance the science of hydrology, Water Resour. Res., 42, W03S04, https://doi.org/10.1029/2005WR004362.

Kotlarski S, Keuler K, Christensen OB, Colette A, Déqué M, Gobiet A, Goergen K, Jacob D, Lüthi D, van Meijgaard E, Nikulin G, Schä C, Teichmann C, Vautard R, Warrach-Sagi K, Wulfmeyer V (2014) Regional climate modeling on European scales: a joint standard evaluation of the EURO-CORDEX RCM ensemble. Geosci Model Dev Discuss 7:217–293. https://doi.org/10.5194/gmdd-7-217-2014

Kourtis, I. M., Vangelis, H., Tigkas, D., Mamara, A., Nalbantis, I., Tsakiris, G., & Tsihrintzis, V. A. (2023). Drought Assessment in Greece Using SPI and ERA5 Climate Reanalysis Data. *Sustainability*, *15*(22), 15999. https://doi.org/10.3390/su152215999

Lavers, D. A., et al. (2022). An evaluation of ERA5 precipitation for climate monitoring. Climate Dynamics, 57(1–2), 1–1

Lenderink, G., Ban, N., Brisson, E., Berthou, S., Cortés-Hernández, V. E., Kendon, E., Fowler, H. J., and de Vries, H.: Are dependencies of extreme rainfall on humidity more reliable in convection-permitting climate models?, Hydrol. Earth Syst. Sci., 29, 1201–1220, https://doi.org/10.5194/hess-29-1201-2025, 2025

Leutwyler D, Lüthi D, Ban N, Fuhrer O, Schär C (2017) Evaluation of the convection-resolving climate modeling approach on continental scales. J Geophys Res Atmos. https://doi.org/10.1002/2016JD026013

Leutwyler, D., Fuhrer, O., Lapillonne, X., Lüthi, D., & Schär, C. (2016). Towards European-scale convection-resolving climate simulations with GPUs: a study with COSMO 4.19. Geoscientific Model Development, 9, 3393–3412. https://doi.org/10.5194/gmd-9-3393-2016

Long, Z., Zha, J., Zhang, H., Chuan, T., Lu, W., Yan, Y., Xia, L., Fan, W., Jiang, H., Zhao, D., & Wu, J. (2025). Deep learning with ERA5 variables accurately simulates near-surface wind speed variations across a complex terrain region. Geophysical Research Letters. https://doi.org/10.1029/2025GL116108

Liu C, Ikeda K, Rasmussen R, Barlage M, Newman AJ, Prein AF, Chen F, Chen L, Clark M, Dai A, Dudhia J, Eidhammer T, Gochis D, Gutmann E, Kurkute S, Li Y, Thompson G, Yates D (2017) Continental-scale convection-permitting modeling of the current and future climate of North America. Clim Dyn 49(1):71–95. https://doi.org/10.1007/s00382-016-3327-9

Lundquist J, Hughes M, Gutmann E, Kapnick S (2020) Our skill in modeling mountain rain and snow is bypassing the skill of our observational networks. Bull Am Meteorol Soc 100(12):2473–2490. https://doi.org/10.1175/BAMS-D-19-0001.1.

Luo, H., Ge, F., Yang, K., Zhu, S., Peng, T., Cai, W. et al. (2019) Assessment of ECMWF reanalysis data in complex terrain: can the CERA-20C and ERA-interim data sets replicate the variation in surface air temperatures over Sichuan China? International Journal of Climatology, 39(15), 5619–5634. https://doi.org/10.1002/joc.6175

Malguzzi, P. et al. (2006). The 1966 'century' flood in Italy: A meteorological and hydrological revisitation. J. Geophys. Res., 111, D24106

Mariani, S., Casaioli, M., Coraci, E., & Malguzzi, P. (2015). New high-resolution BOLAM-MOLOCH suite for the SIMM forecasting system: assessment over two HyMeX intense observation periods. *Natural Hazards and Earth System Sciences*, 15, 1–24. https://doi.org/10.5194/nhess-15-1-2015

https://doi.org/10.5194/essd-2025-789
Preprint. Discussion started: 31 March 2026

Maraun, D., Wetterhall, F., Ireson, A. M., et al. (2010). *Precipitation downscaling under climate change: Recent developments to bridge the gap between dynamical models and the end user*. Reviews of Geophysics, 48(3)

Masseroni, D., Cislaghi, A., Camici, S., Massari, C., & Brocca, L. (2017). A reliable rainfall–runoff model for flood forecasting: Review and application to a semi-urbanized watershed at high flood risk in Italy. Hydrology Research, 48(3), 726-740.

Masson V, Le Moigne P, Martin E et al (2013) The SURFEXv7.2 land and ocean surface platform for coupled or offline simulation of earth surface variables and fluxes. Geosci Model Dev 6(4):929–960

Mearns, L. O., Lettenmaier, D. P. & McGinnis, S. Uses of results of regional climate model experiments for impacts and adaptation studies: the example of NARCCAP. *Curr. Clim. Chang. Rep.* **1**, 1–9 (2015)

Mitchell, T. D., & Jones, P. D. (2005). An improved method of constructing a database of monthly climate observations and associated high-resolution grids. International Journal of Climatology: A Journal of the Royal Meteorological Society, 25(6), 693-712.

Mistry, M.N., Schneider, R., Masselot, P. *et al.* Comparison of weather station and climate reanalysis data for modelling temperature-related mortality. *Sci Rep* **12**, 5178 (2022). https://doi.org/10.1038/s41598-022-09049-4

Muñoz-Sabater, J., E. Dutra, A. Agustí-Panareda, C. Albergel, G. Arduini, G. Balsamo, S. Boussetta, et al. 2021. "ERA5-Land: A State-of-the-Art Global Reanalysis Dataset for Land Applications." *Earth System Science Data* 13: 4349–4383. https://doi.org/10.5194/essd-13-4349-2021.

Nguyen, N. T., He, W., Zhu, Y., & Lü, H. (2020). Influence of calibration parameter selection on flash flood simulation for small to medium catchments with MISDc-2L model. Water, 12(11), 3255.

Olauson, J. (2018). *ERA5: The new champion of wind power modelling?* Renewable Energy, 126, 322–331. https://doi.org/10.1016/j.renene.2018.03.056

Pavan, V., Antolini, G., Barbiero, R. *et al.* High resolution climate precipitation analysis for north-central Italy, 1961–2015. *Clim Dyn* 52, 3435–3453 (2019). https://doi.org/10.1007/s00382-018-4337-6

https://doi.org/10.5194/essd-2025-789
Preprint. Discussion started: 31 March 2026

Pichelli, E. et al. The first multi-model ensemble of regional climate simulations at kilometer-scale resolution part 2: historical and future simulations of precipitation. *Clim. Dyn.* **56**, 3581–3602 (2021)

Poncet, N., Lucas-Picher, P., Tramblay, Y., Thirel, G., Vergara, H., Gourley, J., and Alias, A.: Does a convection-permitting regional climate model bring new perspectives on the projection of Mediterranean floods?, Nat. Hazards Earth Syst. Sci., 24, 1163–1183, https://doi.org/10.5194/nhess-24-1163-2024, 2024

Prein, A., Langhans, W., Fosser, G., Ferrone, A., Ban, N., Goergen, K., Keller, M., Tölle, M., Gutjahr, O., Feser, F., Brisson, E., Kollet, S., Schmidli, J., Lipzig, N., & Leung, L. (2015). A review on regional convection-permitting climate modeling: Demonstrations, prospects, and challenges. *Reviews of Geophysics, 53*(3), 346–378. https://doi.org/10.1002/2014RG000475

Raffa, M., Reder, A., Marras, G.F., Mancini, M., Scipione, G., Santini, M., & Mercogliano, P. (2021). VHR-REA_IT dataset: Very high resolution dynamical downscaling of ERA5 reanalysis over Italy by COSMO-CLM. Data, 6(8), 88. https://doi.org/10.3390/data6080088

Reder, A., Raffa, M., Padulano, R., Rianna, G., & Mercogliano, P. (2022). Characterizing extreme values of precipitation at very high resolution: An experiment over twenty European cities. Weather and Climate Extremes, 35, 100407. https://doi.org/10.1016/j.wace.2022.100407

Ridal, M., Bazile, E., Le Moigne, P., Randriamampianina, R., Schimanke, S., Andrae, U., Berggren, L., Brousseau, P., Dahlgren, P., Edvinsson, L., El-Said, A., … & Others. (2024). CERRA, the Copernicus European Regional Reanalysis system. Quarterly Journal of the Royal Meteorological Society. https://doi.org/10.1002/qj.4764

Roebber, P. J. (2009). Visualizing multiple measures of forecast quality. *Weather and Forecasting*, **24**(2), 601–608. https://doi.org/10.1175/2008WAF2222159.1

Rolland, C. (2003). Spatial and seasonal variations of air temperature lapse rates in Alpine regions. *Journal of climate*, *16*(7), 1032-1046.

Rossa, A., P. Nurmi, and E. Ebert, 2008: Overview of methods for the verification of quantitative precipitation forecasts. Precipitation: Advances in Measurement, Estimation and Prediction, S. Michaelides, Ed., Springer, 419–452.

https://doi.org/10.5194/essd-2025-789
Preprint. Discussion started: 31 March 2026

Sacchetti, D., Cassola, F., Corazza, M., Pedemonte, L., Tizzi, M., Drofa, O., & Davolio, S. (2024). The ARPAL atmospheric operational modeling chain and its applications: description and validation. *Bulletin of Atmospheric Science and Technology*, 5. https://doi.org/10.1007/s42865-024-00064-z

Schulzweida, Uwe. (2023). CDO User Guide (2.3.0). Zenodo. https://doi.org/10.5281/zenodo.10020800

Schwartz, C. S., Kain, J. S., Weiss, S. J., Xue, M., Bright, D. R., Kong, F., ... & Coniglio, M. C. (2010). Toward improved convection-allowing ensembles: Model physics sensitivities and optimizing probabilistic guidance with small ensemble membership. *Weather and Forecasting*, **25**(1), 263–280.

Senior, C. A., and Coauthors, 2021: Convection-Permitting Regional Climate Change Simulations for Understanding Future Climate and Informing Decision-Making in Africa. *Bull. Amer. Meteor. Soc.*, **102**, E1206–E1223, https://doi.org/10.1175/BAMS-D-20-0020.1

Sevruk B (1985) Correction of precipitation measurements. Proc workshop on the correction of precipitation measurements. WMO/IAHS/ETH, Zürich, pp 13–13

Shangguan, W., Zhang, R., Li, L., Zhang, S., Zhang, Y., Huang, F., Li, J., & Liu, W. (2022). Assessment of Agricultural Drought Based on Reanalysis Soil Moisture in Southern China. *Land*, *11*(4), 502. https://doi.org/10.3390/land11040502

Singh T, Saha U, Prasad V et al (2021) Assessment of newly-developed high resolution reanalyses (IMDAA, NGFS and ERA5) against rainfall observations for indian region. Atmos Res 259(105):679

Soares, P. M. M. et al. The added value of km-scale simulations to describe temperature over complex orography: the CORDEX FPS-Convection multi-model ensemble runs over the Alps. *Clim. Dyn*. https://doi.org/10.1007/s00382-022-06593-7 (2022).

Stocchi, P. (2026). MOLOCH-downscaled ERA5 REanalysis (MORE) [Data set]. Institute of Atmospheric Sciences and Climate. https://doi.org/10.82214/EQ2W-2580

Stocchi, P.; Pichelli, E.; Torres Alavez, J.A.; Coppola, E.; Giuliani, G.; Giorgi, F. Non-Hydrostatic Regcm4 (Regcm4-NH): Evaluation of Precipitation Statistics at the Convection-Permitting Scale over Different Domains. Atmosphere 2022, 13, 861. https://doi.org/10.3390/atmos13060861

Taylor, K. E. (2001). Summarizing multiple aspects of model performance in a single diagram. Journal of Geophysical Research: Atmospheres, 106(D7), 7183–7192. https://doi.org/10.1029/2000JD900719

Teichmann, C., Jacob, D., Remedio, A.R. *et al.* Assessing mean climate change signals in the global CORDEX-CORE ensemble. *Clim Dyn* **57**, 1269–1292 (2021). https://doi.org/10.1007/s00382-020-05494-x

Tiedtke M (1989) A comprehensive mass flux scheme for cumu- lus parameterization in large-scale models. Mon Weather Rev 117(8):1779–1800

Tomasi E., (arXiv:2406.13627) https://doi.org/10.48550/arXiv.2406.13627

Trigo, I. F., Davies, T. D., and Bigg, G. R.: Objective climatology of cyclones in the Mediterranean region, *J. Climate*, 12, 1685–1696, https://doi.org/10.1175/1520-0442(1999)012<1685:OCOCIT>2.0.CO;2, 1999

Trini Castelli, S., Bisignano, A., Donateo, A., Landi, T.C., Martano, P. and Malguzzi, P., 2019. Evaluation of the turbulence parametrization in the MOLOCH meteorological model. *Quarterly Journal of the Royal Meteorological Society*, 145(725), pp.3271–3286. https://doi.org/10.1002/qj.3661

Velikou, K., Lazoglou, G., Tolika, K., & Anagnostopoulou, C. (2022). Reliability of the ERA5 in Replicating Mean and Extreme Temperatures across Europe. *Water*, *14*(4), 543. https://doi.org/10.3390/w14040543

Vergara-Temprado, J., N. Ban, D. Panosetti, L. Schlemmer, and C. Schär, 2020: Climate Models Permit Convection at Much Coarser Resolutions Than Previously Considered. J. Climate, **33**, 1915–1933, https://doi.org/10.1175/JCLI-D-19-0286.1.

Viterbo, F., Sperati, S., Vitali, B., D'Amico, F., Cavalleri, F., Bonanno, R., & Lacavalla, M. (2024). MERIDA HRES: A new high-resolution reanalysis dataset for Italy. Meteorological Applications, 31(6), e70011. https://doi.org/10.1002/met.70011

Vitolo, C., Di Giuseppe, F., Barnard, C. *et al.* ERA5-based global meteorological wildfire danger maps. *Sci Data* 7, 216 (2020). https://doi.org/10.1038/s41597-020-0554-z

Wang, Y., Jianping, W., Yang, X., Peng, J. & Pan, X. (2022) Orographic construction of a numerical weather prediction spectral model based on ASTER data and its application to simulation of the Henan 20-7 extreme rainfall event. Remote Sensing, 14(15), 3840. Available from: https://doi.org/10.3390/rs14153840

https://doi.org/10.5194/essd-2025-789
Preprint. Discussion started: 31 March 2026

1405 Weisman, M. L., Davis, C. A., Wang, W., Manning, K. W., & Klemp, J. B. (2008). Experiences with 0–36-h explicit convective
1406 forecasts with the WRF-ARW model. *Weather and Forecasting*, **23**(3), 407–437.
1407
1408 Weusthoff, T., F. Ament, M. Arpagaus, and M. W. Rotach (2010), Assessing the benefits of convection-permitting models by
1409 neighborhood verification: Examples from MAP D-PHASE, *Mon. Weather Rev.*, **138**(9), 3418–3433,
1410 doi: 10.1175/2010MWR3380.1.
1411
1412 Wilks, D. S. (2011). Statistical Methods in the Atmospheric Sciences. Academic Press
1413
1414 Wyngaard, J. C. (2004), Toward numerical modeling in the "Terra Incognita", *J. Atmos. Sci.*, 61, 1816–1826.
1415
1416 Zhang W, Villarini G, Scoccimarro E et al (2021) Examining the precipitation associated with Medicanes in the high-resolution
1417 ERA-5 reanalysis data. Int J Climatol 41:E126–E132